Improving Machinability of Alloy Steel

M.Tech Thesis

By

Naresh Kumar Wagri

Discipline of Mechanical Engineering

Indian Institute of Technology Indore

July 2016

Improving Machinability of Alloy Steel

A Thesis

Submitted in partial fulfillment of the

Requirements for the award of the degree

of

Master of Technology

In

Mechanical Engineering

with specialization in

Production and Industrial Engineering

by

Naresh Kumar Wagri

Discipline of Mechanical Engineering

Indian Institute of Technology Indore

July 2016

Indian Institute of Technology Indore

Candidate's Declaration

I hereby certify that the work which is being presented in the thesis entitled "**Improving Machinability of Alloy Steel"** in the partial fulfillment of the requirements for the award of the degree of **Master of Technology** in **MECHANICAL ENGINEERING** with specialization in **PRODUCTION and INDUSTRIAL ENGINEERING** and submitted in the **Discipline of Mechanical Engineering, Indian Institute of Technology Indore**, is an authentic record of my own work carried out during the time period from May 2015 to June 2016 under the supervision of **Prof. Neelesh Kumar Jain** of Discipline of Mechanical Engineering.

The matter contained in this thesis has not been submitted by me for the award of any degree from any other institute.

NARESH KUMAR WAGRI

This is to certify that the above statement made by the candidate is correct to the best of my knowledge.

Prof. Neelesh Kumar Jain

Naresh Kumar Wagri has successfully completed his M.Tech Oral Examination, held on **……**

Signature of M.Tech Thesis Supervisor
Date:

Signature of Convener, DPGC
Date:

Signature of PSPC Member 1
Date:

Signature of PSPC Member 2
Date:

Signature of Chairman, Oral Examination Board with date

Acknowledgements

This thesis is a result of research carried out at Indian Institute of Technology, Indore. During this period, I came across people who supported and helped me and in my research in various ways and would thereby take this opportunity to thank them and their incredible support for my work. It is my great pleasure to convey my gratitude to all of them.

First, I would like to thank and highly indebted to my mentor **Prof. Neelesh Kumar Jain** for providing the opportunity to work on this project under his guidance. He has been great as a mentor and has motivated me throughout my entire work duration. I am thankful to him for being so patience with me and providing inspiring guidance, constructive criticism and valuable suggestion to complete this thesis.

My gratitude is extended towards my PSPC members **Dr. Bhupesh Kumar Lad** and **Dr. Amod C. Umarikar**. I also would like to express grateful acknowledgment of financial support received from the IIT Indore and I am also grateful to **Prof. Pradeep Mathur,** Director of IIT Indore for providing the essential facilities, without which this work would not have been possible.

I would like to thank Indo German Tool Room, Indore for providing their facilities for CNC turning machine to carry out the research work.

I am specially thankful to my uncle **Mr. Anoop Bali** who courage me all the time. I am also grateful to Mr. Anand Petare Assistant Superintendent of Central Workshop, Mr. Santosh Sharma, Lab-in-Charge of Metrology lab and Suresh Bhagore, Deputy Manager of Tribology and Metallography lab. A special acknowledge to machine operators Pawan Chouhan, Deepak Rathore, Vinay Mishra, Deepak Dhepte for their efficient work. I am also thankful to all the teachers and staff of the discipline of mechanical engineering for helping me to clear my doubts or other issues which were hindering in my thesis.

I am thankful to my colleagues Swagat Dwibedi, Pravin Rai, Muneer alam and Vibhor Pandhare who helped me in this duration. I am also grateful to PhD student Sudhanshu Ranjan Das from mechanical engineering department, NIT Jamshedpur. And last but not the least, my sincere thanks to God and my parents who have been patiently extended all sort of help for accomplishing this undertaking and providing me with opportunities throughout the life.

Dedicated to my family

Abstract

In this study the improvement of machinability of an annealed AISI 4340 ALLOY STEEL workpiece material was investigated by using coated carbide tool insert with CVD multilayer coating consisting of (Ti/TiCN//ZrCN) cylindrical straight turning under dry environment. By annealing this material a coarse pearlitic microstructure developed and this effect of mechanical properties on the machinability of workpiece. This led to an increase in ductility and therefore the decrease in hardness and increases the tool life for better the machinability. Here also discussed optimized the machining parameters for minimum cost and maximum production rate in terms of depth of cut. In this work a series of experiment were conducted in order to determine the machinability index n, p, q and C based on (VB = 0.3 mm) flank wear of tool insert, the effects of tool material and type of coating on the insert (for coated tools). The experimental data were further analyzed to predict the optimal range of cutting velocity, feed rate and depth of cut. The machining of furnace cool (coarse pearlite structure) workpiece material was carried out in a high speed lathe to assess the machinability. The influence of machining parameters such as cutting velocity, feed rate and depth of cut on machining force, surface roughness, maximum flank wear, chips thickness and chips morphology was studied. Optical and scanning electron microscope were used to find the tool insert wear and chip morphology. The machining force data used in the analyses and this forces measured by a three-dimensional force dynamometer (piezoelectric type). By adopting techniques such as two way general linear model analysis of variance ANOVA, the consequences of cutting parameters (cutting velocity, feed and depth of cut) on surface roughness (R_a, R_{max} and R_z), machining forces (F_f, F_c, and F_r) and maximum flank wear (VB_{max}) are explored with 95% confidence level. Also the statistical significance has been checked (depending on P value, F value and percentage of contribution). The results show that feed rate is the principal machining parameter influencing surface roughness, followed by cutting velocity. The machining forces parameter leads to increase significantly with majorly an increase in cutting velocity and depth of cut. However, flank wear is affected by the cutting speed and depth of cut. Chip morphology indicates the formation saw-tooth/serrated chips at higher feed rate.

CONTENTS

List of figures

List of Tables

Table Number and its Caption **Page No.**

Nomenclature

C	Taylor constant
C_1	Machining cost per piece (Rs./piece)
C_2	Tool cost or tool regrinding cost per piece (Rs./piece)
C_3	Tool changing cost per piece (Rs./piece)
C_4	Setup or Ideal time cost per piece (Rs./piece)
d	Depth of cut (mm)
$d_{opt(min.cost)}$	Optimum depth of cut for minimum cost (mm)
$d_{opt(max.prod.)}$	Optimum depth of cut for maximum production rate (mm)
	Minimum value of optimum depth of cut for minimum cost (mm)

	Maximum value of optimum depth of cut for maximum production rate (mm)
D	Diameter of the cylindrical workpiece to be turned (mm)
f	Feed rate (mm/rev)
$f_{opt(min.cost)}$	Optimum feed rate for minimum cost (mm/rev)
$f_{opt(max.prod.)}$	Optimum feed rate for maximum production rate (mm/rev)
	Minimum value of optimum feed rate for minimum cost (mm/rev)
	Maximum value of optimum feed rate for maximum production rate (mm/rev)
F_f or F_x	Feed force i.e. cutting force in x-direction (N)
F_c or F_y	Cutting force i.e. cutting force in y-direction (N)

F_r or F_z	Radial force i.e. cutting force in z-direction (N)
h_f	Flank wear (mm)
k	Constant
L	Length of the cylindrical workpiece to be turned (mm)
	Minimum range of optimum cutting speed for minimum cost (rpm)
	Maximum range of optimum cutting speed for maximum production rate (rpm)
n, p, q	Exponent index
R_a	Average surface roughness (µm)
R_{max}	Maximum surface roughness (µm)

R_z	Maximum or peak-to-valley height roughness (μm)
T	Tool life (min)
T_m	Machining time per piece (min/piece)
$T_{opt(min.cost)}$	Optimum tool life for minimum cost (min)
$T_{opt(max.prod.)}$	Optimum tool life for maximum production rate (min)
T_s	Setup or Idle time per piece (min/piece)
T_{tct}	Tool changing time (min/insert)
V	Cutting velocity (m/min)
$V_{opt(min.cost)}$	Optimum cutting velocity for minimum cost (m/min)

$V_{opt(max.prod.)}$ Optimum cutting velocity for maximum production rate (m/min)

Minimum value of optimum cutting speed for minimum cost (m/min)

Maximum value of optimum cutting speed for maximum production rate (m/min)

$VB_{max.}$ Maximum value of flank wear (mm)

α_b Back rack angle (degrees)

α_s Side rack angle (degrees)

δ_e End relief angle (degrees)

δ_s Side clearance angle or Relief angle (degrees)

γ_e End cutting edge angle (degrees)

γ_s Side cutting edge angle (degrees)

Labor or Overhead cost per min (Rs./min)

Cost of setting the tool for regrinding (Rs./tool)

Tool regrinding cost per mm (Rs./mm)

Sum of two cost (Rupees)

Abbreviations

Adj MS	Adjusted mean of squares
Adj SS	Adjusted sum of squares
AISI	American iron and steel institute
ANOVA	Analysis of variance
BHN	Brilness hardness number
BUE	Build-up-edge
CI	Confidence interval
CNC	Computerized numerical control

CVD	Chemical vapor deposition
DF	Degree of freedom
EDM	Electric discharge machining
F	Variance ratio
HRC	Rockwell hardness
HV	Vickers hardness
MRR	Metal removal rate
N	Number of experiment
P	Statistical parameter
PVD	Physical vapor deposition
Seq SS	Sequential sum of squares

Organization of the Thesis

This thesis is organized into SIX chapters with following contents:

Chapter 1 presents introduction of machinability, its evaluation criterion, factors influencing machinability, methods for improving machinability, challenges in machining of AISI 4340 alloy steel and details of cutting tool material.

Chapter 2 presents review of past work on machinability using different processes machining, past work for surface roughness, machining forces, chip morphology, tool wear and tool life. Research gaps identified based on this review, research objectives defined based on the identified research gaps and research methodology.

Chapter 3 design and optimized machining parameters, selection and optimized machining parameter, optimizing machining parameters for minimum cost, optimizing the machining parameter for Production rate.

Chapter 4 describes planning and details of experiments carried out for the present work. It presents the planning and designing main experiment.

Chapter 5 presents experimental results and their analysis focusing on the effects of machining parameters (cutting velocity, feed rate and depth of cut) on the surface roughness, machining forces, maximum flank wear, chips thickness and their morphology. It also presents analysis of variance ANOVA for outcomes results.

Chapter 6 highlights the conclusions derived from the present work and scope for future work based on the limitations of the present work.

Chapter 1

Introduction

1.1 Concept of Machinability

Machinability is tentatively defined as 'ability of being machined' or the ease of removal of material from the workpiece to an expected surface finish. It is property of a material characterizing its ability to be machined easily while removing extra material to shape it into an engineering component **(Das *et al*., 2015).** Machining performance of a material can determined by machinability. Following factors highlight of importance of machinability of a material:

- Machining process is associated with severe deformation, which results in high energy consumption, high local temperatures and wear of the cutting tool. Some of the new high performance tool steels are difficult-to-machine. Machining dominates the cost in tool production. Hence, enhanced machinability would reduce the cost of machining operations through less cutting tool consumption, power consumption and operation time (**Suresh *et al***., **2012**).
- Engineering industries strive to achieve either a minimum cost of production or a maximum production rate in machining. Use of high speed machining has become more relevant in recent years i.e. cutting velocities have increased many folds than normal speeds. Thus, it is becoming increasingly necessary to relate the available engineering raw materials and semi-finished products to specify machinability ratings. It is advantageous for the industries to know in advance the behavior of wear and tool life with respect to specific steel grades which needs to be processed (**Noordin *et al.*, 2003**).
- Good machinability is a critical requirement to extend the market share and identify new applications for through hardened low alloyed martensitic steels. The market for these steels is mainly in the tool and molds industry and hence good machinability is economically very attractive. It is proposed present the results from the machinability study of such steels at two hardness levels and compare with the machinability of commercially available steels aimed at the same market (**Isik *et al.*, 2007**).

1.2 Evaluation of Machinability

Overall goal of machining is to remove a certain volume of material at highest possible rate with as low cost as possible. Good machinability is defined as a combination of low power consumption, low tool wear and good surface finish. Machinability can be judged by following criteria:

- **Tool life criterion:** Tool life criterion is expressed as cutting speed for a given tool life. Machinability of a material is also defined by the relative cutting speed for a given tool life of the tool machining that material compared to a standard material machined with the same tool material. Tool life is one important factor in metal cutting from an economical point of view and has been used as machinability criterion in the present work.
- **Production rate criterion:** If tool life is expressed in terms of MRR then production rate may be taken as machinability criterion. Higher the cutting speed for a given tool life, greater will be MRR and higher will be production rate. Surface finish could be considered by altering the cutting conditions to obtain the best production rate for a fixed tool life and required surface finish.
- **Power consumption criterion:** Power consumption criterion is related to machining forces and cutting velocity.
  - A material requiring high cutting force (higher power consumption and higher production cost) will have lower machinability index.
  - Limiting the cutting force is necessary to avoid excessive vibration and chatter during machining.
  - Generically the cutting force acting in each of the speed directions contributes to the power consumption P during a cutting process.
  - Conventionally, the cutting force occurring during any machining operations is decomposed into three components namely the main cutting force F_c, feed force F_f and radial force F_r. Figure 1.1 depicts these cutting forces.
  - The required motor power of the machine tool during any machining operation is always greater than the energy consumed by the cutting process.
- **Surface finish criterion:** Some materials may permit higher cutting or induce lower cutting forces but give poor surface finish.
  - Evaluation of a machined surface can be divided into two parts, surface finish and surface integrity.
  - The term surface finish is commonly used in order to describe the geometric features of a surface while surface integrity has a wider definition also pertaining to all

material properties influenced by the machined surface such as fatigue life, corrosion resistance, residual stresses, etc.

- The arithmetic mean surface roughness R_a is one of the most commonly used in industry. Other common definitions include the maximum peak-to-valley surface roughness R_{max} as well as the slightly modified mean peak-to-valley surface roughness R_z.
- A material that produces better surface finish under a given set of conditions may be considered to have better machinability rating.

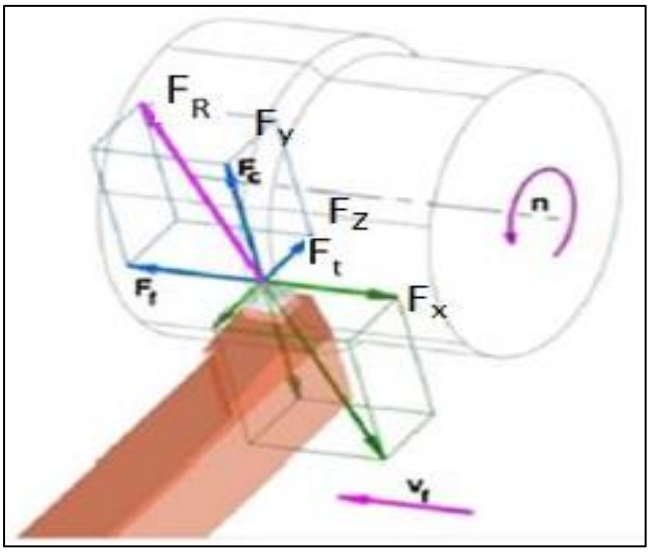

Fig. 1.1: Schematic three machining forces.

In some cases these four criteria may not be sufficient to describe the machinability of a material and therefore other criteria like friction coefficient, cutting temperatures, layer formation, rim zone properties or built-up edge formation have to be taken into account. However, these criteria are closely linked to the four main evaluation criteria and therefore they should not be considered as separate machinability measures. Sometimes some phenomena influencing these evaluation criteria are also considered. Since, machining of free cutting steels is often performed on multi-spindle machines and auto lathes, the applicable rotational speeds are low. In combination with small workpiece diameters this results in low cutting speeds. Subsequently, the formation of built-up edges (BUE) may have strong impact on tool life and surface quality. Further, the cutting temperatures have to be considered as chip formation, tool life, cutting force and dimensional quality depend on cutting temperatures. Temperatures on the rake of the tool also may give information about the tribological conditions in the contact zones of tool and workpiece. Another important phenomenon is formation of built-up edge of various chemical compositions on flank and rake faces of cutting tools which may result in a reduction of cutting forces and temperatures and consequently reduce tool wear.

1.3 Factors Influencing Machinability

Factors affecting the machinability are:

- Mechanical properties of the material such as shear strength, strain hardening, hardness, toughness, wear resistance, thermal conductivity, microstructure
- Physical properties
- Chemical composition of the material
- Shape and size of workpiece
- Machining parameter namely cutting speed, feed and depth of cut

1.4 Improving Machinability

Machinability of a material can be improved by:

- Optimizing the machining parameters
- Reducing cutting forces and power consumption
- Reducing tool wear or increasing tool life
- Increasing material removal rate
- Improving surface finish produced i.e. reducing parameters of surface roughness
- Improving dimensional accuracy or tolerance
- Making chips uniform or short
- Making disposal of chips easy.
- Reducing tendency of built up edge (BUE) formation

1.5 Importance of Machinability of Alloy Steel

Nickel based alloy steel AISI 4340 has the combined properties of high mechanical strength and high heat and corrosion resistance at an elevated temperature. Table 1.1 presents chemical composition of this alloy steel. The austenite nickel matrix reacts with Chromium (Cr), Cobalt (Co), Molybdenum (Mo), Sulphur (S) to become alloy. Chromium present in the alloy reacts with the oxygen present in the air and form a protective scale layer of Chromium Oxide (Cr_2O_3). This protective layer prevents outward diffusion of metallic element. Molybdenum helps for solid solution strengthening at elevated temperature. Precipitation hardening also strengthens the nickel based super alloy with silicon.

Table 1.1: Chemical composition of AISI- 4340 alloy steel.

Elements	Fe	Ni	Cr	Mn	C	Mo	Si	S	P
Wt. %	95.19	1.65	0.70	0.60	0.370	0.20	0.150	0.040	0.035

Table 1.2 present physical and mechanical properties of AISI 4340 alloy steel which has superior mechanical properties, high strength and corrosion resistance for which it is widely used in following applications

- Suitable for shock loading or stress concentration applications such as shafts, gears, bolts, nuts, pins and couplings
- Aerospace components such as aircraft landing gear, shafts and other
- Power transmission gears
- Gas turbine blades
- Exhaust valve in internal combustion engines
- Submarines
- Structural applications

Table 1.2: Physical and mechanical properties of AISI 4340 alloy steel.

Property	**Value**
Density	7.85 g/cm^3
Melting point	1427°C
Coefficient of thermal expansion (20°C specimen oil hardened 600°C temper	12.3 µm/m°C
Thermal conductivity	44.5W/mK
Shear modulus	80 GPa
Elastic modulus	190-210 GPa
Poisson's ratio	0.27-0.30
Elongation at break	22%
Reduction of area	50%
Hardness, Brinell	264
Hardness, Knoop (converted from Brinell hardness)	240
Hardness, Rockwell B (converted from Brinell hardness)	95
Hardness, Rockwell C (Converted from Brinell hardness. Value below normal HRC range for comparison purposes only)	25
Hardness, Vickers (converted from Brinell hardness)	288
Machinability (annealed and cold drawn. Based on 100 machinability For AISI1212 steel.)	50

1.5.1 Challenges in Machining AISI 4340 Alloy Steel

Casting, forging and other advanced technique are used to manufacture components from nickel based AISI 4340 alloy steel. It is quite difficult to machine intricate shaped components from this alloy steel due to following reasons:

- During machining high strength and hot hardness of AISI 4340 alloy cause deformation of cutting tool.
- The workpiece get welded with the cutting tool edge resulting unstable build up edge formation, which hamper the surface roughness of workpiece during machining.
- Presences of the abrasive particle in the microstructure resulting rapid tool wear due to the different wear mechanism.
- The combined properties of mechanical strength and resistance to corrosion at elevated temperature of AISI 4340 alloy steel resulting poor machinability.

During machining precision is required in terms of surface finish, shape with the minimal removal of material from the workpiece to achieve economic benefit. Machinability of steels is affected by many factors such as machining process, cutting tool geometry, cutting fluid type, machining parameters namely cutting speed, feed and depth of cut, rigidity of tool holder and machine tool. Therefore, assessment of the machinability of steel becomes a matter of prime activity to make proper decision and improve its productivity. Machinability can be improved using optimum machining parameters, different cutting tools, proper heat treatment and alloying of the alloy steel. Coated carbide insert tool provide a bit better machinability.

1.6 Cutting Tool Materials

During machining AISI 4340 alloy steel the cutting tool is subjected to extreme mechanical and thermal stress near to the cutting tool which accelerate tool wear. Notching at the nose and depth of cut line, flank wear, crater wear, chipping are the typically observed tool failure. To overcome this challenges the cutting tool should have enough hot hardness to withstand high temperature during high speed condition. Coated carbide tool, ceramic, CBN/PCBN tool are generally used for high speed machining of AISI 4340 alloy steel while uncoated carbide tool are used for low speed machining condition. Effective machining of workpiece can be achieved depending up on the type of cutting tool material used while machining

1.6.1 Different Cutting Tool Materials

There are different types of cutting tool material (**Rao, P.N and Mehta, N.K.)** discussed given below:

1.6.1.1 Coated and uncoated carbide tool

Straight and mixed grade carbide are two often used carbide tool material for commercial machining purpose. The straight carbide tool has cobalt 6% by weight, 94% WC with the range of cobalt 5-15 %. The mixed grade carbide is Titanium carbide (TiC), tantalum carbide (TaC). Titanium carbide improves the wear resistance of carbide tool. The tough ness of the carbide id reduced with the increase concentration of titanium. The hot hardness of the tool can be improved with inclusion of tantalum carbide. The plastic deformation can be prevented while machining at high speed. High cobalt content and coarse grain tungsten carbide are required to resist high shock. The performance of the cutting tool can be achieved using ceramic coating. They have high temperature resistance property and resistance to diffusion wear, high hot hardness, oxidation wear resistance. The lowering cutting temperature during machining can be achieved due to the improved lubricating properties of chip –tool and toll-workpiece interface. Higher cutting speed also achieved using coated ceramic tool.

1.6.1.2 HSS (High speed steel)

High carbon ferrous alloy with the constituent of Cr, Co, W, Mo and V. In the form of Cast, wrought and sintered (using power metallurgy technique) HSS are available. It is of less expansive compared to other cutting tool material. Fracture toughness and fatigue resistance were the feature properties of HSS. It is applicable for a short range of velocity i.e. 30-50 m/min due to its limited wear resistance and chemical stability. It is classified depending up on the dominating alloying element T-type steels having tungsten as the dominant alloying element and M-type steels molybdenum is the dominant alloying element.

1.6.1.3 Cemented carbide

Mixing, compacting and sintering are the process of manufacturing cemented carbide cutting tool material .In case of Sintering process primarily tungsten carbide (WC) and cobalt (Co) powders were used. For tungsten carbide (WC) grain Co acts as a binder. The carbide tool has good electrical and thermal conductivity as they have strong metallic character. These cutting tools are chemically stable. They possess high stiffness and lower friction, and operate at higher cutting velocities compared to HSS. This material is expansive and brittle in nature. Generally used for machining gray cast iron, nonmetallic material and nonferrous metal. M grade carbides are alloyed with tungsten carbide (WC) to have the application in machining austenitic stainless steel. The maximum hardness and toughness position of a material is achieved from the number assigned to grade with in a group. P grades are rated from P01 to P50, M grades from M10 to M40, and K grades from K01 to K40. Cobalt percentage and grain size of carbide determine the performance of carbide cutting tool.

1.6.1.4 Cermet

Cermets are ceramic material in metallic binder. Co and Mo are the softer binder which held the constituent hard particles of TiC, TiN, or TiCN. These materials are operated on high cutting velocities and hence suitable for machining steel, cast iron. They possess lower thermal conductivity and resistance to fracture.

1.6.1.5 Ceramics

Ceramic are nonmetallic material and subjected to extreme temperature during machining. The uniqueness of this type material is to retain the stiffness and hardness of the material at elevated temperature equal to 1000° C.

Basically two types of ceramic tool available for commercial machining purpose

- Alumina-based ceramics which consists of pure oxide, mixed oxides, and silicon carbide (SiC) whisker reinforced alumina ceramics.
- Silicon nitride-based ceramics.

1.6.2 Tool Wear

Machining for a prolonged period the cutting tool destroyed due to high strength and temperature resistance of workpiece major tool wear studied during machining were discussed below:

1.6.2.1 Crater Wear

During machining chip slide over the tool face resulting formation of concave section in the chip tool interface .Crater wear increase rake angle resulting easier machining but simultaneously it reduces the strength of cutting tool which influences tool failure during machining.

1.6.2.2 Flank Wear

The friction between workpiece surface and tool flank resulting flank wear at the tool flank. It generally appears in the form of wear land which affects machining. The increase in flank wear resulting in cutting forces which in excess resulting tool failure. VB (flank wear>0.3mm) tool failure occur.

1.6.2.3 Corner Wear

This tool wear took place in the tool corner.it is also called a part of wear land as there were no definite boundary between flank wear land and corner wear. The reduction of cutting tool length results in increase in the dimension of machined surface gradually Apart from this wear other types of wear are present, these were:

• **Adhesion wear:** The fragment of workpiece welded with tool surface at high temperature during machining is called adhesion wear.

• **Abrasion wear:** The bottom part of chip rub against the tool surface and part of it is break away which is called abrasive wear.

• **Diffusion wear:** Chip and tool diffuses during machining is called diffusion wear.

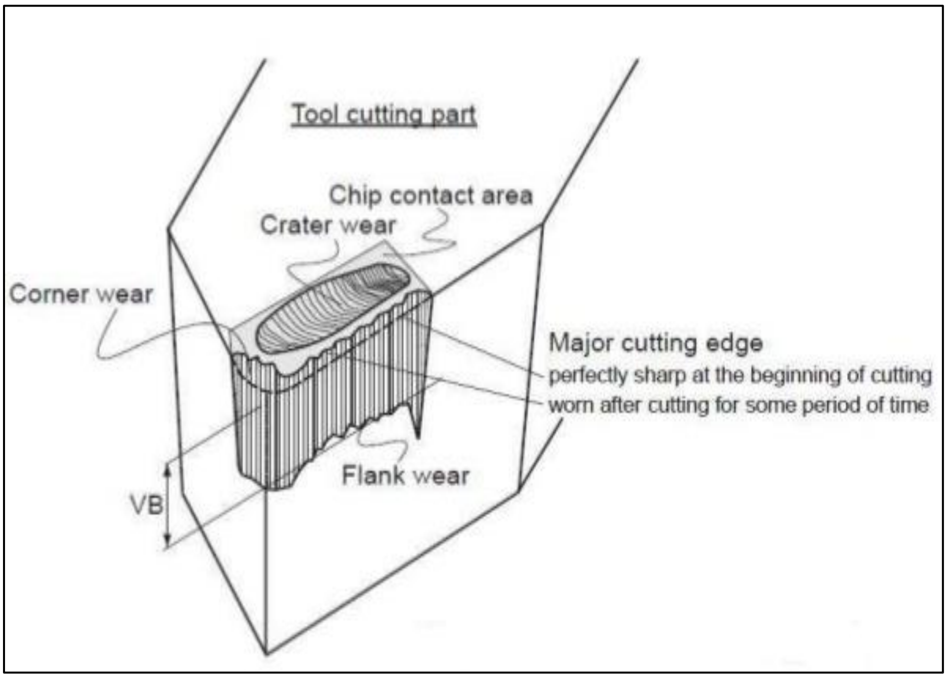

Fig. 1.2: Different type of tool wear.

1.6.3 Tools Insert Designation

Tool insert designation is Coated carbide tools insert (KENNAMETAL) SCMT 12 04 08 (ISO DESIGNATION).

S = Insert shape (square)

C= Clearance angle (6º)

M = Tolerance

T = Insert type

12 = Cutting edge length

04 = Insert thickness

08 = Nose radius.

1.6.4 Description of tool geometry

There are some points about tool geometry discussed given below:

- **Shank:** It is main body of tool. The shank used to grip in tool holder.
- **Flank:** The surface or surface below the adjacent of the cutting edge is called flank of the tool.
- **Face:** It is top surface of the tool along which the chips slides.
- **Base:** It is actually a bearing surface of the tool when it is held in tool holder or clamped directly in a tool post.
- **Heel:** It is the intersection of the flank & base of the tool. It is curved portion at the bottom of the tool.
- **Nose:** It is the point where side cutting edge & base cutting edge intersect.
- **Cutting edge:** It is the edge on face of the tool which removes the material from work piece. The cutting edges are side cutting edge (major cutting edge) & end cutting edge (minor cutting edge)
- **Tool angles:** Tool angles have great importance. The tool with proper angle, reduce breaking of tool, cut metal more efficiently, generate less heat.
- **Noise radius:** It provide long life & good surface finish sharp point on nose is highly stressed, & leaves grooves in the path of cut longer nose radius produce chatter.

1.6.5 Tool signature:

Coated carbide tool insert with CVD multilayer coating consisting of ($Ti/TiCN/Al_2O_3/ZrCN$) ISO SCMT120408 (KENNAMETAL).

[-6°,-6°, 6°, 6°, 15°, 75°, 0.8 {mm}] ASA or ANSI {American system association}

Where,

-6° = Back rake angle

-6° = Side rake angle

6° = End clearance angle

6° = Side clearance angle

15° = End cutting edge angle

15° = Side cutting edge angle

75° = Approach angle

0.8(mm) = Nose radius.

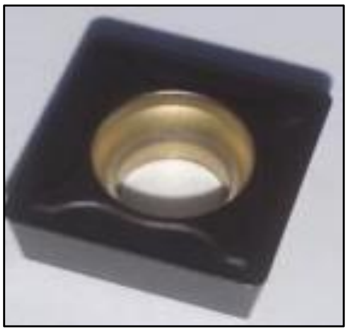

Fig. 1.3: Coated carbide insert

- **Back rack angle α_b:** It is the angle between the face of the tool and the face of the shank or holder, and is usually measured in a plane perpendicular to the base and parallel to the length of the tool. It affects the ability of the tool to shear the work material and form the chip. In turning positive back rack angle takes the chips away from the machined surface, whereas negative back rack angle directs the chip on to the machined surface.
- **Side rack angle α_s:** It is the angle between the face of the tool and the base of the shank or holder and is usually measured in a plane perpendicular to the base and parallel to the width. Increase in the side rack angle reduces the chip thickness in turning.
- **End relief angle δ_e:** It is the angle between the portion of the end flank immediately below the end cutting edge and a line draw through this cutting edge perpendicular to the base. It is usually measured in a plane perpendicular to the end flank. The end relief angle prevents friction on the flank of the tool.
- **Side relief angle δ_s:** It is the angle between the portion of the side flank immediately below the side cutting edge and a line drawn through this cutting edge perpendicular to the base. It is measured in a plane perpendicular to the side flank.
- **End cutting edge angle γ_e:** The end cutting edge angle is the amount is that the end cutting edge slopes away from the nose of the tool, so that it will clear the finished surface on the workpiece, when cutting with the side cutting edge. It prevents the trailing end of the cutting edge of tool from rubbing against the workpiece (due to wear out). A larger end cutting edge angle weakens the tool.
- **Side cutting edge angle γ_s:** It is the angle which prevents interference as the tool enters the work materials. Larger this angle greater the component of forces tending to separates the work and the tool (may in due chatter) i.e. chattering effects. At its increased values it will have more of its length in action for a given depth of cut and also its increased value it produce thinner and wider chip that will distributes the cutting heat (increase tool life). Side

cutting edge angle has no effects on cutting force and cutting power consumptions. Zero is desirable when machining casting and forging with hard and scaly skins, because of the least amount of tool edge should be expressed to the distribution action of the skin.

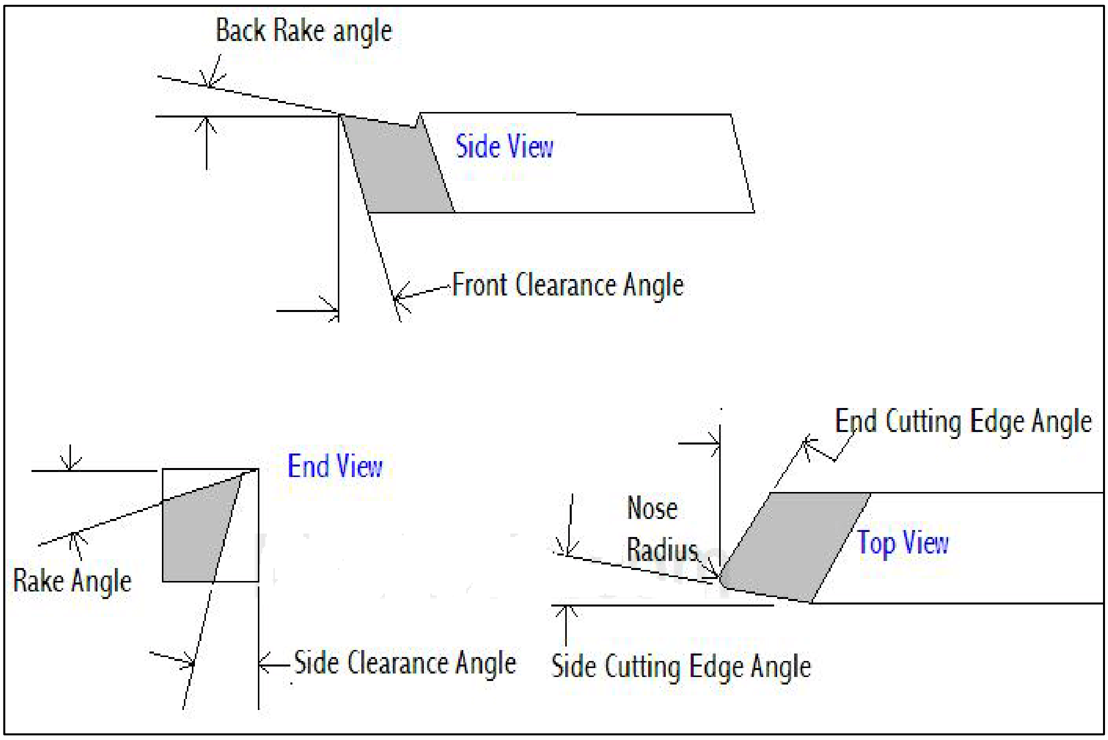

(a)

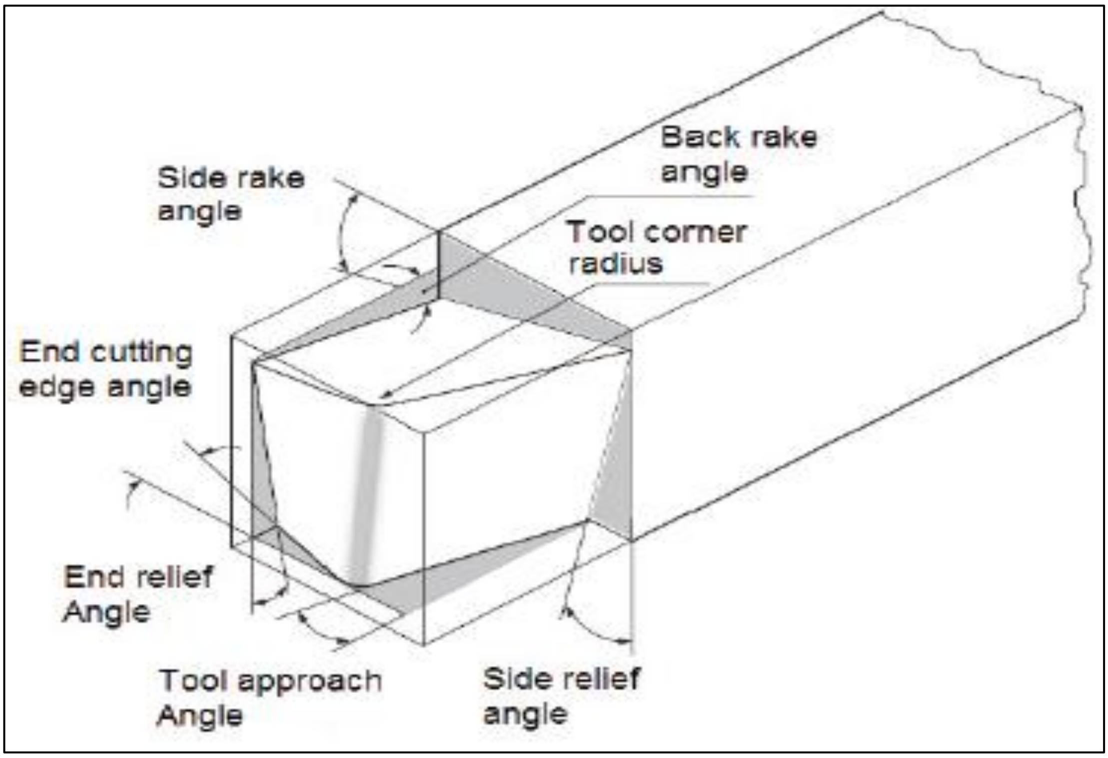

(b)

Fig. 1.4: (a) and (b) Represent different type of tool angles.

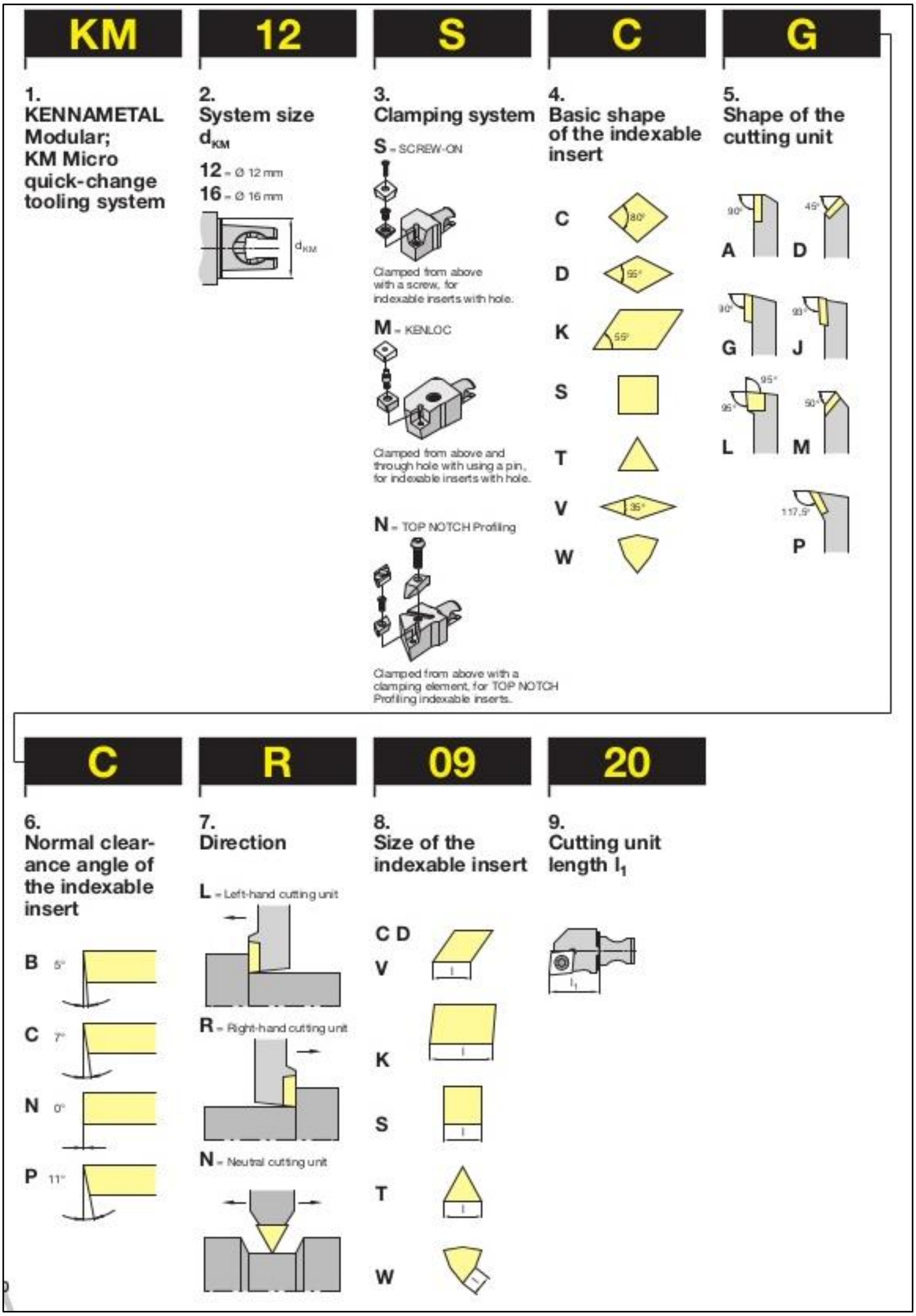

Fig. 1.5: Designation code of tool insert.

1.7.6 Tool holder designation:

Tool holder designation is ISO DESIGNATION (KENNAMETAL) SSBCR2020K12.

Where,

S= Clamping method

S= Insert shape

B = Style

C = Clearance or relief angle

R = Cutting direction

20 = Tool holder shank height

20 = Shank width

K = Tool holder length

12 = Cutting edge length

Fig. 1.6: Tool holder images.

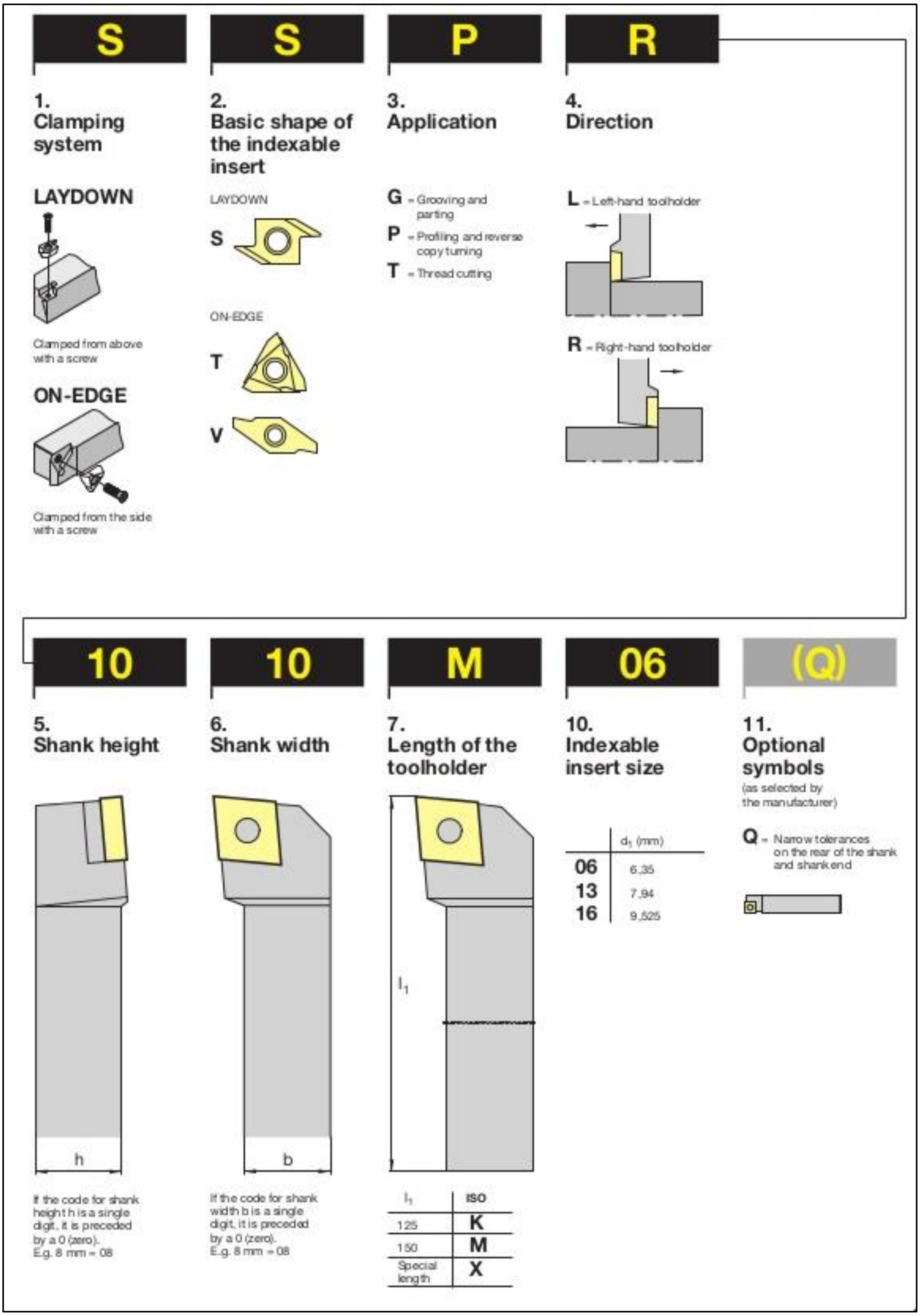

Fig. 1.7: Designation code of tool holder.

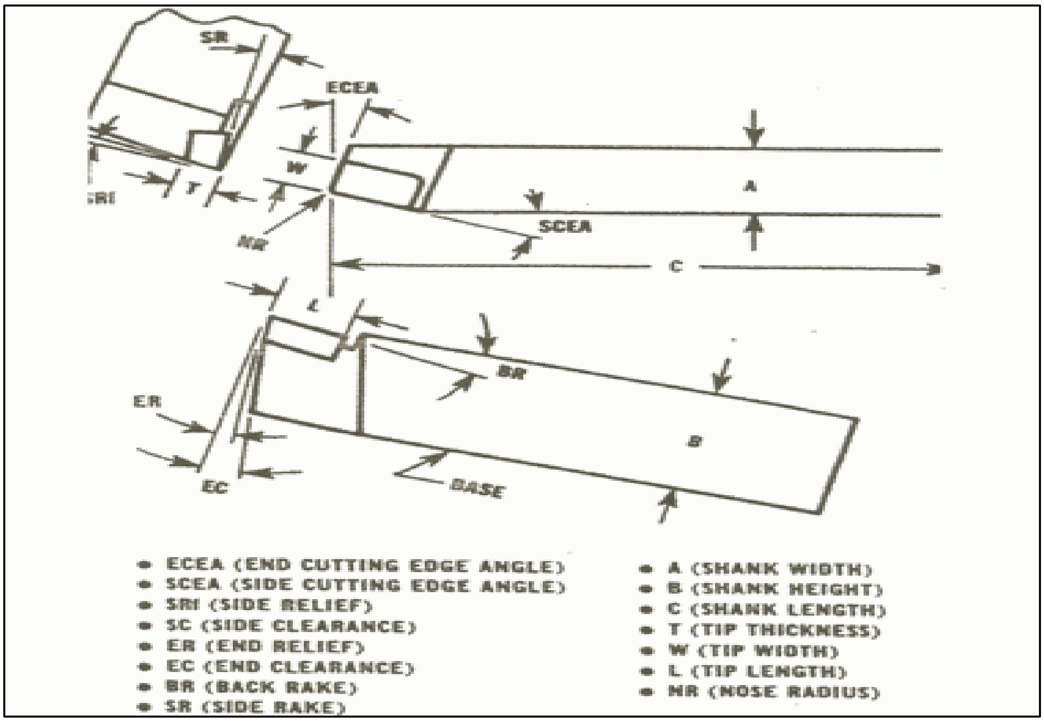

Fig. 1.8: Schematic assembly of tool inserts and tool holder for viewing angles.

Next Chapter presents review of the past works done in this field, research gaps identified, research objective of the present work and research methodology used to meet them.

Chapter 2

Review of Past Work and Research Objectives

2.1 Review of Past Work

Several experiment studies have been executed in order to determine the influence of various process parameters on the surface roughness, tool wear, chip morphology and machining forces using different workpieces and tool insert during machining process.

2.1.1 Effect of cutting parameter on surface roughness

Mashal *et al.* (2001) carried out the interaction and effects of machining parameters, namely, feed rates, cutting speed and depth of cut on the average surface roughness of Al–8Fe–4Ce were studied during cutting operation. Response surface methodology was used to improve the experimentation design. The interaction and effect of the cutting parameters on the response (R_a) were reported. It was found that combining small depth of cut and small feed rates with high cutting speed caused a significant reduction in R_a.

Das *et al*. (2014) observed the hard turning has been performed successfully to obtain finish surface on AISI 4140 steel using PVD TiN coated Al_2O_3+ TiCN mixed ceramic inserts under dry environment. The process parameters are optimally controlled in order to compose the lower surface roughness with minimal flank wear from the experimental investigation and modeling. Taguchi's OA design coupled with response surface methodology (RSM) which is employed in this investigation established to be an efficient tool for machinability evaluation. For AISI 4140 steel roughness, the machined surface is a function of the wear profile of TiN coated ceramic insert. When increasing cutting speed, flank wear (*VB*) of the tool insert increases and causes immediate deterioration of the machined surface quality. Despite the growth of flank wear up to permissible limit (*VB* = 0.3 mm), R_a does not exceed the 1.6 µm. The extensive experimental research shows the effectiveness and potential of PVD-TiN coated Al_2O_3+TiCN mixed ceramic tool for hard turning process under dry condition as a productive and cost-effective option to replace the cylindrical grinding operations. This experimental investigation helped in explaining the machined surface characterization of AISI 4140 steel, wear mechanism of coated mixed ceramic tools and chip formation mechanism of generated chips during hard turning under various cutting conditions, which will give valuable knowledge to manufacturers in proper selection of cutting parameters.

Sornakumar *et al.* (2008) studied bronze–alumina composite was developed using stir-casting method. The machining experiments were performed on bronze and bronze–alumina composite using a tungsten carbide tool insert. The flank wear of carbide tool is higher on machining of bronze–alumina composite than on machining bronze. The surface roughness produced on the bronze and the bronze–alumina composite after machining with the carbide tool was compared. Surface roughness produced on the bronze–alumina composite is higher than that on the bronze. The cutting force encountered during machining of bronze and bronze–alumina composite decreases with increasing cutting speed. The bronze–alumina composite underwent higher cutting force than the bronze. In summary, the bronze–alumina composite was developed and its machinability evaluated and it compares well with bronze.

2.1.2 Past Work for tool life

Yahya Isik (2007) observed that the experiments concerning the relationship between the tool life and the tool wear, it was observed that amongst all wear types flank wear was the most encountered wear type. No crater wear was detected. The results related to tool wear are such that wear rate slows down after the rapid increase at the beginning and starts to increase linearly. When the tool approaches the end of tool life, the wear rate increases rapidly again and if the cutting is carried on, the tool fractures. In turning operations, feed rate is the most influential parameter on surface roughness, cutting depth is the second most one, and cutting speed is the least influential parameter. The influence of cutting speed is negligible compared with those of the other cutting parameters. In the experiments which were conducted by using coated tools, it was observed that the flank wear is a more influential parameter for the fracture than the crater wear. There is a direct relationship between cutting forces and flank wear. Therefore, with the help of a model that will be developed, operator can obtain information related to the probability of tool fracture, through the analysis of the wear amount. But it is always possible that the tool fracture occurs unexpectedly.

Jawaid *et al.* (2000) studied the conclusions drawn from the face milling of titanium alloy Ti-6Al-4V with PVD-TiN and CVD-TiCN+Al_2O_3 coated carbide inserts are used. The best cutting conditions with respect to the highest tool life of 30 min was achieved by both the PVD and the CVD tools at the cutting speed of 55 m/min and a feed of 0.1 mm per tooth. However, when considering the volume of material removed, the CVD tool produced the highest volume of 503 cm^3 at a cutting speed of 55 m/min and a feed of 0.15 mm per tooth. Generally, the CVD coated tool outperformed the PVD coated tool in most cases when face milling Ti-6Al-4V. Non-uniform flank wear was the dominant wear pattern exhibited by both the PVD and CVD tools. Excessive chipping at the cutting edge and flaking and/or chipping on the rake face were the dominant failure modes. Plastic deformation of the cutting edge was also found, along with an observed wear mechanism, for most cutting conditions. Coating delamination, galling on the rake face and adhesion of work material at the cutting edge were responsible for the initial wear mechanism for both of the coated tools. Attrition and diffusion wear mechanisms were responsible for the flank and rake face wear of both of the coated tools. Evidence of the diffusion of cobalt and tungsten into the adhered workpiece was found at the flank and rake faces of the tools. The thermal cracks observed were thought to be responsible for the severe chipping and/or flaking of the inserts at both the rake and flank faces.

Salak *et al*. (2006) observed that the short time face turning is presented as a new method for machinability testing of PM steels, using common ring-shaped test specimens and performed at constant revolution of the lathe. This method represents a contemporary interrupted-cut method (tool entry–exit) which machining mode is frequent in powder metallurgy. The increase of apparent hardness of the machined surfaces and of microhardness of machined subsurface areas, as the consequence of the deformation and work hardening caused by turning was demonstrated. The presented face turning method is easy and simple, fulfilling many of the criteria for the characterization of machinability of the PM materials in relation to the tool material and geometry and/or cutting conditions

2.1.3 Past work for machining forces

Medvedeva *et al.* (2011) studied the machinability of the steels of varying nickel content from 1 to 5 wt.% was estimated in the prehardened condition in end milling and drilling operations. The machinability was characterized by measuring the cutting forces, and estimation of tool/chip interface temperature. Nickel content showed to have a strong influence on the machinability of the hot-work tool steel. The steels with higher nickel content exhibited considerably higher tool life with respect to flank wear and number of produced holes in end milling and drilling, respectively. The difference in machinability was related to the nickel influence on the steel microstructure and mechanical properties. In end milling, machining the lower nickel containing steels generated higher cutting forces and temperatures, which promoted the material adhesion to the cutting edge and easier built up edge formation. As a consequence, the tool wear accelerated resulting in a more rapid failure. The decrease in cutting forces with nickel content was mainly related to the decrease of the elevated temperature yield strength. In drilling, the main reason for longer tool life is considered to be lower thrust forces when drilling the steels with higher nickel content. The reduced forces are the result of lower yield strength of these materials and improved chip breaking by fine dispersed carbides in their microstructure.

Halil *et al.* (2009) carried out in this work, the machinability behavior of solution heat treated (SHT) and solution heat treated and aged (SHTA) 6061 Al-alloy was studied in artificially aged conditions. Turning tests were performed on the as-received, SHT and SHTA workpieces using multilayer coated cemented carbide tools. The conclusions derived from this study the variation in the cutting forces depending on the workpiece aging heat treatment are not very prominent. The most prominent variation is seen at low cutting speeds in the machining of SHT workpieces which had the lowest hardness among the others due to quenching after solution heat treatment. The cutting forces drop generally with increasing cutting speed for all the workpieces. These drops in the forces are partly caused by a decrease in tool-chip contact area and partly by a drop in shear strength in the flow-zone as the temperature rises with increasing cutting speed.

S. To *et al.* (2013) studied experimental on the enhancement effect of hydrogen ion implantation on the machinability of silicon. The improved machinability of silicon is verified in the machined groove characteristics of the three distinct cutting zones and the semi-quantitative analysis of cutting force signals with power spectrum density analysis. The developed power spectrum density analysis method is effective to capture the ductile/brittle cutting characteristics. This paper provides a novel approach for surface modification of silicon wafer for ductile-regime cutting with the improved machinability.

2.1.4 Past Work for tool wear

Paulo *et al.* (2007) observed the cutting parameters used and the characterization of the machinability evaluation in hard turning of cold tool work steel (D2) using ceramic tools. The tool wear is highly influenced by the cutting velocity (57.4%) and in a smaller degree by cutting time (13.4%). The excessive flank tool wear existent in the ceramic tools which works with high cutting velocity has a correspondent reduction on surface roughness. The specific cutting pressure is strongly influenced by the feed rate (64.1%). The surface roughness is influenced by feed rate (29.6%) and cutting time (32%).

Zedan e*t al.* (2013) studied the drilling tests, maximum wear takes place at the outer corner edge of the drill, whereas minimum wear occurs at or near the point of the drill tip. When the corners of the drill are rounded off, the drill then sticks to the workpiece and breaks if the cutting process is not halted in time. The chip breakability of the alloys containing Al_2Cu phase is superior to that of the alloys containing Mg_2Si. Thus combined additions of Cu and Mg are expected to further refine the size of the chips produced**.**

Rajshekhar *et al*. (2014) observed the face turning method presented here for tool wear development of bearing steels represents the contemporary machining involving interrupted cuts and the development of tool wear and machinability aspects for the two work-materials is in line with traditional longitudinal turning method. Behavior of wear mechanism of carbide tool for the said steels is in good agreement with the published literature. The face turning method demonstrated good sensitivity even for slight change in the percentage of chemical compositions of carbon, manganese, and chromium in these steels. The SEM and surface profile investigations reveal varying effect of alloying elements (namely chromium in AISI 52100) on machinability. The face turning method of machinability test can be used to monitor engineered changes in industries to improve machinability, as development of tool wear for the two work materials is in line with traditional machining methods. The machinability of AISI 51100 is better than AISI 52100, considering tool wear, surface finish and chip morphology.

Persson *et al.* (2001) studied the face milling test using round cemented carbide inserts in a test mode comparable to that in the available standard to grade the machinability of low alloyed martensitic steels. For the considered class of martensitic steel alloys, good correlation between bulk hardness and milling machinability was observed. Within the group of steels in the hardness range of 310 to 340 HV30, the new grade TOOLOX 33 displayed the best machinability, exceeding the commercial grades CS1 by almost 300% and CS2 by 80% at a cutting speed of 350 m/min. In general all wear results displayed scatter for flank wear > 0.1 mm probably due to the milling mode and associated wear mechanisms.

2.1.5 Past work on chip characteristics

Thakur *et al.* (2014) investigated the influence of cutting speed and tool coating on chip characteristics and tool wear during dry machining of Inconel 825. In this study loose arc and connected arc type of chips were obtained at lower cutting speed, (i.e. V_c = 51 m/min). Increase in cutting speed combined with progression of machining duration resulted in continuous snarled ribbon like chips and serrated chips. Chips formed during dry machining of Inconel 825 were characterized by lateral flow and shear cracks. The lateral flow of material and shear cracks increased with increase in cutting speed. CVD multilayer coated tool resulted in the reduction of both side flow as well as severity in shear cracks. There is a general trend of decrease in chip thickness ratio except at low cutting speed. The difference between chip thickness ratio obtained after machining with uncoated and coated tools was less. However, coated tool exhibited a marginally lower value in the entire range of cutting speed. Tool wear during dry machining of Inconel 825 was characterized by adhesion, plastic deformation, diffusion, and catastrophic failure. The average flank wear increased with both cutting speed as well as machining duration.

The multilayer coating consisting of TiN+TiCN+Al_2O_3+ZrCN plays a major role in improving resistance to wear particularly at higher cutting velocity. The uncoated tool suffered catastrophic failure at high cutting speed (i.e. V_c = 124 m/min.) only after 150 s of machining. The same uncoated cemented carbide insert resulted in favorable machinability characteristics in terms of chip formation and tool wear at 51 m/min. The machined surface quality obtained after machining with coated tool was clearly superior compared to that with its uncoated counterpart. The thickness of deformed layer obtained during machining with the multilayer coated tool was significantly lower than that obtained with the uncoated tool.

Sivaramana *et al.* (2012) investigated the influence of cutting parameters such as cutting speed, feed rate and depth of cut on chip morphology and cutting forces. The multi-phase micro-alloyed steel having a yield strength of 1384 MPa recorded less cutting force as compared to existing high strength low alloy steel (HSLA). This shows better machinability for FBM steel. Chips formed were similar to the chips obtained during machining of HSLA steel and saw tooth formation was observed.

2.1.6 Past work for selection of workpiece material and machining process

Rajshekhar *et al.* (2013) studied the ensuing tool-work pair combination, the face turning operation has favorably exhibited as a method to determine the machinability of low alloy steels. The face turning method presented here for tool wear development of low alloy steels represents the contemporary machining involving interrupted cuts and the development of tool wear and machinability aspects for the two work-materials is in line with traditional longitudinal turning method. Also behavior of wear mechanism of carbide tool for the said steels is in good agreement with the published literature. The face turning method of machinability test can be used to monitor engineered changes in industries to improve machinability, as the development of tool wear for the two work materials is in line with traditional machining methods. The machinability of AISI 9320 is better than AISI 4340, considering tool wear, surface finish and chip morphology. The proposed tool life equations for the AISI 9320 and AISI 4340 are validated. The experimental uncertainty of tool life lies within limit of ±5%. The face turning method is simple and effective means to characterize machinability of steels.

Nourredine *et al.* (2003**)** observed that the result of this study shows that the developed machinability indicators provide a number advantage. A cost of effective method for machinability testing. Future research efforts include the development of a methodology to rank more than two materials at a time, in order of machinability. This will include the development of a computerized database, in which the user would only need to select the material needed for evaluation, the desired cutting condition, and corresponding weights in the computation.

Yusuf *et al.* (2003) mentioned that optimum machinability was achieved only on the microstructure of 90 mm diameter SAE 1050 steel as hot rolled. The heat treatments of annealing and normalizing applied to this steel reduced the tool life and machinability rating. No significant correlation between the mechanical properties, such as hardness and tensile strength, and machinability could be observed. Especially, the effects of microscopic heterogeneity of the phase distribution (e.g. ferrite þ pearlite banding) on tool life make the mechanical properties-tool life relations indefinite. While the increase in the BUE sizes especially, at the lower cutting speeds is determined together with the decrease in the hardness of specimen these cause the surface roughness to get worse. It is observed that heat treatments did not affect the cutting forces significantly. However, the minimum horizontal force was observed during cutting the low hardness steel at the ultimate cutting speeds.

2.2 Identified Research Gaps

From the literature review it can be concluded that:

- Very limited work has been done for selection of optimized input machining parameter (feed, cutting velocity and depth of cut) before performing the experiment.
- No work has been done on optimization of the machining parameter considering depth of cut for evaluation of optimum cutting velocity, feed rate and tool life etc. for condition of minimum cost and maximum production.
- Limited work has been done on combination of AISI 4310 alloy steel workpiece material with CVD coated carbide tool insert for particular given tool signature.
- There is lot of scope to understand machining or metal cutting process of different grades of alloy steel workpiece using several tool material obtain better quality of machinability.

2.3. Objective of the Present Work

Present research work was undertaken with the following research objectives defined on the basis of the research gaps:

- Improving machinability of AISI 4340 alloy steel cylindrical workpiece.
- Optimization of three machining parameters considering depth of cut for evaluation of optimum cutting velocity, feed rate and tool life etc. for condition of for minimum cost and maximum production.

- Annealing of AISI 4340 alloy steel workpiece at 500 °C for 2 hour and furnace cooled for 24 hour to develop coarse pearlite structure for reducing cutting forces.
- Experiments using soft turning of annealed AISI 4340 alloy steel using coated carbide CVD deposited multilayer coating of $TiN/TiCN/Al_2O_3/ZrCN$ tool to study effects of cutting velocity, feed rate and depth of cut on surface roughness, machining forces, flank wear and chip morphology as measure of machinability.
- To find significant parameters using ANOVA analysis of the experimental results.

2.4 Research Methodology

Fig.2.1 presents the research methodology used in the present work to meet the identified research objectives.

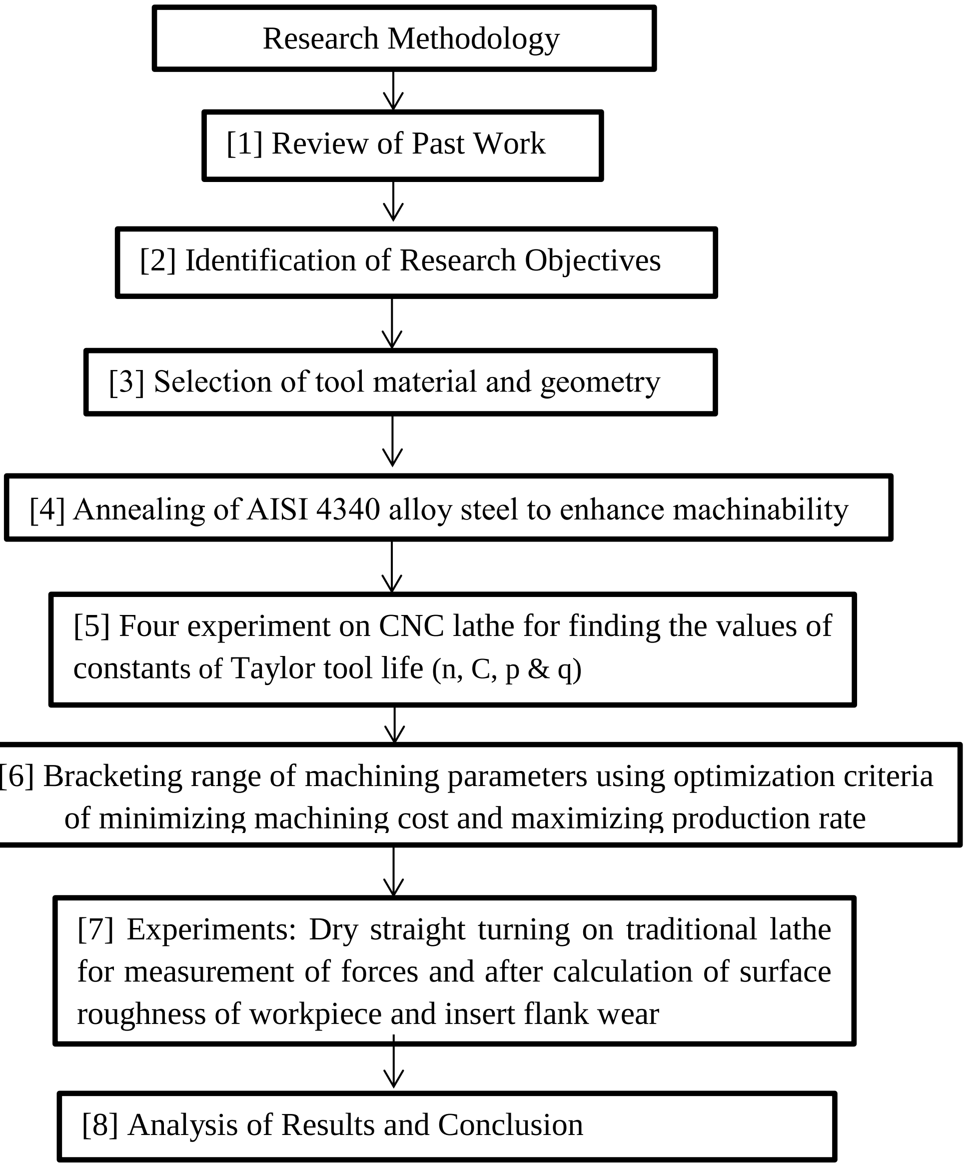

Fig.2.1: Research Methodology of the present work

Next Chapter presents in details about design and optimized machining parameters.

Chapter 3

Selection of Optimized Machining Parameters

3.1 Optimizing Machining Parameters

Optimum values of machining parameters can be selected according to conflicting criteria such as:

- Total machining cost (summation of machining cost, tool cost or tool regrinding cost, tool changing cost, setup and idle cost).
- Production rate i.e. total machining time (summation of total machining time, machining time, setup or idle time and tool changing time).

Following generalized Taylor's tool life equation can be used for optimizing the machining parameters:

$$VT^{n} f^{p} d^{q} = C \tag{3.1}$$

Where,

V	Cutting velocity (m/min)
d	Depth of cut (mm)
f	Feed rate (mm/rev)
T	Tool life (min).
C, n, p, q	Empirical constants

$$T = \frac{C^{\frac{1}{n}}}{V^{\frac{1}{n}} f^{\frac{p}{n}} d^{\frac{q}{n}}} \tag{3.2}$$

Let $k = C^{\frac{1}{n}}$

$$T = \frac{k}{V^{\frac{1}{n}} f^{\frac{p}{n}} d^{\frac{q}{n}}} \tag{3.3}$$

$$T_m = \frac{\pi DL}{1000Vf} \tag{3.4}$$

Where,

L	Length of the cylindrical workpiece to be turned (mm)
D	Diameter of the cylindrical workpiece to be turned (mm)

T_m Machining time per piece (min/piece)

$$\frac{T_m}{T} = \frac{\pi DLV^{\left(\frac{1}{n}\right)} f^{\left(\frac{p}{n}-1\right)} d^{\left(\frac{q}{n}\right)}}{1000k} \quad (3.5)$$

Relationship of machining cost:

$$C_1 = \lambda_1 T_m = \lambda_1 \frac{\pi DL}{1000 fV} \quad (3.6)$$

Where,

C_1 Machining cost per piece (Rs./piece)

λ_1 Labor or Overhead cost per min (Rs./min)

$$C_2 = \left(\lambda_2 + \lambda_3 h_f \tan \delta_s\right) \frac{T_m}{T} \quad (3.7)$$

Where,

λ_2 Cost of setting the tool for regrinding (Rs./tool)

λ_3 Tool regrinding cost per mm (Rs./mm)

C_2 Tool cost or tool regrinding cost per piece (Rs./piece)

δ_s Side clearance angle or relief angle (degrees)

h_f Flank wear (mm)

$$C_3 = \lambda_1 T_{tct} \frac{T_m}{T} \quad (3.8)$$

Where,

C_3 Tool changing cost per piece (Rs./piece)

T_{tct} Tool changing time (min/insert)

$$C_4 = \lambda_1 T_s \quad (3.9)$$

Where,

C_4 Setup or Ideal time cost per piece (Rs./piece)

Therefore, the total machining cost:

$$C_t = C_1 + C_2 + C_3 + C_4 \quad (3.10)$$

Where,

C_t Total machining cost of a component (Rs.)

Since,

$$C_t = \lambda_1 \frac{\pi DL}{1000\, fV} + \left(\lambda_2 + \lambda_3 h_f \tan\delta_s\right)\frac{T_m}{T} + \lambda_1 T_{tct}\frac{T_m}{T} + \lambda_1 T_s \quad (3.11)$$

$$C_t = \lambda_1 \frac{\pi DL}{1000\, fV} + \left[\left(\lambda_2 + \lambda_3 h_f \tan\delta_s\right) + \lambda_1 T_{tct}\right]\frac{T_m}{T} + \lambda_1 T_s \quad (3.12)$$

For using equation: (3.5)

$$C_t = \lambda_1 \frac{\pi DL}{1000\, fv} + \left[\left(\lambda_2 + \lambda_3 h_f \tan\delta_s\right) + \lambda_1 T_{tct}\right]\frac{\pi DLV^{\left(\frac{1}{n}\right)} f^{\left(\frac{p}{n}-1\right)} d^{\left(\frac{q}{n}\right)}}{1000k} + \lambda_1 T_s \quad (3.13)$$

3.1.1 Optimizing Machining Parameters for Minimum Cost

Total machining cost is summation of machining cost, tool cost or tool regrinding cost, tool changing cost, and setup or idle cost. Therefore, optimizing machining parameters for minimum cost are given below:

- ❖ Optimum cutting speed for a given feed and depth of cut to Minimize Total Machining cost is given by:

$$\left[\frac{\partial C}{\partial V}\right]_{opt} = 0 \quad (3.14)$$

$$V_{opt(\min.\cos t)} = \left[\frac{nk\lambda_1}{(1-n)\left(\lambda_1 T_{tct} + \lambda_4\right) d^{\frac{q}{n}} f^{\frac{p}{n}}}\right]^n \quad (3.15)$$

Where,

$V_{opt(\min.\cos t)}$ Optimum cutting velocity for minimum cost (m/min).

$$\lambda_4 = \left(\lambda_2 + \lambda_3 h_f \tan\delta_s\right)$$

,

- ❖ Optimum feed for a given cutting speed and depth of cut to Minimize Total Machining cost, is given by:

$$\left[\frac{\partial C}{\partial f}\right]_{opt} = 0 \quad (3.16)$$

$$f_{opt(\min.\cos t)} = \left[\frac{nk\lambda_1}{(p-n)(\lambda_1 T_{tct} + \lambda_4) V^{\frac{1}{n}} d^{\frac{q}{n}}} \right]^{\frac{n}{p}} \tag{3.17}$$

Where,

$f_{opt(\min.\cos t)}$ Optimum feed rate for minimum cost (mm/rev)

- ❖ Optimum tool life for a given cutting speed, feed and depth of cut to Minimize Total Machining cost is given by:

$$\left[\frac{\partial C}{\partial T} \right]_{opt} = 0 \tag{3.18}$$

$$T_{opt(\min.\cos t)} = \left[T_{tct} + \frac{C_2}{C_1} \right] \left[\frac{(1-n)}{n} \right] \tag{3.19}$$

Where,

$T_{opt(\min.\cos t)}$ Optimum tool life for minimum cost (min)

From equation: (3.6) and (3.7).

$$T_{opt(\min.\cos t)} = \left[T_{tct} + \frac{(\lambda_2 + \lambda_3 h_f \tan \delta_s) V^{\frac{1}{n}} f^{\frac{p}{n}} d^{\frac{q}{n}}}{\lambda_1 k} \right] \left[\left(\frac{1-n}{n} \right) \right] \tag{3.20}$$

- ❖ Optimum depth of cut from generalized Taylor tool life equation for minimum machining cost is given by:

$$V_{opt(\min.\cos t)} T^{n}_{opt(\min.\cos t)} f^{p}_{opt(\min.\cos t)} d^{q}_{opt(\min.\cos t)} = C \tag{3.21}$$

$$d_{opt(\min.\cos t)} = \frac{C^{\frac{1}{q}}}{V^{\frac{1}{q}}_{opt(\min.\cos t)} T^{\frac{n}{q}}_{opt(\min.\cos t)} f^{\frac{p}{q}}_{opt(\min.\cos t)}} \tag{3.22}$$

Where,

$d_{opt(\min.\cos t)}$ Optimum depth of cut for minimum cost (mm)

3.1.2 Optimizing Machining Parameters for Maximum Production Rate

Optimizing the machining parameter for maximum production i.e. (minimum production time). Therefore the total machining time is summation of machining time, setup time and tool changing time are given below:

Therefore, Total Machining TimeT_t,

$$T_t = T_m + T_s + T_{tct}\frac{T_m}{T} \tag{3.23}$$

Where,

T_t	Total Machining Time (min)
T_s	Setup or Idle time per piece (min/piece)

$$T_t = \frac{\pi DL}{1000Vf} + T_s + T_{tct}\frac{\pi DL}{1000k}V^{\left(\frac{1}{n}-1\right)} f^{\left(\frac{p}{n}-1\right)} d^{\frac{q}{n}} \tag{3.24}$$

From equation: (3.4) and (3.5)

- ❖ Optimum cutting speed for a given feed and depth of cut to minimize total machining time is given by:

$$\left[\frac{\partial T_t}{\partial V}\right]_{opt} = 0 \tag{3.25}$$

$$V_{opt(\max.prod.)} = \left[\frac{nk}{T_{tct}\left(1-n\right) f^{\frac{p}{n}} d^{\frac{q}{n}}}\right]^{n} \tag{3.26}$$

Where,

$V_{opt(\max.prod.)}$ Optimum cutting velocity for maximum production rate (m/min)

- ❖ Optimum feed for a given cutting speed and depth of cut to minimize total machining time is given by:

$$\left[\frac{\partial T_t}{\partial f}\right]_{opt} = 0 \tag{3.27}$$

$$f_{opt(\max.prod.)} = \left[\frac{nk}{T_{tct}\left(p-n\right) V^{\frac{1}{n}} d^{\frac{q}{n}}}\right]^{\frac{n}{p}} \tag{3.28}$$

Where,

$f_{opt(\max.prod.)}$ Optimum feed rate for maximum production rate (mm/rev)

❖ Optimum Tool life to Minimize Total Machining time is given by:

$$\left[\frac{\partial T_t}{\partial T}\right]_{opt} = 0 \tag{3.29}$$

$$T_{opt(\max.prod.)} = T_{tct}\left[\frac{(1-n)}{n}\right] \tag{3.30}$$

Where,

$T_{opt(\max.prod.)}$ Optimum tool life for maximum production rate (min)

❖ Optimum depth of cut from generalized Taylor tool life equation for maximum production:

$$V_{opt(\max.prod.)} T^{n}_{opt(\max.prod.)} f^{p}_{opt(\max.prod.)} d^{q}_{opt(\max.prod.)} = C \tag{3.31}$$

$$d_{opt(\max.prod.)} = \frac{C^{\frac{1}{q}}}{V^{\frac{1}{q}}_{opt(\max.prod.)} T^{\frac{n}{q}}_{opt(\max.prod.)} f^{\frac{p}{q}}_{opt(\max.prod.)}} \tag{3.32}$$

Where,

$d_{opt(\max.prod.)}$ Optimum depth of cut for maximum production rate (mm)

3.2 Bracketing Ranges of Machining Parameters

Ranges of the machining parameters were bracketed using the optimization criteria for the minimizing the total cost and maximizing the production rate. Four feasible values of cutting velocity, feed and depth of cut were selected in these bracketed ranges for further experiments and keeping in view availability on the values on the lathe machine used.

❖ **Selected Range for Cutting Velocity:**

$$\left[V_{opt(\min.\cos t)_{\min}} - V_{opt(max.prod.)_{\max}}\right] \rightarrow V_1, V_2, V_3, V_4$$

Where,

V_1, V_2, V_3, V_4	Selected data of cutting velocity (m/min).
$V_{opt(\min.\cos t)_{\min}}$	Minimum range of optimum cutting speed for minimum cost (m/min).
$V_{opt(max.prod.)_{\max}}$	Maximum range of optimum cutting speed for maximum production rate (m/min).

Also,

$$\left[N_{opt(\min.\cos t)_{\min}} - N_{opt(max.prod.)_{\max}} \right] \rightarrow N_1, N_2, N_3, N_4$$

Where,

N_1, N_2, N_3, N_4	Selected data of cutting velocity (rpm).
$N_{opt(\min.\cos t)_{\min}}$	Minimum range of optimum cutting speed for minimum cost (rpm).
$N_{opt(max.prod.)_{\max}}$	Maximum range of optimum cutting speed for maximum production rate (rpm).

- **Selected Range for Feed Rate:**

$$\left[f_{opt(\min.\cos t)_{\min}} - f_{opt(\max.prod.)_{\max}} \right] \rightarrow f_1,\ f_2,\ f_3,\ f_4$$

Where,

f_1, f_2, f_3, f_4	Selected data of feed rate (mm/rev)
$f_{opt(\min.\cos t)_{\min}}$	Minimum range of optimum feed rate for minimum cost (mm/rev)
$f_{opt(\max.prod.)_{\max}}$	Maximum range of optimum feed rate for maximum production rate (mm/rev)

- **Selected Range for Depth of Cut:**

$$\left[d_{opt(\min.\cos t)_{\min}} - d_{opt(\max.prod.)_{\max}} \right] \rightarrow d_1, d_2, d_3, d_4$$

Where,

d_1, d_2, d_3, d_4	Selected data of depth of cut (mm)
$d_{opt(\min.\cos t)_{\min}}$	Minimum range of optimum depth of cut for minimum cost (mm)
$d_{opt(\max.prod.)_{\max}}$	Maximum range of optimum depth of cut for maximum production rate (mm)

Next Chapter presents in details about planning and details of experimental investigation.

Chapter 4

Plan of Experimental Investigations

This chapter presents the planning and details of experiments carried out in the present study. It describes the different sub-systems and the components of the experimental apparatus used in the present research work and planning of different experiments required for investigations on machinability of workpiece AISI 4340 annealed alloy steel under dry environment using coated carbide tool insert with proper tool holder for cylindrical straight tuning operation.

4.1 Experimental Apparatus

The experiments for the present work were conducted on non-traditional CNC lathe machine and traditional lathe machine. This experimental apparatus consists of following major systems are

- Traditional lathe machine
- Dynamometer
- Amplifiers
- Acquiring/Analyzing

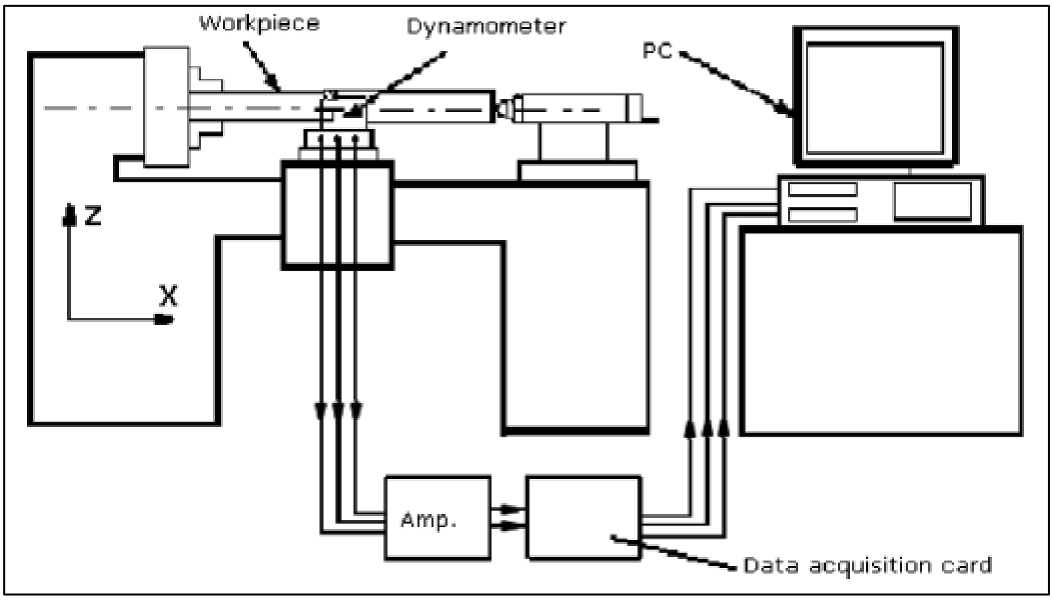

Fig. 4.1: Schematic diagram of experimental apparatus.

4.1.1 Traditional lathe machine

Medium size all geared and high speed precision lathe HMT (Model no. NH 22/1000). Machining is one of the most important material removal methods in the technology of manufacturing. It is basically a collection of material working processes that involves other processes such as turning, drilling, shaping, sawing, planning, reaming, and grinding among others. Velocity range of this machine are (40, 52, 60, 68, 88, 102, 114, 148, 175, 192, 250, 290, 325, 420, 490, 550, 715, 840, 930, 1210, 1430, 1575, and 2040) rpm.

Fig. 4.2: Traditional lathe machine.

Fig.4.3: Force measurement setup.

4.1.2 Dynamometer

Piezoelectric type of dynamometer 6 channel type of KISTLER instrument AG Winter Thur Switzerland Type 5697 A 5132 (Model no. 4289124). Voltage range (18 to 36 Volts) and power supply (5 watt). Dynamometers are used to measure the forces during turning with the help of dynoware software. These dynamometers are modular in structure and are usually mounted on the turret of the machine tool with the aid of a suitable adapter. The tool is fastened to the dynamometer with a tool holder, whereby the dynamometer is embedded between the tool and the turret. With this structure, the forces at work can be acquired accurately and highly dynamically so that even the smallest changes in the process chain can be quantified at once. The cutting force created by the turning process is broken down immediately into the three components cutting force F_c, feed force F_f and radial force F_r with the aid of multi-component dynamometers.

Fig. 4.4: Piezoelectric type dynamometer

4.1.4 Amplifier

Amplifiers are necessary in order to utilize effectively the charge difference that arises when piezoelectric sensors are loaded. These electronics are essentially comprised of an inverting charge amplifier with high inner amplification and convert the charge signals into proportionate voltage signals. Dynamometers that measure more than one component require the corresponding number of charge amplifiers. The multi-channel charge amplifiers developed by Kistler are optimized for measurement tasks such as cutting force measurement and are very modular in their design to some extent. This makes it possible to combine force and acceleration signals very readily in the same device. Depending on the Type, the adjustment of the parameters can be undertaken directly using menus on the charge amplifier or conveniently at the computer.

Fig.4.5: Amplifier

4.1.5 Acquiring/Analyzing

Acquiring/Analyzing Kistler offers optimized software for data acquisition and analysis with cutting force measurement. With the Kistler DynoWare, it is possible to set all of the parameters of the respective charge amplifiers that are important for data acquisition. The acquired data is presented in a graphics form and facilitate, together with various functions, the signal processing and analysis of the measurement signals. With DynoWare, it is easy to document and export the data.

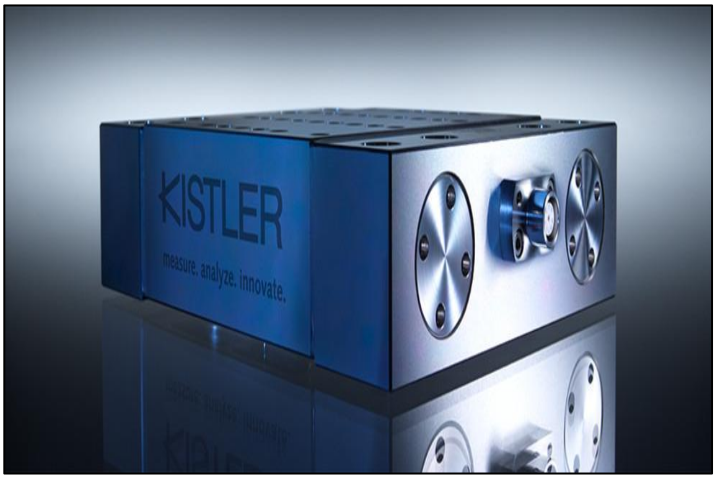

Fig.4.6: Acquiring/Analyzing

4.2 Selection of material

Selection of workpiece material and tool material discussed in detail.

4.2.1 Workpiece material

A cylindrical shaped of 50 mm diameter and 150 mm of length of AISI 4340 alloy steel is the work material for the machining operation. The chemical composition of the workpiece AISI 4340 alloy steel was measured by Spectro metal analyzer (Spectro Max) from GOPI ALLOY STEEL Company Kolkata West Bengal.

Table 4.1: Chemical composition of AISI 4340 ALLOY STEEL in weight (Workpiece material).

Elements	Fe	Ni	Cr	Mn	C	Mo	Si	S	P
Wt. %	95.19	1.65	0.70	0.60	0.370	0.20	0.150	0.040	0.035

4.2.2 Tool inserts and tool holder

Coated carbide four sided tool insert with CVD multilayer coating consisting of ($Ti/TiCN/Al_2O_3/ZrCN$).

ISO SCMT120408 (KENNAMETAL)

[-6º,-6º, 6º, 6º, 15º, 75º, 0.8 {mm}]

Tool holder DESIGNATION

ISO SSBCR2020K12 (KENNAMETAL)

4.3 Plan of Experimentation

Several experiments were planned and performed to determine the machinability of workpiece. First of all here performed heat treatment of workpiece than after four experiments perform for finding the value of tool life based on 0.3 mm flank wear for better finishing condition.

4.3.1 Heat treatment

Heat treatment of workpiece material i.e. Annealing of workpiece material therefore, billet workpiece material AISI 4340 alloy steel: Length = 180 mm, Diameter = 51 mm, heat treated (annealed at 500 °C) for 2 hour in PIT TYPE of electric furnace purpose to increase ductility or make it soft & enhance machinability. Than after furnace cool of workpiece for 24 hour to developed coarse pearlite structure. Coarse pearlite microstructure leads to lesser value of τ_s (shear strength) and reduce hardness of workpiece material and comparison with tool insert hardness than lesser force will require between them during machining.

Fig.4.7: Pit type electric furnace. **Fig.4.8**: Annealed AISI 4340 alloy steel.

4.3.2 Mounting of sample

The workpiece sample cut from wire EDM (Electro discharge machine) 1 cm^3 size two piece for cold and hot mounting and for that workpiece sample are polished with fine to very fine sand paper having grade 100, 200, 500, 800, 1200, 1600, 2000 and 2400 to developed the mirror images of workpiece sample after that chemical compound nital etchant solution is used for developing the grain boundaries of workpiece sample. Therefore the polished sample is given below and microscopic images of this polished sample taken by LEICA DFC295 Inverted metallurgical microscope. Refer fig.5.1 and fig5.2.

Fig.4.9 Polishing machine.

❖ **Before Annealing:**

- Workpiece AISI 4340 sample
- Polished with nital etchant
- Cold mounting sample

Fig.4.10 Cold mounting of workpiece sample 10 x10 mm size

- **After Annealing:**
- Sample AISI 4340 Alloy steel
- Polished sample with nital etchant
- Hot mounting sample

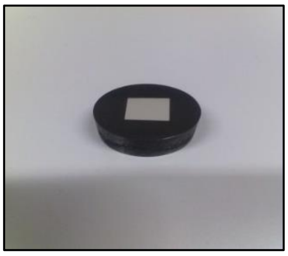

Fig.4.11 Hot mounting of workpiece sample 10 x10 mm size

4.3.3 Hardness

UHL VMH-002 from Walter UHL GmbH, Germany, ASTM E8 384: 0.2 kg, Indentation Speed 25 µm/s, Dwell Time: 15 sec Base metal AISI 4340 ALLOY STEEL Hardness measure in kg/mm^2.

Fig.4.12: Vickers micro hardness

- **Vickers Micro Hardness (HV) before annealing:**
  - 279HV0.2
  - 255HV0.2
  - 256HV0.2

- Load =200 gm.
- Average HV: 264 Kg/mm^2
- BHN= 264
- HRC = 25

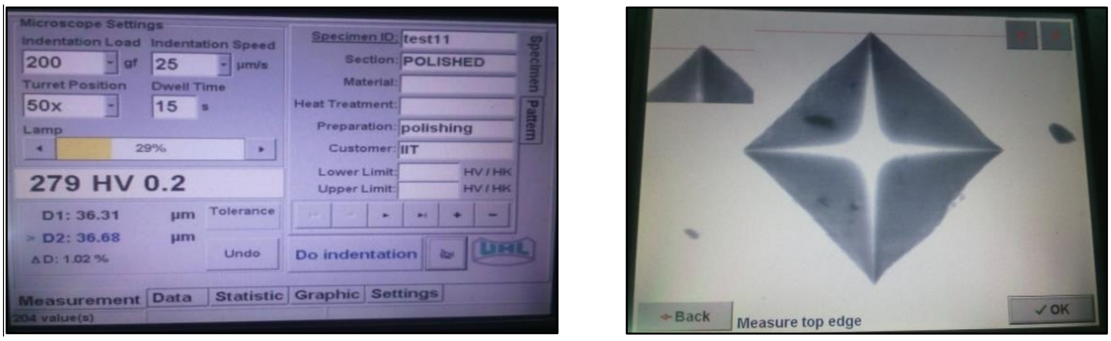

(a) (b)

Fig.4.13: (a) Hardness data image and (b) Vickers indentation of workpiece sample before annealing

- ❖ **Vickers Micro Hardness (HV) after annealing:**
  - ➢ 238HV0.2
  - ➢ 235HV0.2
  - ➢ 251HV0.2
- Load=200 Kg
- Average HV: 242 Kg/mm^2
- BHN=242
- HRC= 21

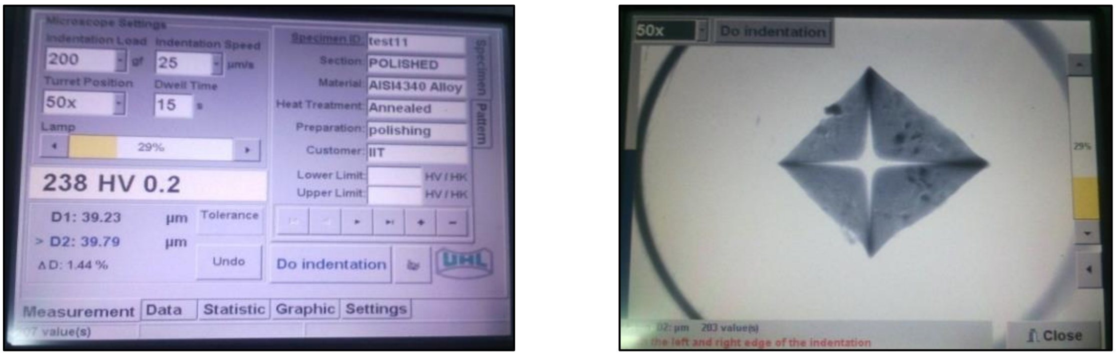

(a) (b)

Fig.4.14: (a) Hardness data image and (b) Vickers indentation of workpiece sample after annealing.

It is clear from above testing, the hardness value of heat treated is low therefore low machining force will require for better machinability.

4.3.4 Tool life evaluation

Here tool life evaluated for finding the value of empirical or exponent Taylor constant *n, p, q* and *C* based on 0.3 mm flank wear for better finishing purpose. There are four experiment performed with four selected level i.e. (cutting velocity, feed rate and depth of cut). A center drill was on the face of the each workpiece to facilitate mounting at the tailstock therefore the entire length is 180 mm out of 30 mm is used for holding. Each workpiece is 51 mm diameter and 0.5 mm depth of cut is given for burr and oxide layer removed from the outer surface of workpiece after annealing. But here on CNC lathe machine there is only one workpiece is used for performed four experiments. Since each experiment performed till approximately 0.3 mm flank wear measured for evaluation of tool life.

Table 4.2: Machining parameters and their levels

s.no.	Cutting parameter	symbol	Unit	Level			
				1	2	3	4
1	Cutting velocity	v	m/min	112	146	190	247
2	Feed rate	f	mm/rev	0.1	0.16	0.2	0.28
3	Depth of cut	d	mm	0.1	0.2	0.3	0.4

❖ **Experimental condition for straight turning:**

Table 4.3: Input machining parameters for experiment.

Workpeice	AISI 4340 Alloy Steel
Tool insert	Coated carbide CVD deposited multilayer coating of (TiN/TiCN/Al_2O_3/ZrCN)
Designation of tool insert	ISO SCMT120408 (KENNAMETAL) ASA or ANSI {American system association}
Designation of tool holder	ISO SSBCR2020K12 (KENNAMETAL)
Geometry of tool	−6°, −6°, 6°, 6°, 15°, 75°, 0.8 (mm)
Cutting velocity	112, 146, 190, 247 (m/min)
Feed rate	0.1, 0.16, 0.2, 0.28 (mm/rev)
Depth of cut	0.1, 0.2, 0.3, 0.4 (mm)
Cutting condition	Dry environment i.e. (no use of cutting fluid)
Workpeice length to be turned	150 mm
Diameter of workpiece	50 mm

4.3.5 Main experiment plan

Main experiment performed on traditional lathe machine and machining process is straight turning under dry environment for finding the value of machining forces than after measurement of maximum flank wear of tool insert, surface roughness values of workpiece material and chip morphology. Here four level of machining parameters and three factors are used and design of experiment by taguchi L16 from MINITAB 16 software. Hence the experiments are shuffled given below table.

Table 4.4: Design of experiment by taguchi L16**.**

Experiment no.	Cutting velocity	Feed rate	Depth of cut
1	112	0.10	0.1
2	112	0.16	0.2
3	112	0.20	0.3
4	112	0.28	0.4
5	146	0.10	0.2
6	146	0.16	0.1
7	146	0.20	0.4
8	146	0.28	0.3
9	190	0.10	0.3
10	190	0.16	0.4
11	190	0.20	0.1
12	190	0.28	0.2
13	247	0.10	0.4
14	247	0.16	0.3
15	247	0.20	0.2
16	247	0.28	0.1

4.3.5.1 Outcome response

The measurement of output responses are machining forces, surface roughness, maximum flank wear and chip morphology.

- **Machining forces:**

Here three forces are measured namely as primary cutting force $\boldsymbol{F_c}$, feed force $\boldsymbol{F_f}$ and radial force $\boldsymbol{F_r}$.

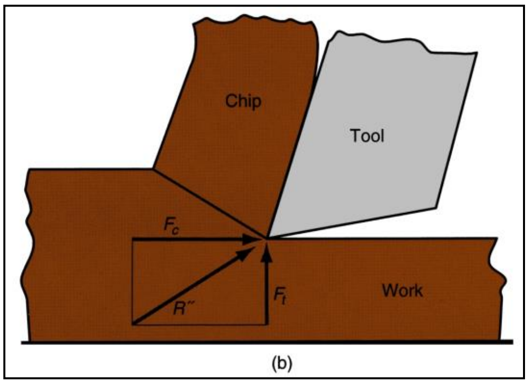

Fig.4.15: Machining forces.

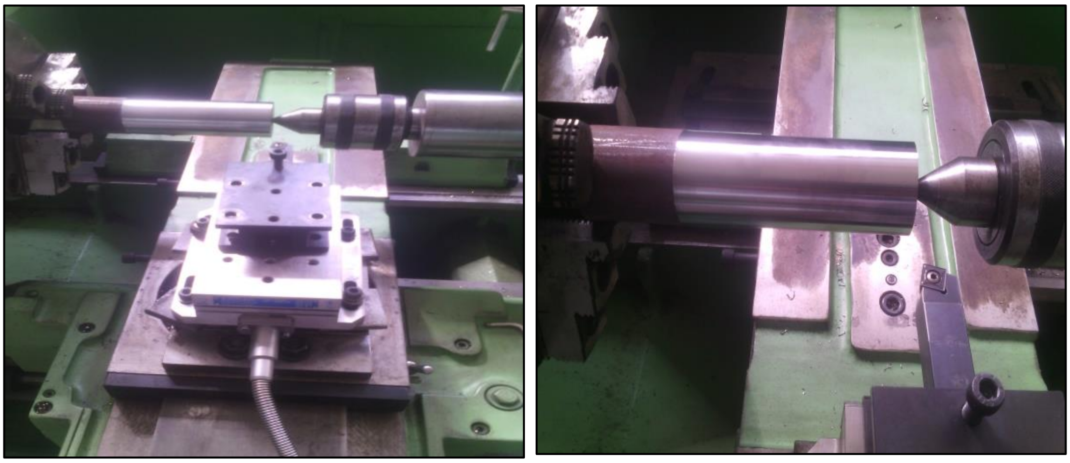

(a) (b)

Fig.4.16: (a) and (b) View of cutting zone.

❖ **Surface roughness:**

Roughness consists of the finer irregularities which generally result from the inherent action of the production process. These include transverse feed marks and other irregularities within the limits of the sampling length. Here three surface roughness measured namely as *Ra* (Average Surface Roughness**),** R_{max} (Maximum surface roughness) and R_z (Maximum peak-to-valley height).

- **Average Surface Roughness:** R_a is the universally recognized parameters of roughness. It is the arithmetic mean of the departures y of the profile from the mean line. It is normally determined as the mean results of several consecutive sampling lengths L

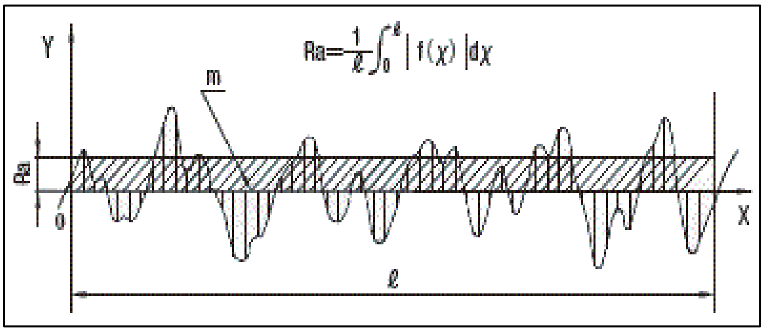

Fig.4.17 Average surface roughness profile.

- **Maximum surface roughness:** R_{max} is the maximum peak-to-valley height within sampling length L. But because of the value can be greatly affected by a spurious scratch or particles of dirt on the surface, it is more usual to use the average of five consecutive sampling lengths.
- **Maximum peak-to-valley height:** R_z ten-point height is the average distance between the five highest peaks and the five deepest valleys within the sampling length and measured perpendicular to it.

❖ **Surface roughness tester:** 3D-Surface roughness cum contour tracing equipment (Mahrsurf LD 130) is used for surface roughness profile and their value.

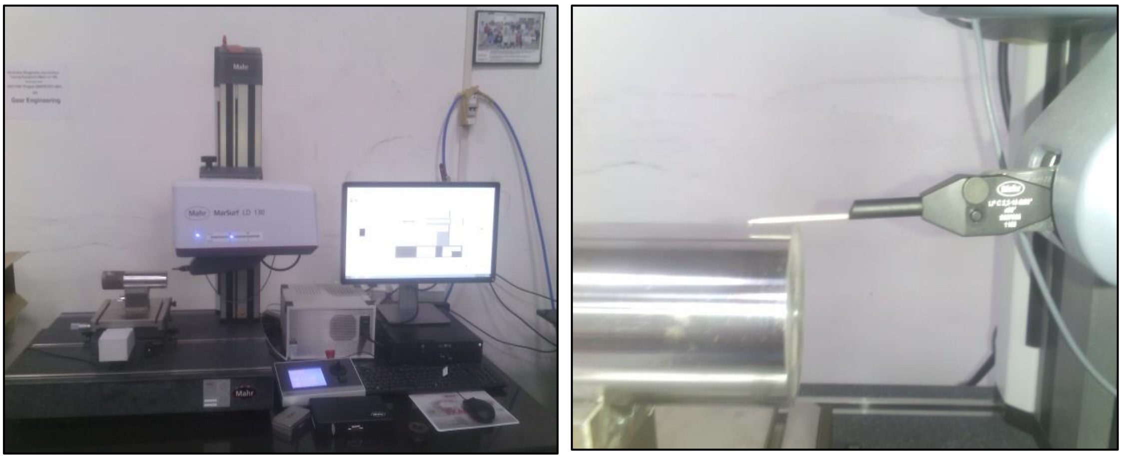

(a) (b)

Fig.4.18: (a) Measuring setup of surface roughness tester and (b) probe mounted on workpiece surface.

❖ **Tool Wear:**

In this experiment VB_{max} maximum flank wear is measured of cutting tool insert with the help of Field Emission Scanning Electron Microscope (FESEM), Carl Ziess Supra 55.

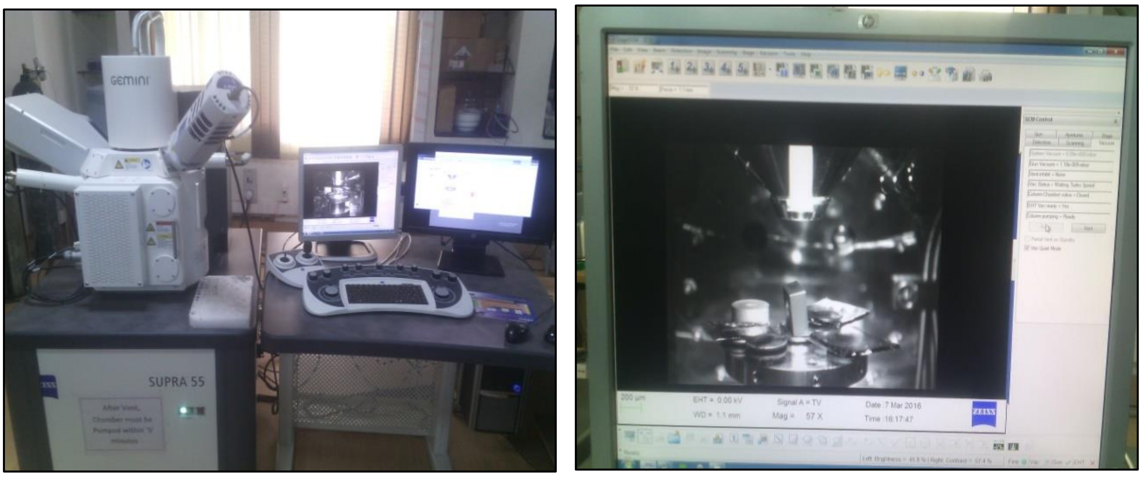

(a) (b)

Fig.4.19: (a) Tool wear measurement setup and; (b) Tool insert inside vacuum chamber.

Chip marphology:

Here chip thickness is measured with help of micrometer (mahr micromar 40A 0-25) and their marpholgy has been studied and chips images were measured on Field Emission

Scanning Electron Microscope (FESEM), Carl Ziess Supra 55. Four basic type of chip in machining are given below:

Fig.4.20: Chip thickness measuring instrument micrometer

- **Discontinuous chip:**

  Brittle work materials (e.g., cast irons), low cutting speeds, large feed and depth of cut and high tool-chip friction.

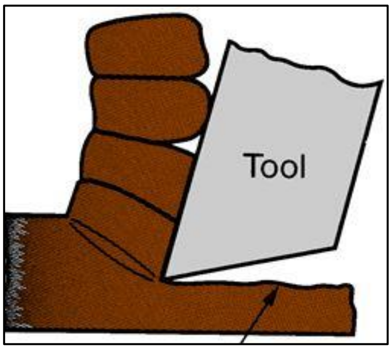

Fig.4.21: Discontinuous chip

- **Continuous chip:**

  Ductile work materials (e.g., low carbon steel), high cutting speeds, small feeds and depths, sharp cutting edge on the tool and low tool-chip friction.

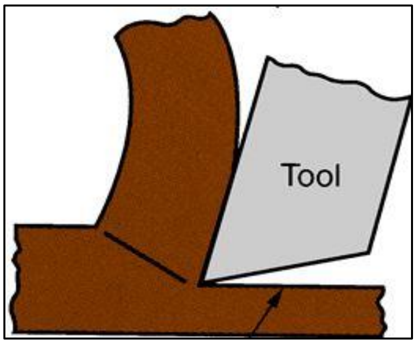

Fig.4.22: Continuous chip

- **Continuous chip with Built-up Edge (BUE):**

Ductile materials, low-to-medium cutting speeds, tool-chip friction causes portions of chip to adhere to rake face and BUE formation is cyclical it forms and then breaks off.

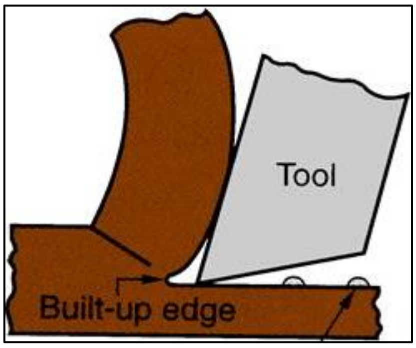

Fig.4.23: Continuous chip with Built-up Edge (BUE)

- **Serrated chip:**

Semi continuous saw-tooth appearance, cyclical chip formation of alternating high shear strain then low shear strain and most closely associated with difficult-to-machine metals at high cutting speeds .

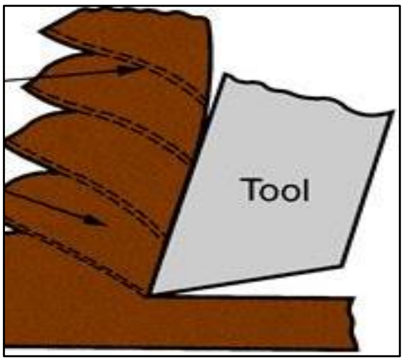

Fig.4.24: Serrated chip

Next Chapter presents in optimum output data compare with selected input data after performing experiments. Detail discussion of results and their analyses.

Chapter 5

Results and Analyses

This chapter describes about the results of the performed experiments, their calculation discussion and analyses. Identification of the optimum values for surface roughness, machining forces and flank wear.

5.1 Microscopic Images of Annealed Alloy Steel

Polished microscopic images of AISI 4340 alloy steel before and after annealing**.** Microscopic images taken from by LEICA DFC295 Inverted metallurgical microscope.

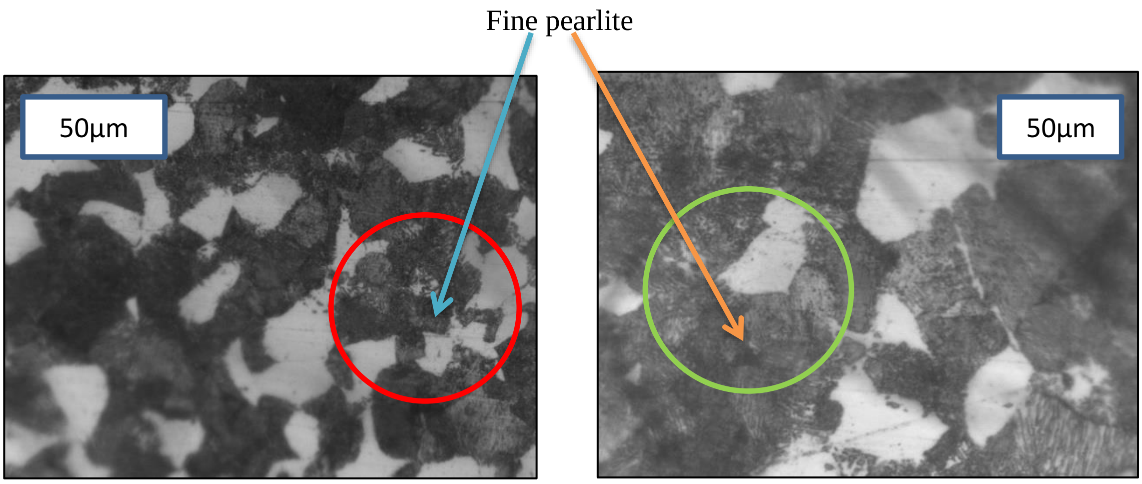

(a) (b)

Fig.5.1: (a) Microscopic images at 50X magnification and (b) microscopic images at 100X magnification under 50µm before annealing.

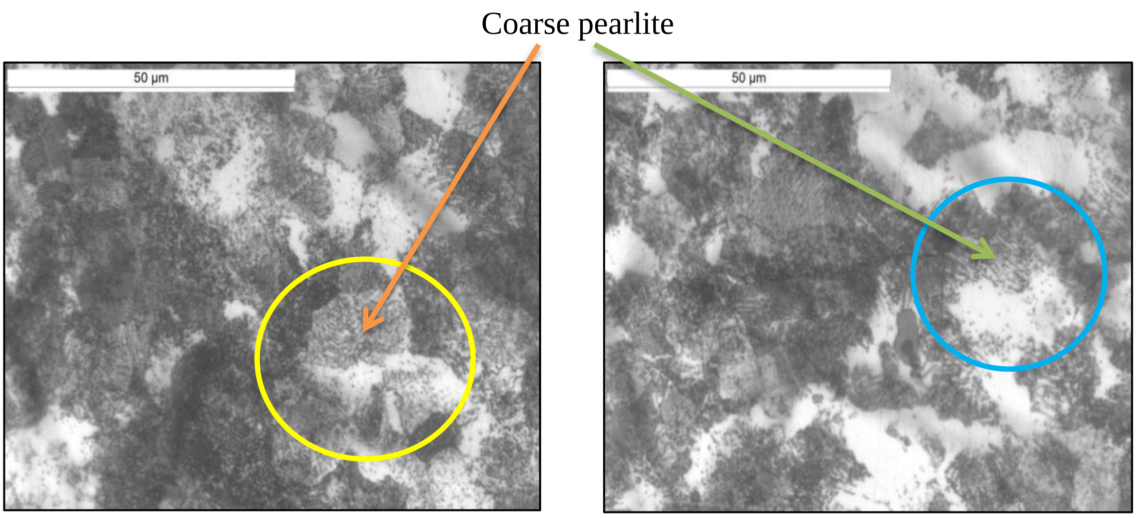

(a) (b)

Fig.5.2: (a) Microscopic image at 50X magnification and (b) microscopic image at 100X magnification under 50µm after annealing.

Fig.5.1 Shows fine pearlite structure and due to fine pearlite the workpiece material property is hard and less ductile. On the other hand fig.5.2 shows coarse pearlite structure that means material property i.e. hardness value less compare with tool insert and make it more ductile for enhance machinability of workpiece.

5.2 Results for Tool Life Evaluation

Four experiments performed on CNC Lathe DX-150, JYOTI, SINUMERIK (SIMENS), VERSION 802 D, Multipass turning operation under dry cutting condition.

Table 5.1: Four experiment performed A, B, C and D.

S.no.	Exp. No..	Input parameters				Out responces	
		Cutting velocity (m/min)	Feed rate (mm/rev)	Depth of cut (mm)	No. of passes for turning	Insert Flank wear (mm)	Tool life (min)
1	A	V_1 (112)	f_1 (0.1)	d_1 (0.1)	40	0.31	T_1(48)
2	B	V_2 (146)	f_2 (0.16)	d_2 (0.2)	15	0.32	T_2(14)
3	C	V_3 (190)	f_3 (0.2)	d_3 (0.3)	14	0.296	T_3(6)
4	D	V_4 (247)	f_4 (0.28)	d_4 (0.4)	17	0.292	T_4(2)

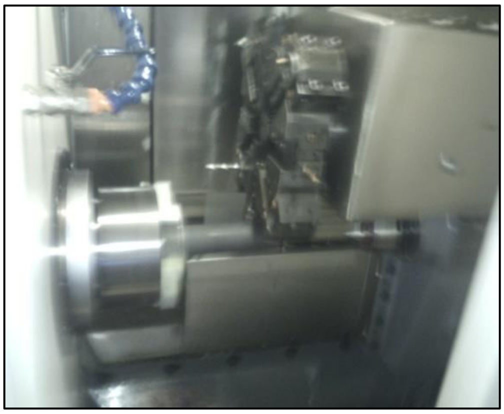

Fig. 5.3: CNC lathe turning set up

5.3 Effect of Machining Parameters on Tool Life

The graph plotted between tool life, cutting velocity, feed rate and depth of cut. It is clearly all figure shows increment of abscissa and decrement of ordinate i.e. tool life is decreased with increasing of cutting speed, feed rate and depth of cut.

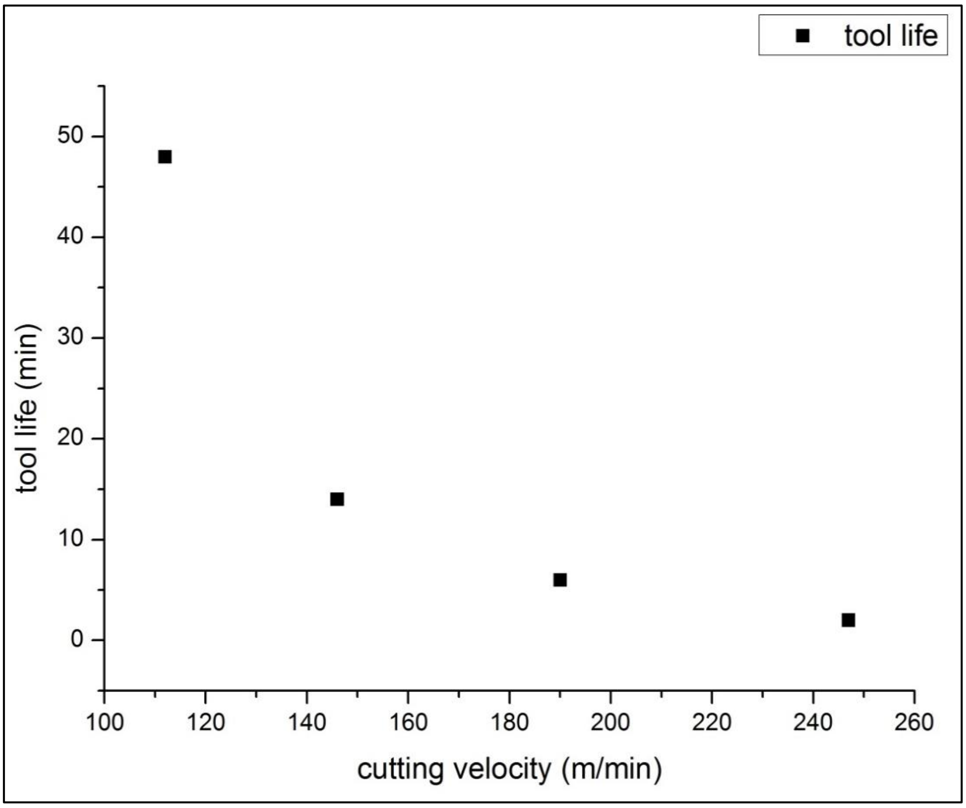
tool life
50
40
30
20
10
0
tool life (min)
100
120
140
160
180
200
220
240
260
cutting velocity (m/min)

(a)

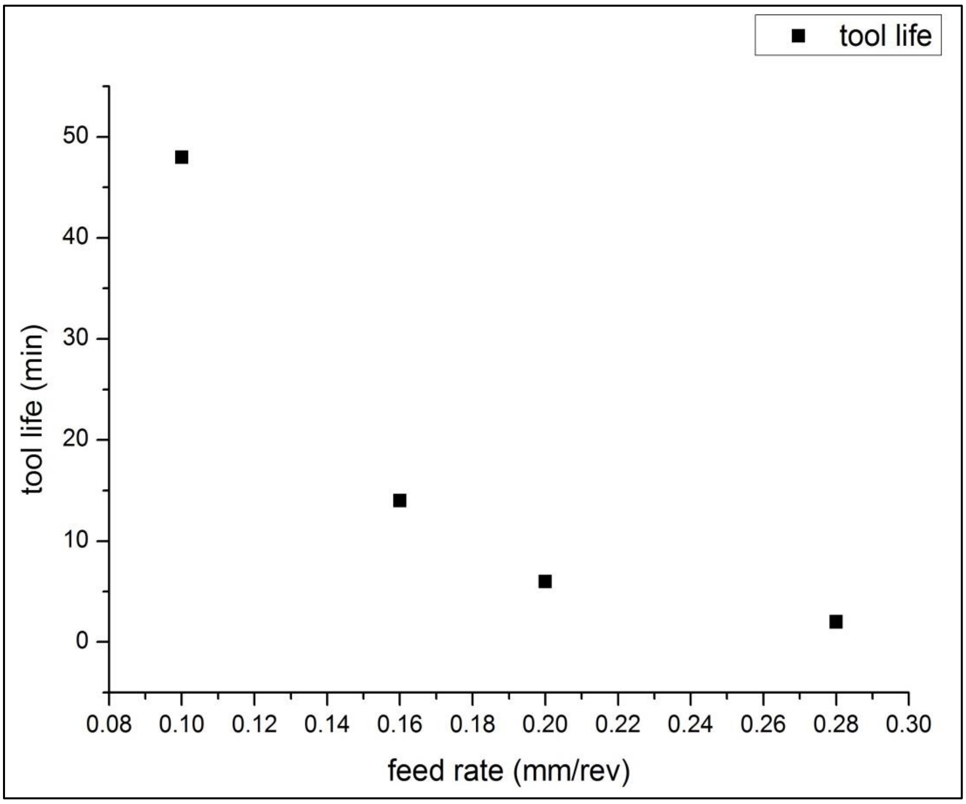
tool life
50
40
30
20
10
0
tool life (min)
0.08
0.10
0.12
0.14
0.16
0.18
0.20
0.22
0.24
0.26
0.28
0.30
feed rate (mm/rev)

(b)

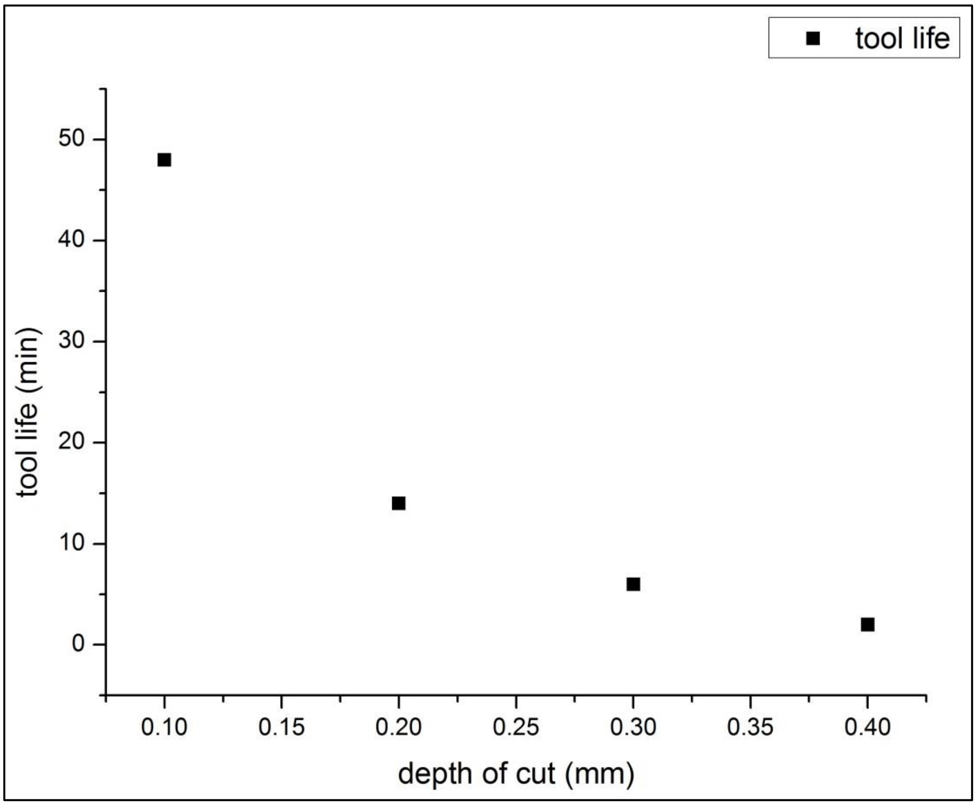

(c)

Fig. 5.4: Results (a) tool life vs. cutting velocity, (b) tool life vs. feed rate and (c) tool life vs. depth of cut.

5.4 Microscopic Images of Coated Carbide Tool Insert

The microscopic images at 5X magnification of each experiment for finding the value of tool wear i.e. flank wear of coated carbide four sided tool insert which is used for performed above four experiments. Images taken from by LEICA DM 2500M Optical microscope.

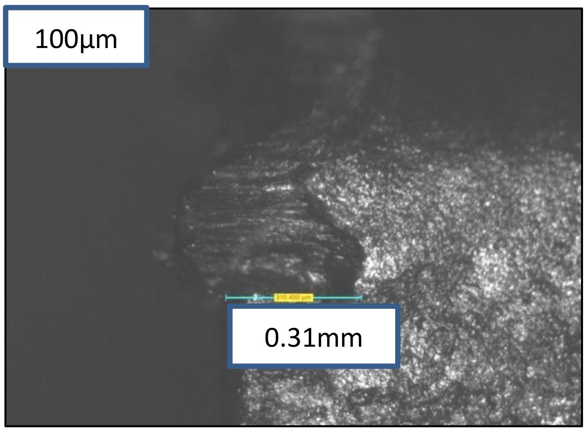

(a)

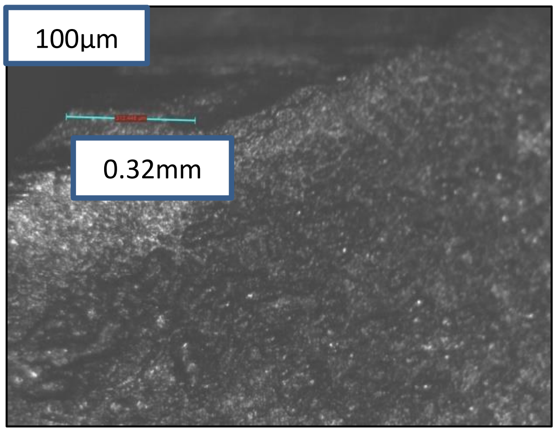

(b)

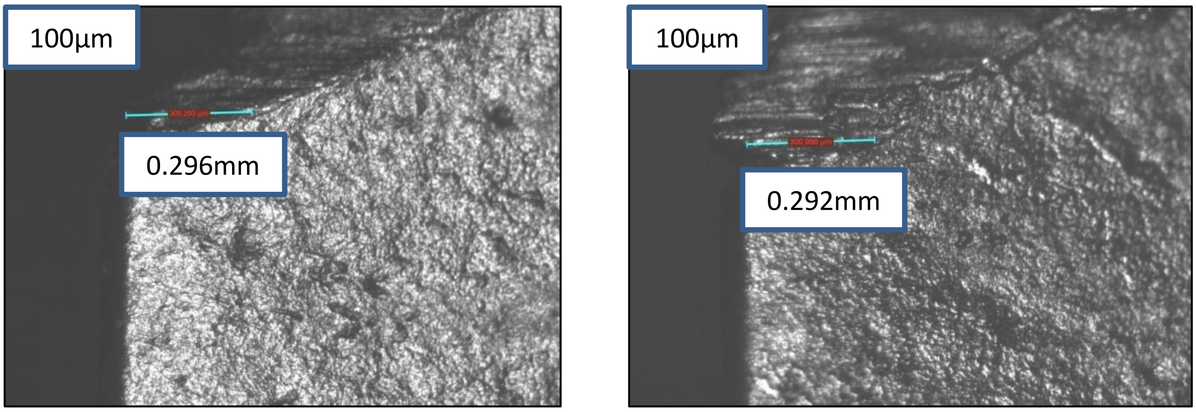

(c) (d)

Fig.5.5: Four optical microscopic images for finding tool wear at (a) 0.31 mm flank wear at T_1= 48min, V_1=112m/min, f_1= 0.1 mm/rev, d_1=0.1mm. (b) 0.32 mm flank wear at T_2= 4min, V_2=146m/min, f_2= 0.1 6mm/rev, d_2=0.2mm. (c) 0.296 mm flank wear at T_3 =6min, V_3=190m/min, f_3=0.2mm/rev, d_3=0.3mm. And (d) 0.292 mm flank wear at T_4 =2min, V_4=247m/min, f_4=0.28mm/rev, d_4=0.4mm.

0.3 mm flank wear each sided

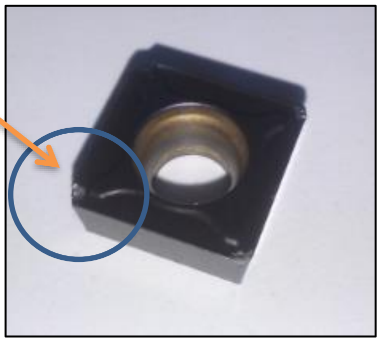

Fig. 5.6: Coated carbide tool insert after turning.

5.5 Evaluation of Constants of Taylor's Tool Life Equation

There are four empirical constant *n, p, q* and *C* for finding the value of this empirical constant we need four equations and for unknown i.e. empirical constant. Finally this empirical constant which help for finding the optimum value of cutting velocity, feed rate and depth of for condition minimum cost and maximum production rate. Than after it is compare with selected input cutting parameter i.e. cutting velocity, feed rate and depth of cut.

$$V_1 T_1^n f_1^p d_1^q = C \tag{4.1}$$

$$V_2 T_2^n f_2^p d_2^q = C \tag{4.2}$$

$$V_3 T_3^n f_3^p d_3^q = C \tag{4.3}$$

$$V_4 T_4^n f_4^p d_4^q = C \tag{4.4}$$

Therefore we have all the above value except *n, p, q* and *C* from table 5.1 than here four unknown and four equations (4.1), (4.2), (4.3) and (4.4) solving by MATLAB 15 software.

- n = 0.4805
- p = 0.9180
- q = - 0.1508
- C = 122.9899

❖ **Constant data:**

- Length of cylindrical workpiece to be turned, L = 150 mm
- Diameter of cylindrical workpiece, D = 50 mm
- Setup time per piece , T_s = 30 min/piece
- Tool changing time, T_{tct} = 2 min
- Labor cost per min, λ_1 = 1.667 Rs./min (800 Rs./day)
- Cost of setting the tool for regrinding, λ_2 = 50 Rupees
- Tool regrinding cost per mm λ_3 = 10 Rs./mm
- Side clearance angle, δ_s = 6º
- And remaining all given data available above table.

Put above data in equations (3.15), (3.17), (3.22), (3.26), (3.28) and (3.32) for finding the value of optimum cutting velocity, feed rate and depth of cut are given below and this output responses comparison with selected input machining parameters. Therefore the optimum output machining parameters are lies in the range of selected input machining parameters. Hence this is the justification of selected machining parameters and these selected machining parameters are further used for main experiments.

Table.5.2: Optimum responses of machining parameters.

Parameters	unit	Optimum output data	Selected data
Range of Cutting velocity	m/min	$[62.61 - 496.768]$	$[112, 146, 190, 247]$
Range of cutting speed in rotation	rpm	$[398.58 - 3162.52]$	$[715, 930, 1210, 1575]$
Range of feed rate	mm/rev	$[0.0687 - 0.5544]$	$[0.1, 0.16, 0.2, 0.28]$
Range of depth of cut	mm	$[0.021 - 0.5385]$	$[0.1, 0.2, 0.3, 0.4]$

5.6 Discussion of Main Results and Analyses

Discussion of the main experiment results, their analysis and detail discussion of surface roughness, machining forces, maximum flank wear and chip morphology results of analysis of variance (ANOVA) to determine the significant parameter and evaluation of main effects plot between cutting velocity, feed rate and depth of cut.

Table 5.3: Experimental results for surface roughness, machining forces, maximum flank wear and chip thickness.

Ex .no	Input parameters			Outcome responses							
	Cutting speed (m/min)	Feed rate (mm/ rev)	Depth of cut (mm)	Surface roughness (μm)			Machining forces (N)			Maximum flank wear (mm)	Chip thickness (mm)
	V	f	d	R_a	R_{max}	R_z	F_f or F_x	F_c or F_y	F_r or F_Z	VB_{max}	t_c
1	112	0.10	0.1	1.58	7.92	7.54	2.554	8.6421	15.981	0.0147	0.15
2	112	0.16	0.2	2.41	12.0	11.6	4.363	12.900	17.279	0.0156	0.25
3	112	0.20	0.3	2.42	13.9	12.0	9.8204	15.225	27.531	0.0166	0.24
4	112	0.28	0.4	3.35	17.9	16.3	12.183	25.668	35.305	0.0275	0.33
5	146	0.10	0.2	0.728	4.37	3.98	4.8501	15.854	37.447	0.0249	0.16
6	146	0.16	0.1	1.11	6.61	6.14	6.9016	13.541	29.942	0.0206	0.14
7	146	0.20	0.4	2.32	13.1	11.3	10.687	27.898	39.235	0.0360	0.34
8	146	0.28	0.3	3.27	14.2	13.6	14.662	21.823	36.393	0.0307	0.25
9	190	0.10	0.3	0.746	4.17	4.15	5.2487	26.141	52.515	0.0358	0.19
10	190	0.16	0.4	1.05	6.80	5.75	9.1786	31.215	60.152	0.0500	0.17
11	190	0.20	0.1	1.56	7.65	7.37	11.185	18.309	41.126	0.0301	0.26
12	190	0.28	0.2	1.12	5.27	5.10	10.894	22.835	45.636	0.0352	0.30
13	247	0.10	0.4	0.812	4.37	4.21	14.892	42.671	65.927	0.0557	0.23
14	247	0.16	0.3	0.960	5.61	5.03	15.137	31.885	57.830	0.0441	0.20
15	247	0.20	0.2	1.55	6.53	6.12	13.647	26.571	51.968	0.0360	0.28
16	247	0.28	0.1	2.78	12.7	12.4	12.065	23.490	47.834	0.0339	0.31

5.7 Surface roughness analysis

The experimental results of surface roughness parameters (R_a, R_{max} and R_z) are analyzed using the analysis of variance (ANOVA) for determining the parameters significantly influencing the surface roughness and the analysis is made by a software package MINITAB16. This analysis was accomplished for a significance level alpha (α) of 0.05 (95% confidence level). Table 5.4 the P-values, i.e. the recognized significance levels, allied with the F tests for each source of variation. Statistical significance to the response is considered when the P-value of its input sources is observed to be lower than 0.05. The last column of the table explains the percent contribution of significant source to the total variation and revealing the degree of impact on the surface roughness.

Table 5.4: Analysis of variance for surface roughness parameters: (a) R_a, (b) R_{max} and (c) R_z

Sources	DF	Seq SS	Adj SS	Adj MS	*F*	*P*	Contr. %	Remark
(a) *Analysis of Variance for R_a*								
v	3	3.7410	3.7410	1.2470	4.61	0.053	30.926	
f	3	6.2705	6.2705	2.0902	7.73	0.017	51.842	Significant
d	3	0.4620	0.4620	0.1540	0.57	0.655	3.819	
Error	6	1.6217	1.6217	0.2703			13.407	
Total	15	12.0952					100	
(b) *Analysis of Variance for R_{max}*								
v	3	111.218	111.218	37.073	9.32	0.011	39.636	Significant
f	3	119.881	119.881	39.960	10.04	0.009	42.729	Significant
d	3	25.991	25.991	8.664	2.18	0.192	9.262	
Error	6	23.869	23.869	3.978			8.506	
Total	15	280.959					100	
(c) *Analysis of Variance for R_z*								
v	3	88.240	88.240	29.413	6.77	0.024	37.808	Significant
f	3	103.460	103.460	34.487	7.94	0.016	44.329	Significant
d	3	15.629	15.629	5.210	1.20	0.387	6.696	
Error	6	26.056	26.056	4.343			11.164	
Total	15	233.386					100	

It is seen in table 5.4, the parameters *v*, *f* and *d* are significant sources on surface roughness parameters: average surface roughness (R_a), maximum surface roughness (R_{max}) and maximum peak-to-valley height (R_z). Feed (the most significant parameter) contributed 51.842% for R_a, 42.729% for R_{max} and 44.329% in case of R_z. The contribution of the second most significant parameter cutting speed was noticed merely 39.636% in case of R_{max} and 37.808% for R_z. Besides this, depth of cut showed the minor role and is not found statistically significant on surface roughness parameters (R_a, R_{max} and R_z), while the cutting velocity is also not significant for average surface roughness (R_a). The error contributions are 13.407%, 8.506% and 11.164% for R_a, R_{max} and R_z respectively. The extremely small percentage of error indicates that any major parameter has been neither neglected nor any significant errors in measurement.

Fig.5.7 (a) to (c) illustrates the main effect plots of three surface roughness parameters (R_a, R_{max} and R_z). The main effect plots in indicate that, the surface roughness leads to increase significantly with an increase in feed. This is predicted as well as known that, the theoretical surface roughness is primarily dependent upon the feed rate, for a certain nose radius of the tool. Subsequently, **(Suresh *et al.*, 2009)** found the reason that with increased feed thrust force increases resulting to vibration and producing extra heat to enhance the plastic deformation of workpiece and thereby resulting higher surface roughness. The normal tendency of curves in is, when cutting speed is increased gradually, the surface roughness values diminish until the lowest value is attained beyond which the surface roughness values increase. The surface finish improves with increase in cutting speed up to 190 m/min can simply illustrated by restricting BUE formation trend with increasing cutting speed. Nevertheless, more increase in cutting speed gives rise to increase in surface roughness which can be explained by either the possibility of chatters due to vibrations or material side flow related to high speeds. No considerable effect is noticed on surface roughness caused by change in depth of cut. However, to reduce the tendency to chatter low depth of cut is to be maintained.

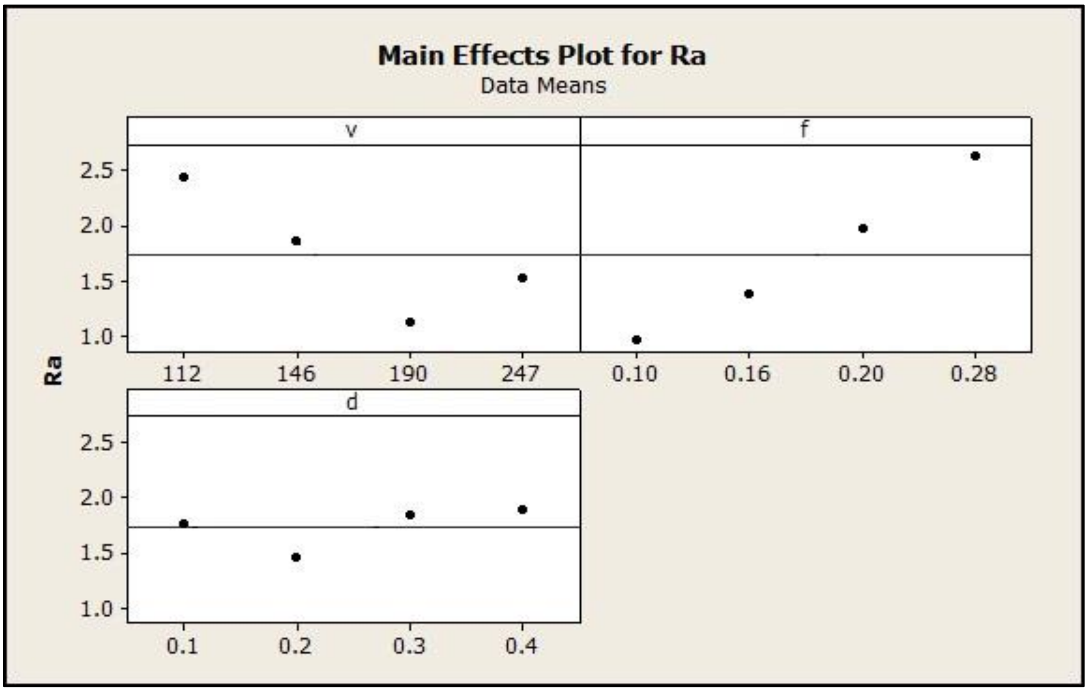

(a)

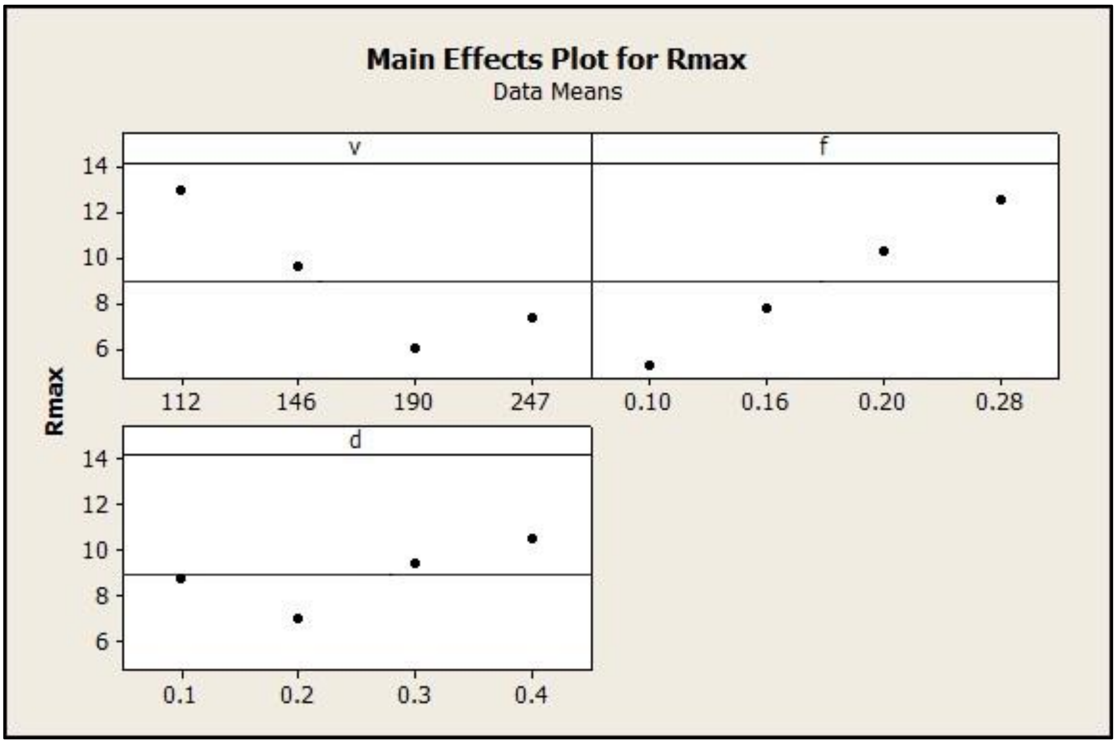

(b)

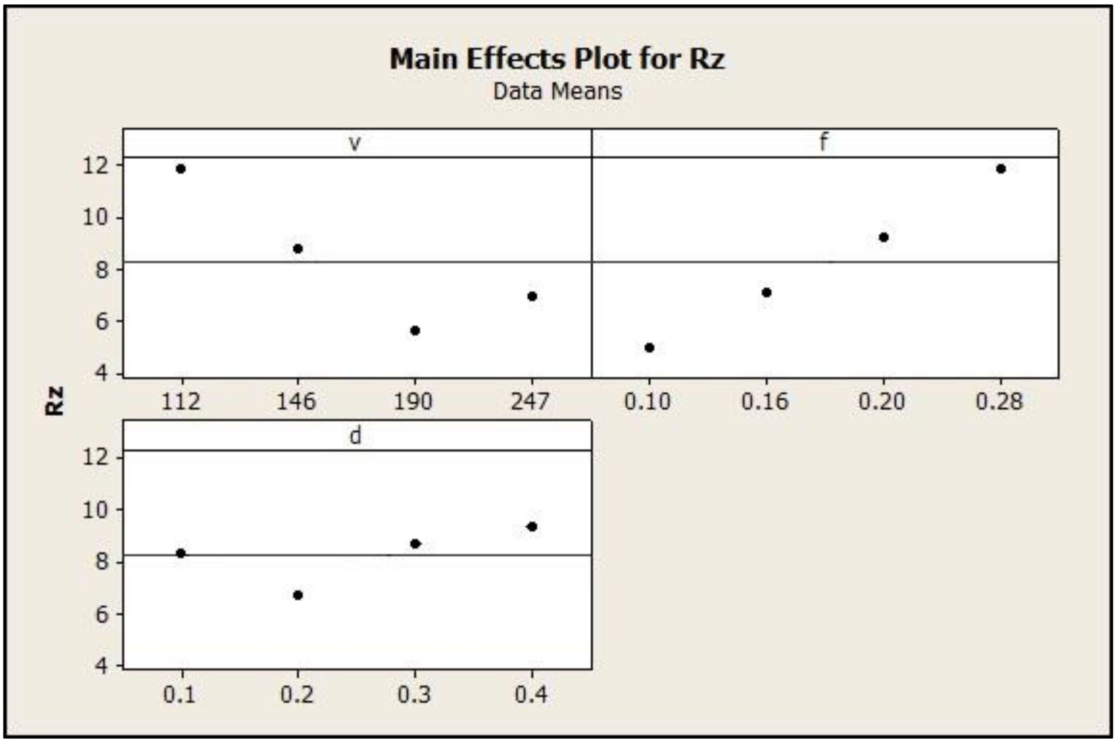

(c)

Fig.5.7: Main effects plot for surface roughness parameters (a) R_a, (b) R_{max} and (c) R_z

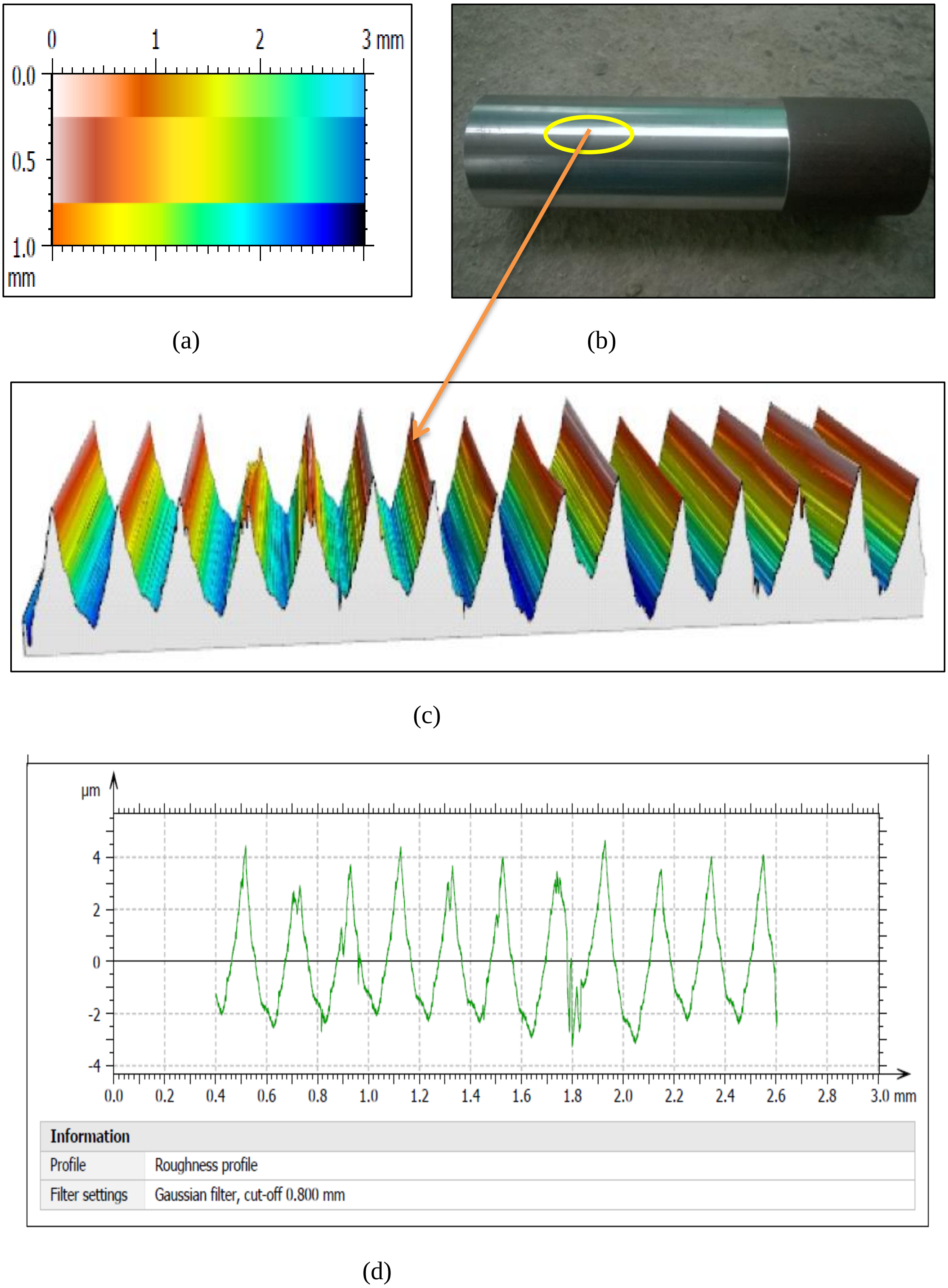

Fig.5.8: (a) 3x1 mm rectangular traced area by probe over the machined surface of workpiece (b) Machined workpiece material, (c) 3D surface roughness plot (d) Roughness profile of workpiece material AISI 4340 alloy steel, at v=112m/min, f=0.1mm/rev and d= 0.1mm.

5.8 Machining Forces Analysis

Forces are very important parameter for judging the machinability and cutting is a process of extensive stresses and plastic deformations. The high compressive and frictional contact stresses on the tool face result in a substantial cutting force F_c. In orthogonal cutting, the total cutting force F is conveniently resolved into two components in the horizontal and vertical direction, which can be directly measured using a force measuring device called a dynamometer. The experimental results of machining forces parameter (F_f, F_c, and F_r) are analyzed using the analysis of variance (ANOVA) for determining the parameters significantly influencing the machining forces.

Table 5.5: Analysis of variance for machining forces: (a) F_f, (b) F_c and (c) F_r

Sources	DF	Seq SS	Adj SS	Adj MS	*F*	*P*	Contr. %	Remark
(a) Analysis of Variance for F_f								
v	3	97.600	97.600	32.533	6.42	0.027	40.082	Significant
f	3	74.636	74.636	24.879	4.91	0.047	30.651	Significant
d	3	40.835	40.835	13.612	2.68	0.140	16.770	
Error	6	30.424	30.424	5.071			12.494	
Total	15	243.495					100	
(b) *Analysis of Variance for F_c*								
v	3	535.86	535.86	178.62	62.02	0.000	47.877	Significant
f	3	6.06	6.06	2.02	0.70	0.585	0.541	
d	3	560.02	560.02	186.67	64.82	0.000	50.036	Significant
Error	6	17.28	17.28	2.88			1.543	
Total	15	1119.22					100	
(c) *Analysis of Variance for F_r*								
v	3	2461.11	2461.11	820.37	73.05	0.000	78.083	Significant
f	3	18.15	18.15	6.05	0.54	0.673	0.575	
d	3	605.27	605.27	201.76	17.96	0.002	19.203	Significant
Error	6	67.38	67.38	11.23			2.137	
Total	15	3151.91					100	

It is seen in table 5.5, the parameters: force in x-direction or feed force F_f, force in y-direction or cutting force F_c and force in z-direction or radial force F_r. Cutting velocity is the (most significant parameter) contributed 40.082% for F_f, 47.877% for F_c and 78.083% in case of F_r. The contribution of the second most significant parameter depth of cut was noticed merely 50.036% in case of F_c and 19.203% for F_r, while the depth of cut is also not significant for feed force (F_f). Besides this, feed rate showed the minor role and is not found statistically significant on machining forces parameters (F_c and F_r), while the feed rate is significant 30.651% for feed force (F_f). The error contributions are 12.494%, 1.543% and 2.137% for (F_f, F_c, and F_r) respectively.

Fig.5.9 (a) to (c) illustrates the main effect plots of three machining forces parameters (F_f, F_c, and F_r). The main effect plots in indicate that, the machining force parameters leads to increase significantly with majorly an increase in cutting velocity and depth of cut. This is predicted as well as known that, the theoretical machining forces are primarily dependent upon the cutting velocity and depth of cut.

Fig. 5.10 (a) to (c) Forces is measured in three direction x, y and z by piezoelectric type dynamometer with using dynoware software at cutting velocity 112 m/min, feed rate 0.28 mm/rev and depth of cut 0.4 mm therefore the graph plotted between machining force versus time and measuring time = 10 sec, sampling rate = 1000 Hz and number of channels used in the dynamometer = 6. Since all force sudden fluctuates in positive quadrant, hence the average forces are 12.183 N for F_f feed force, 25.668 N for F_c main cutting force and 35.305 N for F_r radial force.

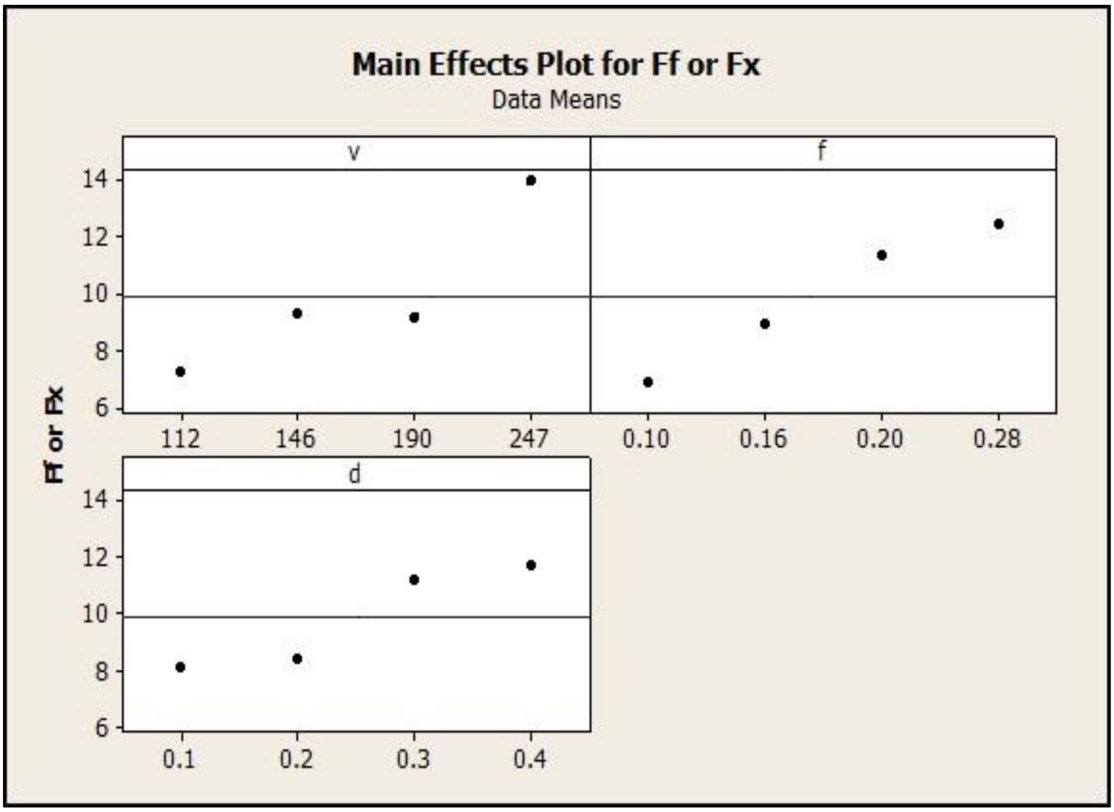

(a)

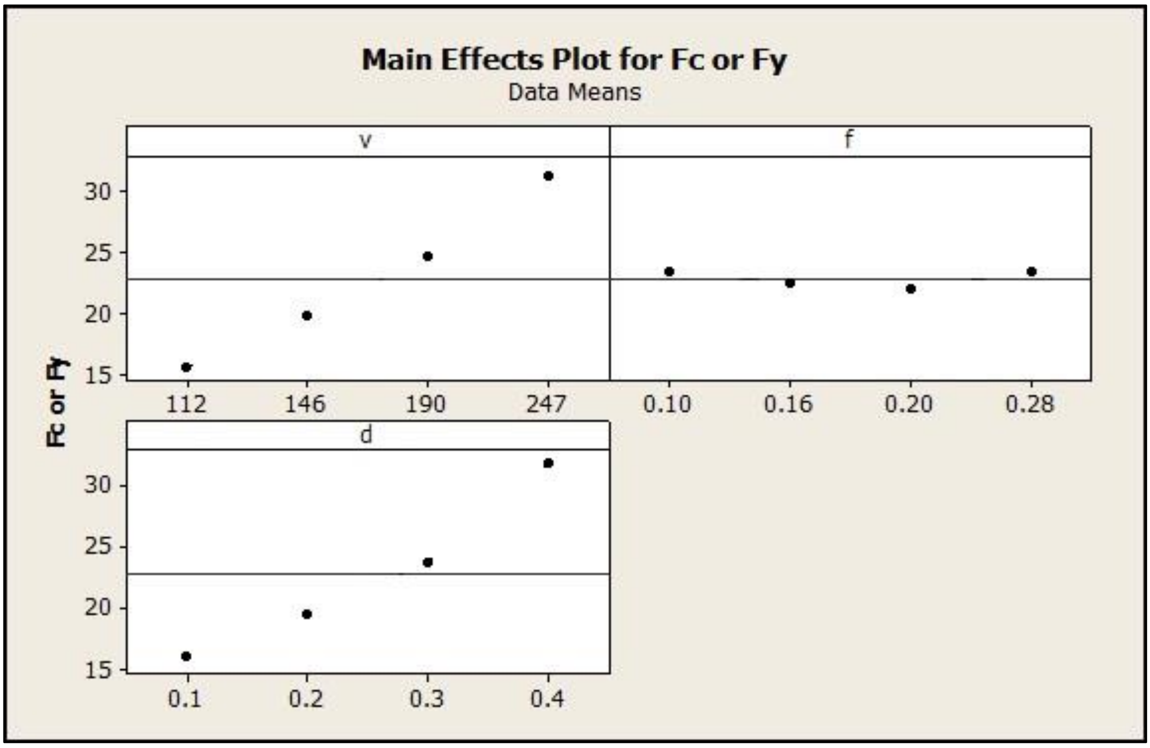

(b)

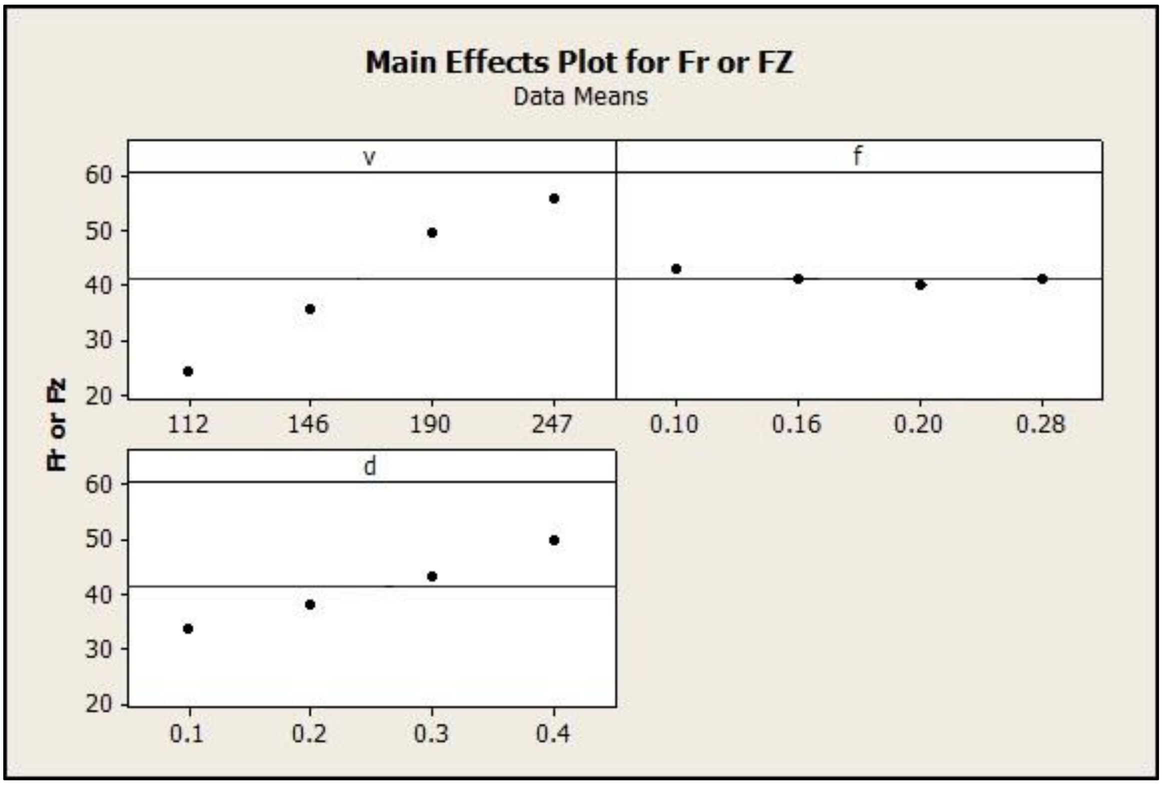

(c)

Fig. 5.9: (a) to (c) main effects plot for machining forces (a) F_f, (b) F_c and (c) F_r.

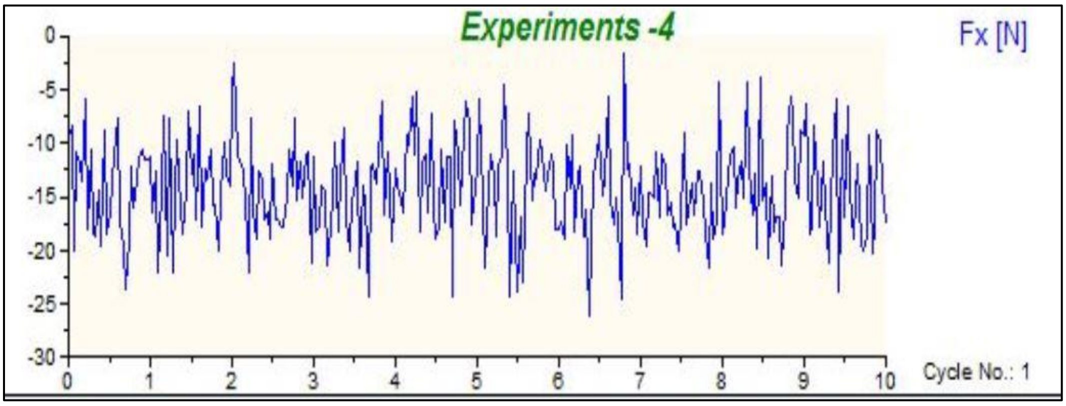

(a)

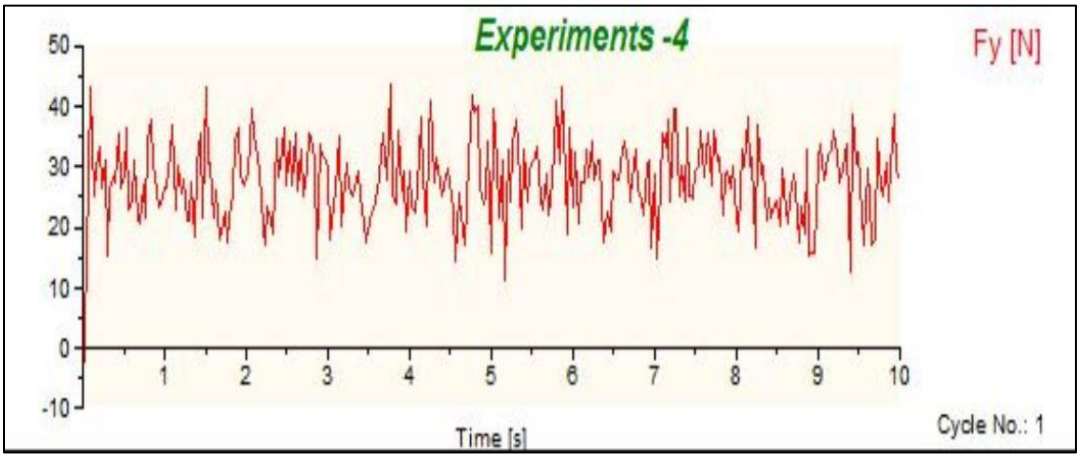

(b)

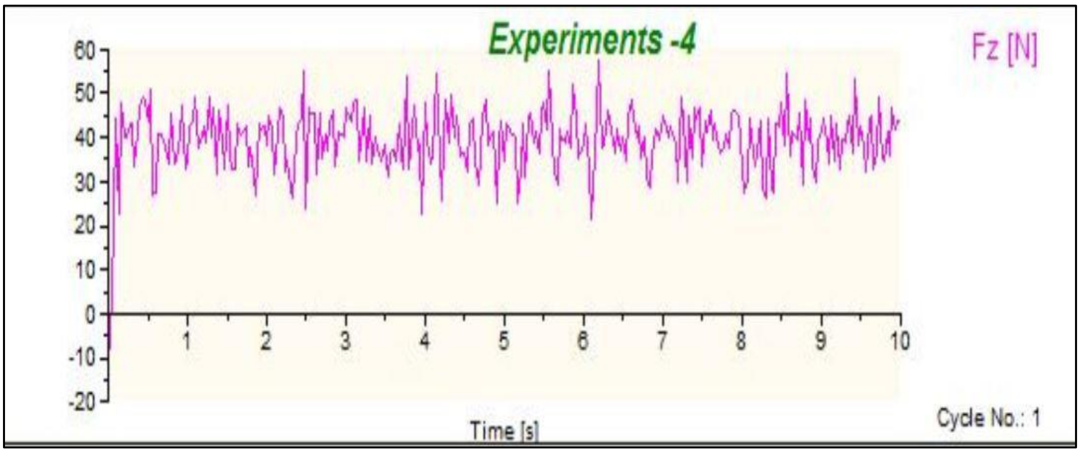

(c)

Fig.5.10: (a) to (c) forces result at cutting velocity 112 m/min, feed rate 0.28 mm/rev and depth of cut 0.4 mm.

5.9 Flank wear analysis

Both crater wear and flank wear can appear on the cutting tool in turning. Although crater wear was observed on rake surface of tools it was not measured. But in this research, flank wear has been accounted as a paradigm, as it is consistently present and is the simplest to measure during turning.

The result of ANOVA of flank wear in machining of workpiece material alloy steel is shown in Table 5.6. Out of the cutting parameters taken into account the effect of cutting speed is predominant (F = 76.97) on the output response of tool maximum flank wear (VB), followed by feed (F = 1.37) and depth of cut (F = 39.82) and P-value is less than 0.05 at 95% confidence level. A better knowledge for the explanation of the outcomes, which exhibits that the percent contribution due to the cutting velocity is 64.06% while depth of cut contributes 33.123% and feed 1.135%. However, maximum flank wear (VB_{max}) was not found statistically significant on feed rate but the flank wear increases marginally with increase in feed rate.

Table 5.6: Analysis of variance for maximum flank wear (VB_{max}).

Sources	DF	Seq SS	Adj SS	Adj MS	*F*	*P*	Contr. %	Remark
(a) Analysis of Variance for VB_{max}								
v	3	0.0013422	0.0013422	0.0004474	76.97	0.000	64.060	significant
f	3	0.0000238	0.0000238	0.0000079	1.37	0.340	1.135	
d	3	0.0006943	0.0006943	0.0002314	39.82	0.000	33.123	significant
Error	6	0.0000349	0.0000349	0.0000058			100	
Total	15	0.0020952						

The main effect plots for flank wear are shown in Fig. 5.11. It is clearly illustrated that flank wear increases with increase in cutting speed and depth of cut. This is in agreement with the findings of **(Sahoo *et al*., 2012 and Suresh *et al*, 2012)** that, increased cutting speed notably increases temperature at the contact tool due to the rapid rubbing action between tool's flank side and machined surface, which even exceeds the limits of the allowed thermal stability of the tool material. Another way to explain, this effect is due to increase in friction at the tool-chip interface causing localized high pressure and temperature at the nose region of the tool inserts and for this reason it results thermal impact. Owing to high cutting temperature, the yield strength of the workpiece material decreases which leads to lesser cutting forces and consequently lesser flank wear (VB<0.3 mm). The reduced tool wear is achieved at a combination of both the lowest cutting speed and depth of cut, and medium feed rate.

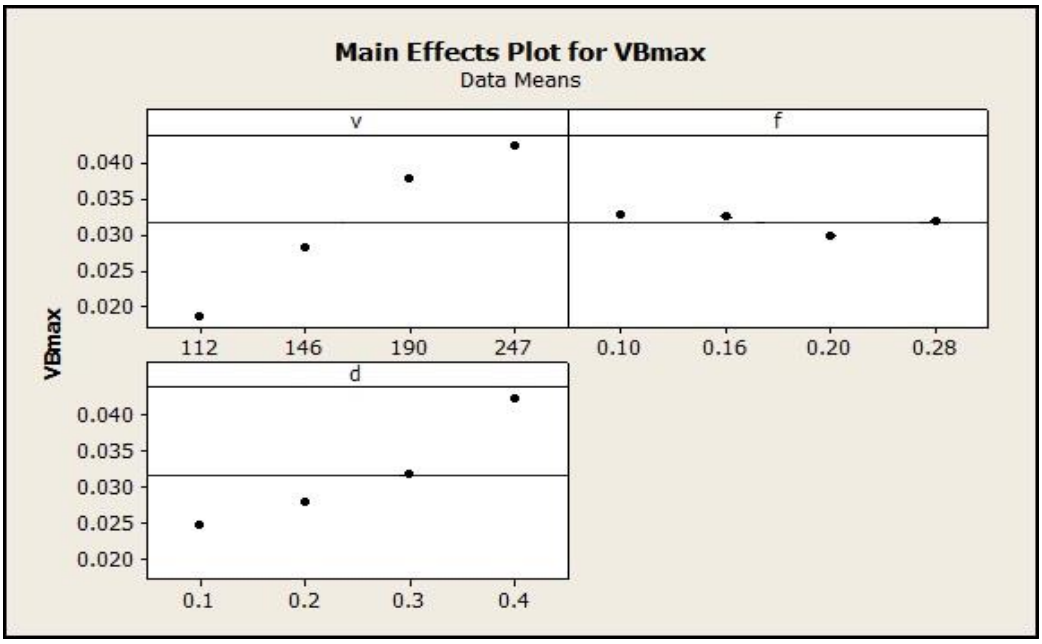

Fig.5.11: Main effects plot for maximum flank wear (VB_{max}).

Flank wear of the tool insert in turning is primarily caused by abrasion for the range of considered input variables for the study, where abrasive wear possesses scars on flank face which is observed in Fig.5.12. This was caused by the abrasive nature of the some hard particles present in the steel work material and it agrees with the observations of **(Pavel *et al,* 2005).** The SEM images of the worn out inserts reveal no chipping and catastrophic failure of cutting edge are noticed for coated carbide CVD deposited multilayer coating of (TiN/TiCN/Al_2O_3/ZrCN) insert. Experiment number one at low feed 0.1 mm/rev, 0.1 mm depth of cut and 112 m/min cutting velocity and experiment number sixteen at 0.28 mm/rev, 0.1 when turning is performed at two different experiment. These effects explain that (TiN/TiCN/Al_2O_3/ZrCN) coating appreciably enhances the fracture resistance as well as wear resistance inserts while turning AISI 4340 alloy steel.

The influences of maximum flank wear on workpiece machined surface roughness from the machining, it has been recorded that 0.01477 mm corresponds to the values of surface roughness criteria R_a, R_{max} and R_z are 1.58, 7.92 and 7.54 µm respectively. When the maximum flank wear attains 0.03392 mm, the increase of surface roughness criteria R_a, R_{max} and R_z is 75.94%, 60.35% and 64.45% respectively. The analysis concludes that surface roughness is closely related and proportional to the flank wear. That means, any progress in flank wear indicates some degradation of the machined surface quality. Similar results can be found in the literature although it is taken that, as long as wear is usual and does not go beyond 0.3 mm, surface roughness (exactly the criterion R_a) increases gradually since R_a does not exceed the 1.6 µm.

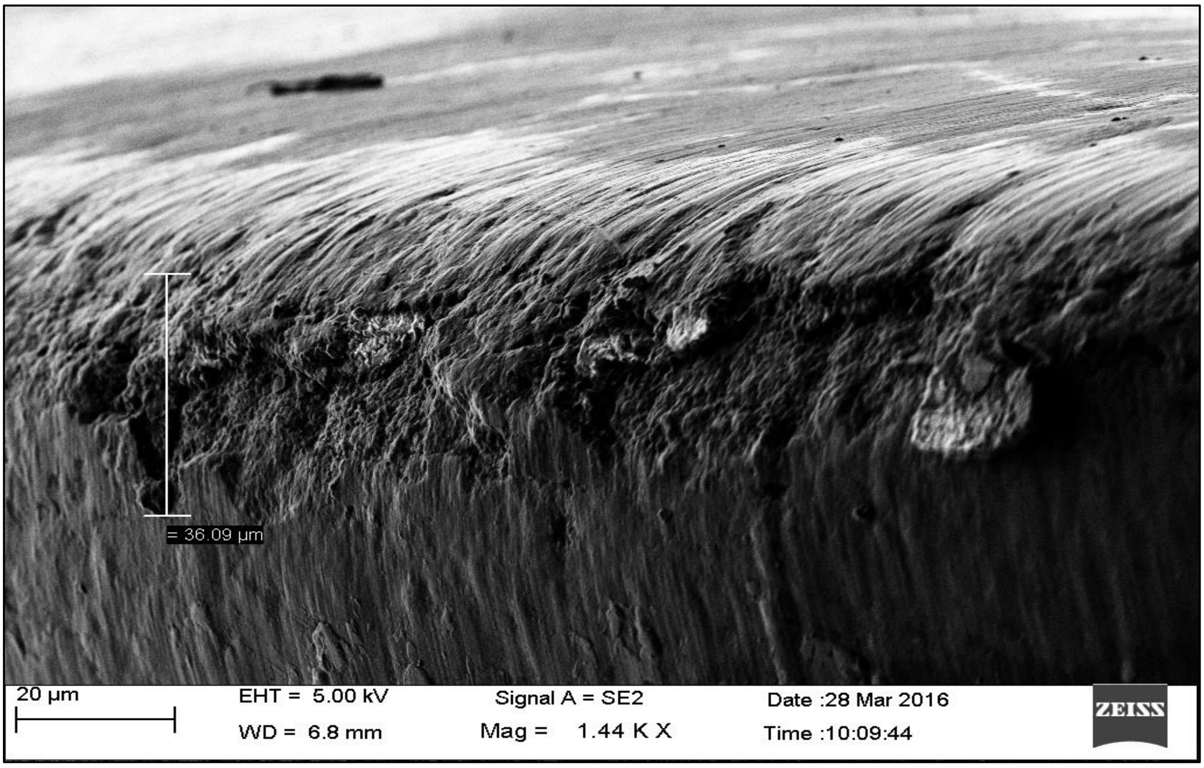

(a)

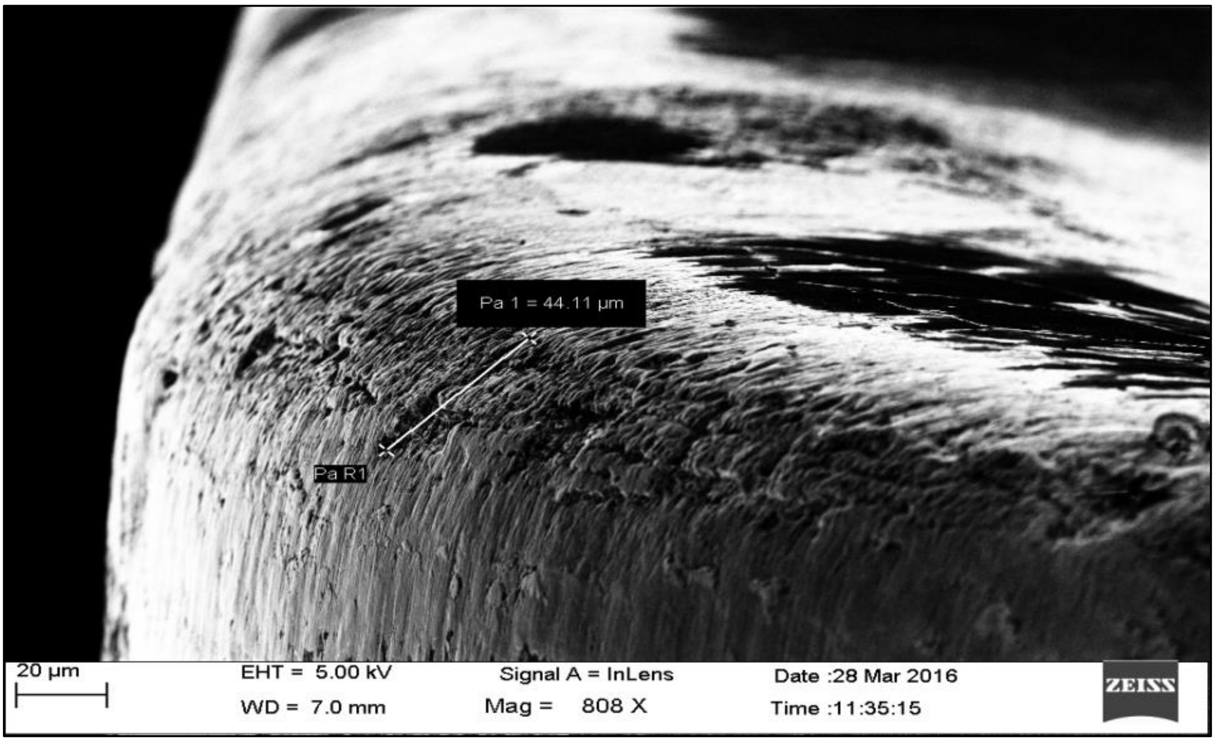

(b)

Fig.5.12: SEM images of the worn out insert (a) v = 146 m/min, f = 0.20 mm/rev and d = 0.4 mm, (b) v = 247 m/min, f = 0.16 mm/rev and d = 0.3 mm

5.10 Chip morphology analysis

To study chip morphology, chip forms are quite important as long chips may cause disturbances in automated manufacturing systems, possibly deteriorate surface quality and also endanger the safety of the machine operator. SEM was employed for the chip samples generated in dry turning of AISI 4340 alloy steel at different feed rates of 0.10 mm/rev, 0.28 mm/rev and 0.4 mm and 0.1 depth of cut Fig. 5.13 (a) and (b). It is to be noted that, with the increase in the feed at constant cutting velocity of 247 m/min therefore, the chip is increasingly scalloped. It means that it takes more and more shape of the sawtooth chip due to cyclic cracking by creating very intensive shear bands.

(Bermingham *et al*., 2011 and Dolinsek *et al*., **2004)** found, increasing temperature (caused by increasing feed) leads to enhancing thermal softening, microstructural deformation (transformation) and consequently, heat generation. It can be viewed from SEM micrograph of chips Fig.5.14 (a) and (b) that there are chip serrations moving over the entire width of the chip at different cutting conditions. There is an indication of distinct serrated elements at the upper-free edge, termed as primary serrated teeth and in some cases larger coagulated elements at the lower-tool nose-side edge of the chip, named as secondary serrated teeth.

Fig.5.15 (a) and (b) the top and bottom surfaces of chip conformed in SEM. The top surface of chip is plastically deformed and continually yields a rough surface mostly with minute wrinkles. The bottom surface of chip, which was sliding over the cutting tool, is noticed to be far smoother, and acquires long scratch marks.

It is observed from Fig.5.16 that on decreasing the feed rate and cutting velocity tends to smaller chip thickness so that the cutting forces and the tool vibrations decrease and subsequently produces the better surface finish. Therefore the 146 m/min is the optimum cutting speed. As reported by **(Noordin *et al*., 2003)** with increase in feed the undeformed chip thickness increases. Consequently, tangential force increases as the shear plane area increase with increase in undeformed chip thickness. The formation of saw-tooth chip directly depends upon the thickness of undeformed chip i.e. increase in undeformed chip thickness leads to bigger saw-tooth.

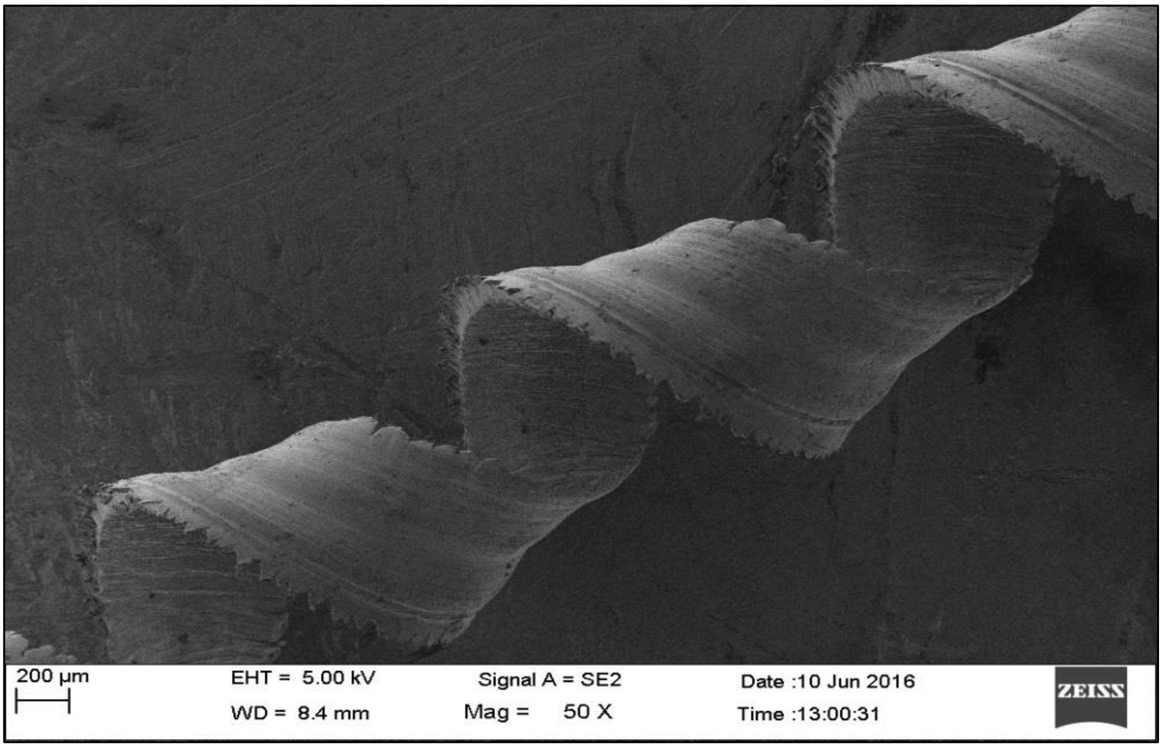

(a)

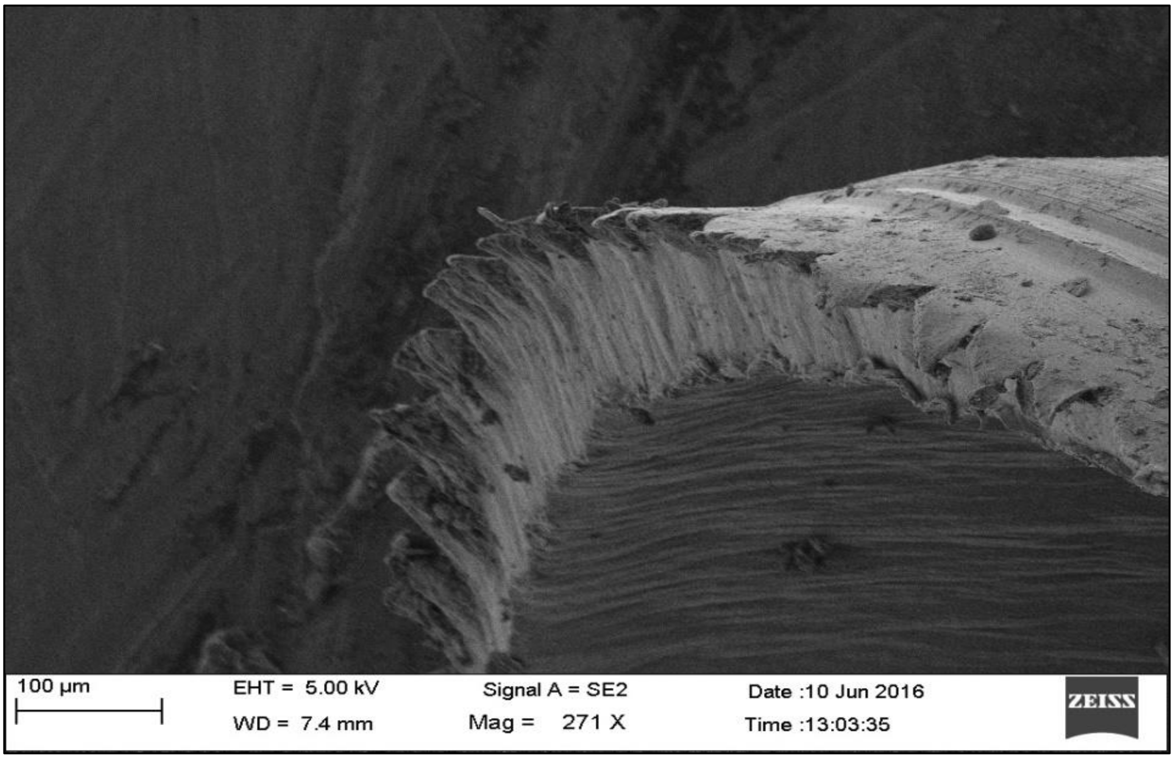

(b)

Fig.5.13: SEM observations of chip morphology at (a) v = 247 m/min, f = 0.10 mm/rev and d = 0.4 mm; (b) at v = 247 m/min, f = 0.28 mm/rev. and d = 0.1 mm.

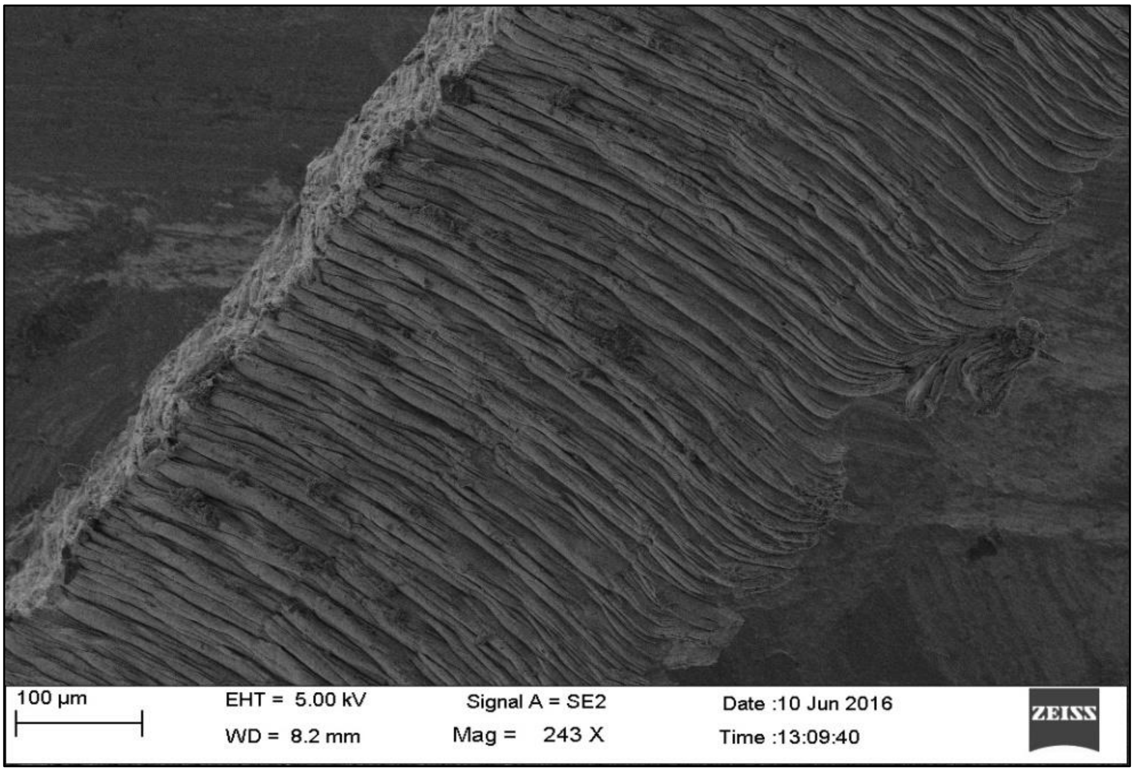

(a)

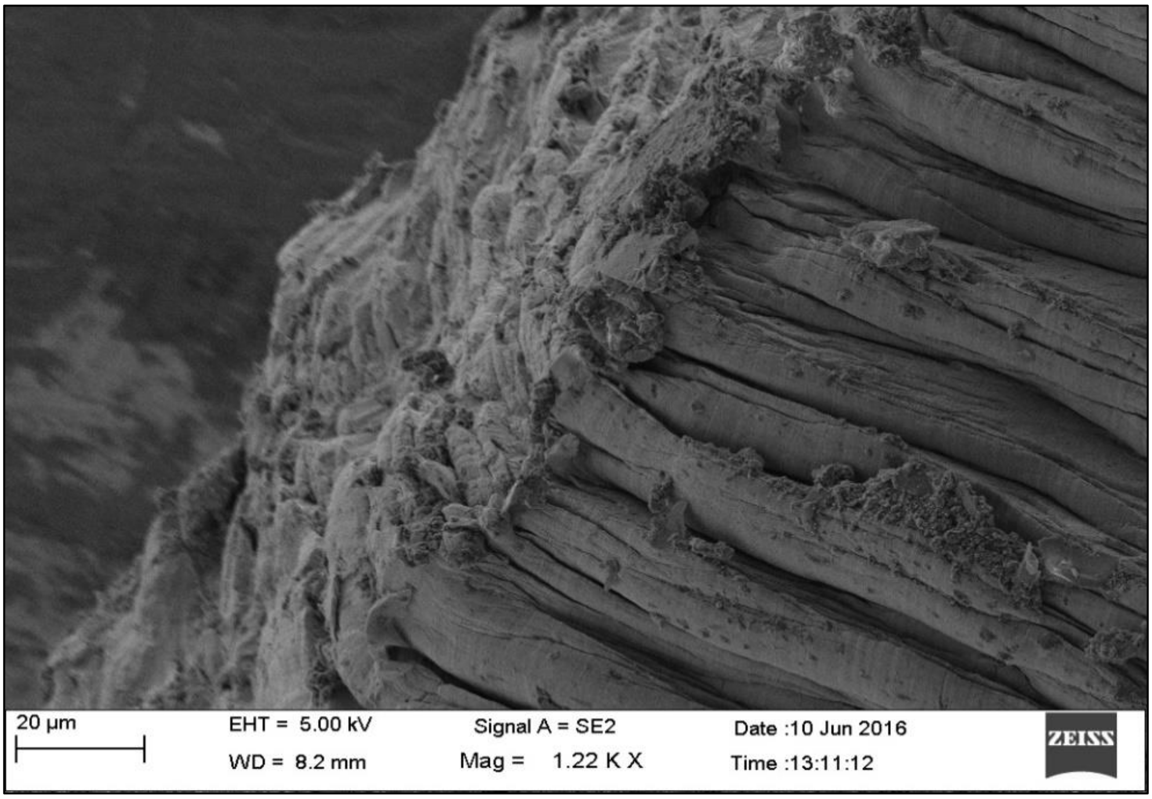

(b)

Fig.5.14: (a) SEM micrograph of chip, showing the primary (along the main body of the chip) and (b) secondary serrated teeth (along the free edge of the chip) formed in turning of AISI 4340 alloy steel at 170 m/min (v), 0.10 mm/rev (f) and 0.3 mm (d) using coated carbide insert

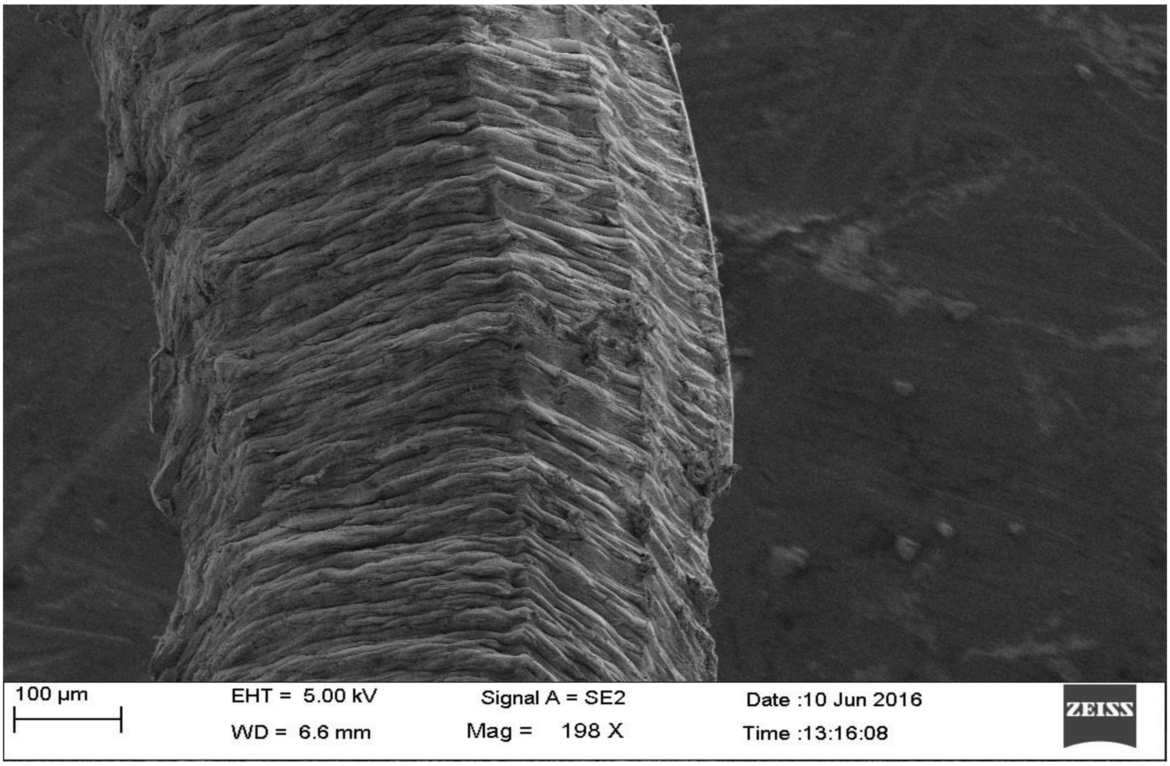

(a)

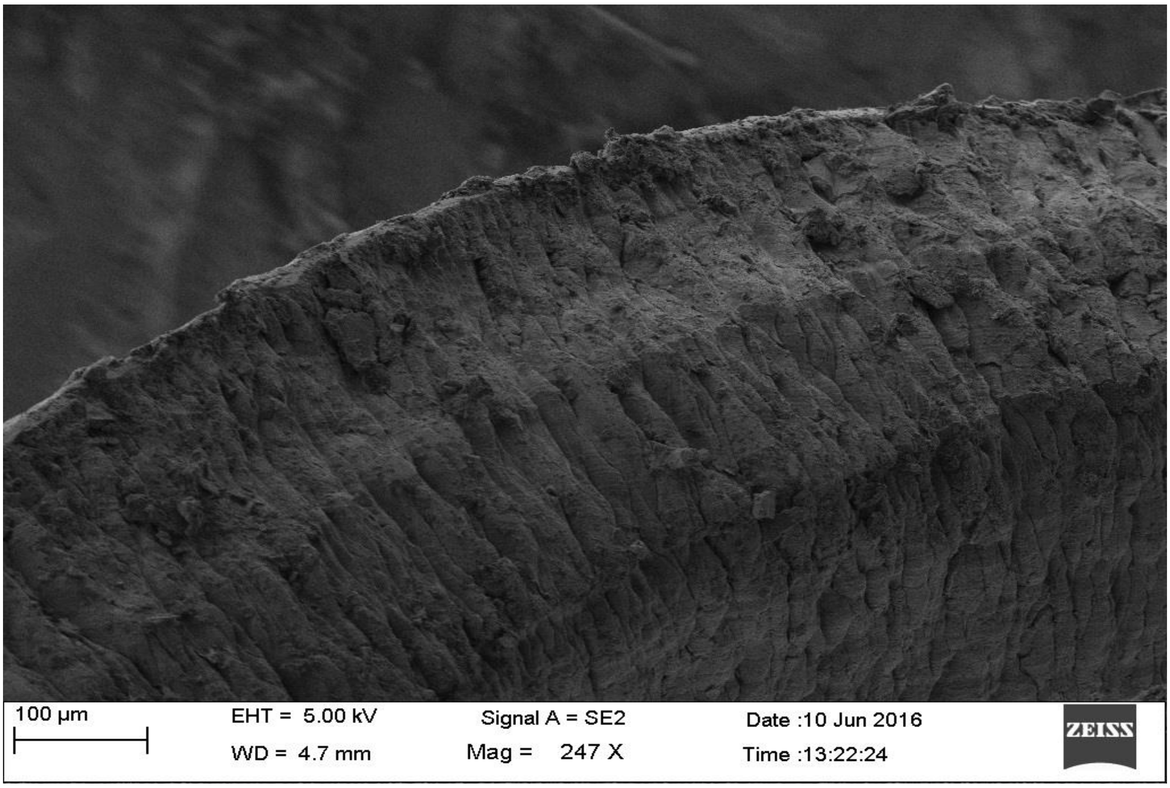

(b)

Fig.5.15: SEM micrograph of chip, (a) top surface and (b) bottom surface at v = 146 m/min, f = 0.10 mm/rev and d = 0.2 mm.

Here continues chips obtained, in general satisfactory chip breaking is sought where the obtained chips are sufficiently short for easy removal from the cutting zone Fig.5.17 (a) to (q). This is however a highly ambiguous definition resulting in the need for a qualitative evaluation of the obtained chips. Thus, “good chip breaking” may vary significantly between different machining cases. In addition to chip breaking, it is also important that the chip flow direction and curvature is such that no chip hammering of either the cutting tool or machined surface occurs. Several authors have attempted to describe chips obtained from a machining process geometrically. For instance has divided differing types of chips into the following categories as a function of their geometrical shape, together with knowledge of the width, thickness and length of the chip this information could be used to define the chip form in its entirety according to stress that improved methods for chip control is becoming increasingly relevant due to the major trend towards fully automated machining processes.

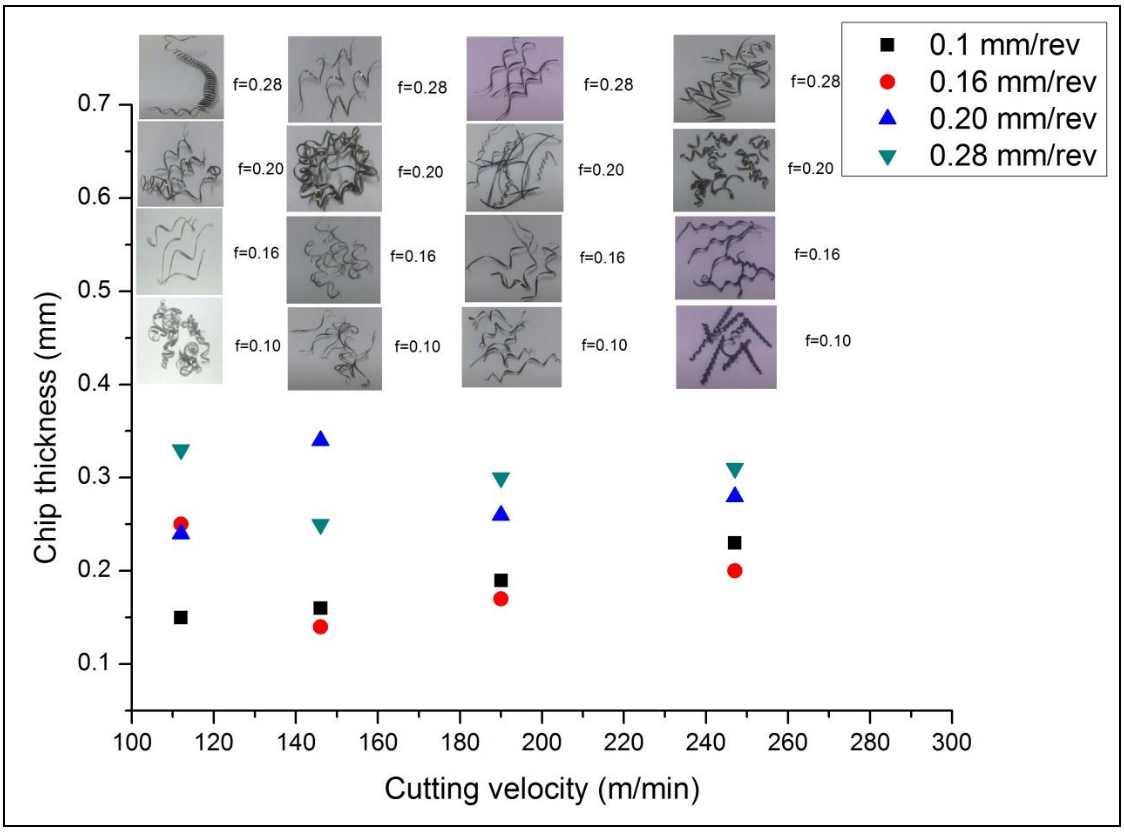

Figs.5.16: Chip thickness at different cutting velocity.


(a) (b)


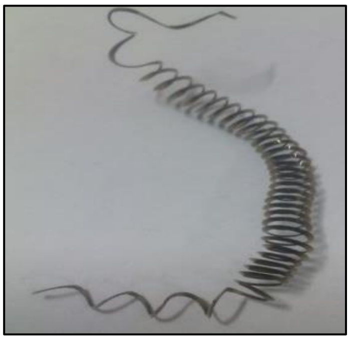

(c) (d)

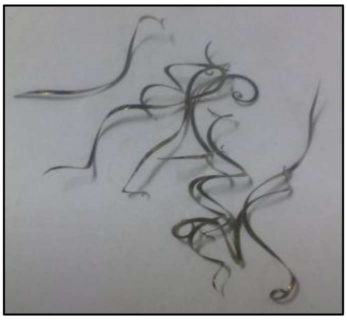


(e) (f)


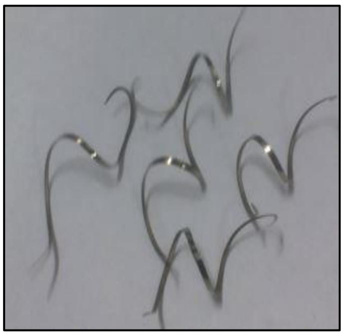

(g) (h)

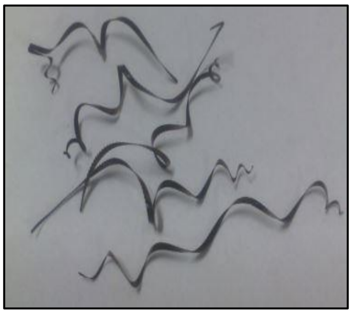

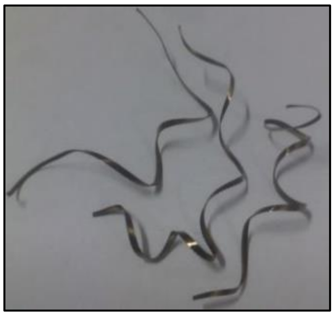

(i) (j)

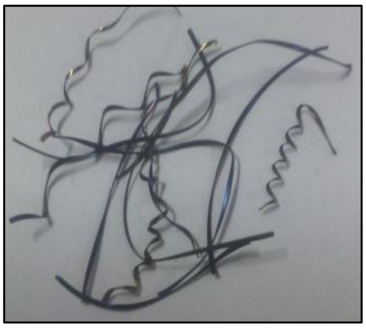

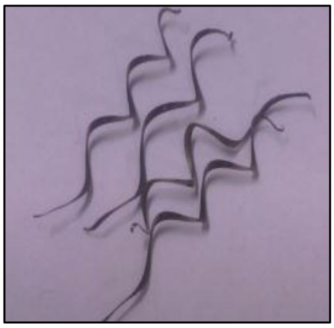

(k) (l)

(m) (n)

(o) (p)

Fig.5.17 (a) to (p) chips at different cutting level parameters

Next Chapter presents about conclusions of the experimental work and scope for future work.

Chapter 6

Conclusions and Scope for the Future Work

This chapter summarizes the significant achievements and conclusions from the present work highlighting the extent to which the aims and objectives are met. It also presents the possibilities for future work based on the outcomes of the research.

6.1 Conclusions

The straight turning has been performed successfully to obtain ultra finish surface on AISI 4340 alloy steel workpiece material using coated carbide CVD deposited multilayer coating of ($TiN/TiCN/Al_2O_3/ZrCN$) inserts under dry environment. The process parameters are optimally controlled in order to compose the lower surface roughness with minimal flank wear from the experimental investigation and modeling to draw the following conclusions:

- Taguchi's L16 design coupled with ANOVA which is employed in this investigation established to be an efficient experiment machinability evaluation.
- For minimum power consumption and maximum tool life criterion having better result at cutting velocity (v = 112 m/min), feed rate (f = 0.10 mm) and depth of cut (d = 0.1 mm). On the other hand for surface finish criterion i.e. higher finished machined surface at (a) Average surface roughness (R_a = 0.728 µm) at (v = 146 m/min), feed rate (f = 0.10 mm) and depth of cut (d = 0.2 mm), (b) Maximum surface roughness (R_{max} = 4.17 µm) at cutting velocity (v = 190 m/min), feed rate (f = 0.10 mm) and depth of cut (d = 0.3 mm) and (c) Maximum or peak-to-valley height roughness (R_z = 3.98 µm) at cutting velocity (v = 146 m/min), feed rate (f = 0.10 mm) and depth of cut (d = 0.2 mm).
- The main effect plot shows, the surface roughness is principally affected by feed rate and the depth of cut has a negligible impact. Whereas cutting speed has a negative effect for all surface roughness parameters (R_a, R_{max} and R_z) are observed with increase in cutting velocity up to 190 m/min. Then roughness value increases further increase of cutting velocity.
- The main effect plots in indicate that, the machining force parameters leads to increase significantly with majorly an increase in cutting velocity and depth of cut. This is predicted as well as known that, the theoretical machining forces are primarily dependent upon the cutting velocity and depth of cut.
- It is evident from ANOVA results the main effect plot that, cutting velocity is the major affecting flank wear (VB) with contribution of 64.060% and depth of cut 33.123%.

Although, the influence of feed rate has not been observed statistically significant, but the flanks wear is an increasing function of cutting velocity and depth of cut.

- For AISI 4340 alloy steel roughness, the machined surface is a function of the wear profile of CVD (TiN/TiCN/Al_2O_3/ZrCN) coated carbide insert. When increasing cutting speed, flank wear (*VB*) of the tool insert increases and causes immediate deterioration of the machined surface quality. Despite the growth of flank wear up to permissible limit (*VB* = 0.3) mm, Ra does not exceed the 1.6 µm.
- The best surface finish (R_a = 0.728, R_{max} = 4.37and R_z = 3.98 µm) was obtained at feed of 0.10 mm/rev, cutting speed of 146 m/min and 0.2 mm depth of cut, whereas the minimum flank wear (*VB* = 0.01477 mm) and machining forces (F_f = 2.554, F_c = 8.6421 and F_r = 15.981 N) was achieved with v = 112 m/min, f = 0.1 mm/rev and d = 0.1 mm. hence these data possess higher machinability
- The SEM images of the chips confirm the formation of saw tooth type of chips due to the cyclic crack propagation and also shear patterns are seen with most of the chips. The experiment also found that, decreasing the feed and cutting velocity approach to smaller chip thickness.
- The higher feed (0.28 mm/rev) favors the formation more saw tooth on the chip because the chip thickness increases hence the degradation of surface quality occurs.
- This experimental investigation helped in explaining the machined surface characterization of AISI 4340 alloy steel, wear mechanism of coated carbide tools insert and chip formation mechanism of generated chips during dry turning under various cutting conditions, which will give valuable knowledge to manufacturers in proper selection of cutting parameters.

6.2 Scope for the Future Work

There is a sufficient scope for future work. Some of the directions for the future work are as follows:

- Hard dry turning with AISI 4340 alloy steel workpeice material and CVD (TiN/TiCN/Al_2O_3/ZrCN) coated carbide tool insert with heat treatment like normalizing and spherodizing.
- Measurement of cutting temperature under dry environment.
- Use of cutting fluid like vegetable based oil for reduction of heat.

References

Bermingham, M.J., Kirsch, J., Sund, S., Palanisamy, S., Dargusch, M.S., 2011 New observations on tool life, cutting forces and chip morphology in cryogenic machining Ti–6Al–4V, *Int. J. Mach. Tools Manuf 51, 500–511.*

Boubekri, N., Rodriguez, J., Asfour, S., 2013. Development of aggregate indicator to assess the machinability of steels. *Journal of Materials Processing Technology 134, 159-165.*

Das, S.R., Dhupal, D., Kumar, A., 2015. Experimental investigation into machinability of hardened AISI 4140 steel using TiN coated ceramic tool. *Measurement 62, 108-126.*

Davim, J. P., Figueira, L., 2007. Machinability evaluation in hard turning of cold work tool steel (D2) with ceramic tools using statistical techniques. *Materials and Design 28, 1186–1191.*

Demir, H., Gündüz, S., 2009. The effects of aging on machinability of 6061 aluminum alloy. *Materials and Design 30, 1480–1483.*

Dolinsek, S., Ekinovic, S., Kopac, J., 2004 A contribution to the understanding of chip formation mechanism in high-speed cutting of hardened steel, *J. Mater. Process. Technol. 157–158, 485–490.*

Gaitonde, V.N., Karnik, S.R., Figueira, L., Davim, J.P., 2009, Analysis of machinability during hard turning of cold work tool steel (Type: AISI D2), *J. Mater. Process. Technol. 24, 1373–1382.*

Isik, Y., 2007. Investigating the machinability of tool steels in turning operations. *Materials and Design 28, 1417–1424.*

Jawaid, A., Sharif, S., Koksal, S., 2000. Evaluation of wear mechanisms of coated carbide tools when face milling titanium alloy. *Journal of Materials Processing Technology 99, 266-274.*

Lalbondre, R., Krishna, P., Mohankumar G.C., 2013. Machinability Studies of Low alloy steels by Face Turning Method: An Experimental Investigation. *Procedia Engineering 64, 632 – 640.*

Lalbondre, R., Krishna, P., Mohankumar G.C., 2014. An Experimental Investigation on Machinability Studies of Steels by Face Turning. *Procedia Materials Science 6, 1386 – 1395.*

Mashal, Y.A-H.,. El-Axir, M.H., Kassem, M.A., 2001. The machinability and tribological characteristics of aluminum alloys with improved elevated temperature properties using rapidly solidified powder. *Wear 250, 518–528.*

Medvedeva, A., Bergström, J., Gunnarsson, S., Krakhmalev, P., Nordh, L.G., 2011. Influence of nickel content on machinability of a hot-work tool steel in prehardened condition. *Materials and Design 32, 706–715.*

Nourredine, M.Y., 2003, Performance evaluation of coated carbide and coated cermet tools when turning hardened tool steel, *PhD Thesis, Universiti Teknologi Malaysia, 2003.*

Ozcatalbas, Y., Ercan, F., 2003. The effects of heat treatment on the machinability of mild steels. *Journal of Materials Processing Technology 136, 227–238.*

Pavel, R., Marinescu, I., Deis, M., Pillar, J., 2005. Effect of tool wear on surface finish for a case of continuous and interrupted hard turning, J. Mater. *Process. Technol. 170, 341–349.*

Persson, U., Chandrasekaran, H., 2001. Machinability Of Martensitic Steels In Milling And The Role Of Hardness.

Sahoo, A.K., Sahoo, **B., 2012**, Experimental investigations on machinability aspects in finish hard turning of AISI 4340 steel using uncoated and multilayer coated carbide inserts, *Measurement 45, 2153–2165*.

Salak, A., Vasilko, K., Seleck´a, M., Danninger, H., 2006. New short time face turning method for testing the machinability of PM steels. *Journal of Materials Processing Technology 176, 62–69.*

Sivaraman, V., Sankaran, S., Vijayaraghavan, L., 2012. Machinability of Multiphase Microalloyed Steel. *Procedia CIRP 2, 55 – 59.*

Sornakumar, T., Senthil, A.K., 2008. Machinability of bronze–alumina composite with tungsten carbide cutting tool insert. *Journal of materials processing technology 202, 402–405.*

Suresh, R., Basavarajappa, S., Gaitonde, V.N., Samuel, G.L., 2012, Machinability investigations on hardened AISI 4340 steel using coated carbide insert, *Int. J. Refract Metal Hard Mater. 33, 75–86.*

Suresh, R., Basavarajappa, S., Samuel, G.L., 2012, Some studies on hard turning of AISI 4340 steel using multilayer coated carbide tool, *Measurement 45, 1872–1884.*

Thakur, A., Gangopadhyay, S., Mohanty, A., 2014. Investigation on Some Machinability Aspects of Inconel 825 During Dry Turning. *Materials and Manufacturing Processes.*

Wang, S. T. H., Jelenković, E.V., 2013. Enhancement of the machinability of silicon by hydrogen ion implantation for ultra-precision micro-cutting. *International Journal of Machine Tools & Manufacture 74, 50–55.*

Zedan, Y., Alkahtani, S., 2013. Influence of the microstructure on the machinability of heat-treated Al–10.8% Si cast alloys: Role of copper-rich intermetallics. *Journal of Materials Processing Technology 213, 167–179.*

Callister, W.D., Rethwisch, D.G., Material Science and Engineering, 2nd Edition, John wiley and Sons publishing company, New Delhi, 2014.

Ghosh, A., Mallik, A.K., Manufacturing science, Affiliated east-west press private limited publishing company, New Delhi, 2010.

Rao, P.N., Manufacturing Technology vol. 1st & 2nd, Tata McGraw hill education private limited publishing company, New Delhi, 2009.

Mehta, N.K., Metal cutting and Design of Cutting Tool, Jigs & Fixtures. Tata McGraw hill education private limited publishing company, New Delhi, 2013.

Appendix-A: Detail of the instrument used

- **Leica inverted microscope**

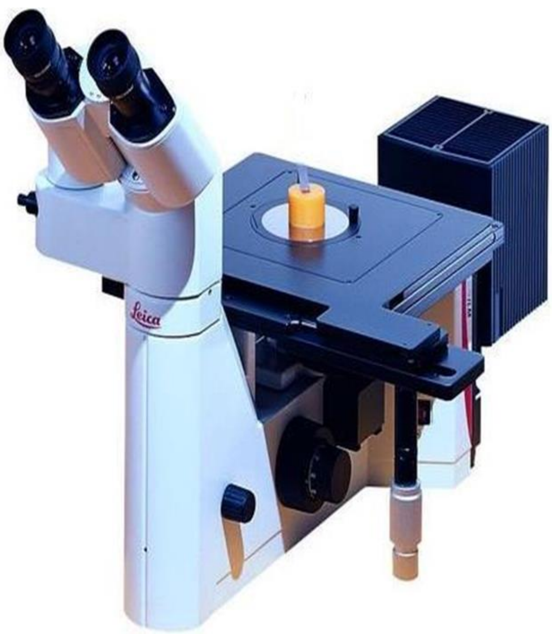

Make	**Leica Microsystems, *Germany***
Model	*DMIL*
Optics	Leica HC optics (infinity corrected) HC objectives: 2.5x-100x
Transmitted-Light	5 watt LED, external power supply (in 100-240, out 5V/2A)
Illuminator	Filter holder for TL filter Ø 32mm, collector, scattering filter
Focus	Coaxial coarse and fine adjustment, travel path 7mm, nosepiece focusing

- **Vickers Microhardness Tester**

Make	**Walter UHL *Technische Mikroskopie GmBH, Germany***
Model	*VMH002 V*
Load Range	1 grams-2000 grams
Type of Indenter	Diamonds square base hexagonal pyramid

- **Field Emission Scanning Electron Microscope**

Make	**Carl Zeiss NTS GmbH, Germany**
Model	**SUPRA 55**
Resolution	1.0 nm @ 15 kV 1.7 nm @ 1 kV 4.0 nm @ 0.1 kV
Acceleration Voltage	0.1 – 30 kV
Magnification	12x – 900,000 x
Stages	5-Axes Motorized Eucentric Specimen Stage X = 130 mm, Y = 130 mm and Z = 50 mm, T = -3° to + 70°, R = 360°

- **3D Surface Roughness-cum-Contour Tracer**

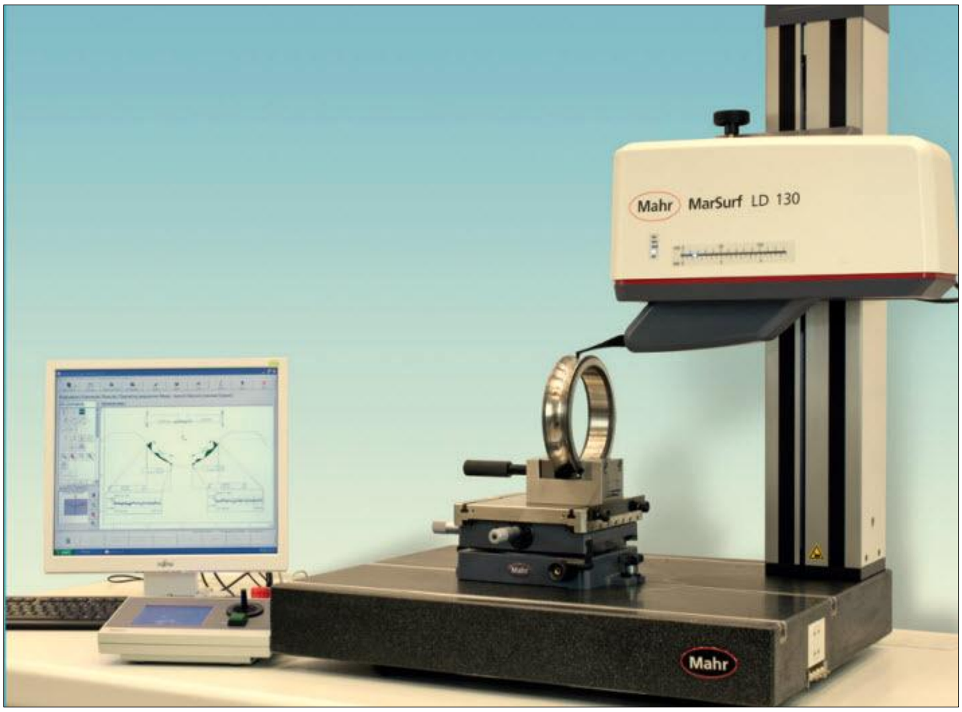

Make:	**Mahr Metrology, Germany**
Model:	**LD-130 with XT Facility**
Tracing length:	0.1 mm to 130 mm
Inclination of the measuring stand: adjustment of the measuring force	±45°; without active
Resolution:	0.8 nm